EUROPEAN COMMISSION
DIRECTORATE-GENERAL
Joint Research Centre

Analysis of Landscape and Climate Parameters for Continental Scale Assessment of the Fate of Pollutants

Alberto Pistocchi
Pilar Vizcaino
David Pennington

IES

2006

EUR 22624 EN

The mission of Institute for Environment and Sustainability is to provide scientific and technical support to the European Union's policies for protecting the environment and the EU Strategy for Sustainable Development.

European Commission
Directorate-General Joint Research Centre
Institute for Environment and Sustainability

Contact information
Address:Via E. Fermi 1, TP 460. Ispra (VA). Italy
E-mail: pilar.vizcaino@jrc.it
Tel.: +39 0332 786281
Fax:

http://ies.jrc.cec.eu.int
http://www.jrc.cec.eu.int

EUR 22624 EN

ISSN 1018-5593
ISBN 92-79-04809

Luxembourg: Office for Official Publications of the European Communities

Printed in Italy

Foreword

Increasingly, environmental management requires a capability to assess the spatial distribution of pollutants implying risks for human health and the ecosystems. Specialist and disciplinary analysis weakens in favor of crosscutting approaches capable of a holistic perspective.

To tackle the goal of an integrated description of the fate and transport of contaminants in the ecosystems and the related risks, at the Institute for Environment and Sustainability (IES) of the JRC an initiative is going on which has been named FATE after the Fate of pollutants in Terrestrial and Coastal Ecosystems.

The initiative consists of the systematic integration and pipelining of laboratory and modeling activities concerning the monitoring and prediction of pollution dynamics in water, soil and all related environmental media. Through the development of specific models, the working group of FATE is now in the condition to provide decision support on a wide range of contamination issues, with particular emphasis for the level of screening of substances with poor monitoring history and high potential of concern for human health and ecosystem risks.

The working scales range from Continental Europe, to large catchments, to site-specific investigations aimed at providing calibration data, benchmark detailed models and criteria for up scaling.

The decision support tools available include databases and atlases of landscape and climate parameters, data on exposure pathways, models for the simulation of the fate, transport and uptake of contaminants along ecological webs and human cohorts, tightly integrated with sampling, laboratory analysis and interpretation of monitoring data.

The analysis presented here concerns environmental parameters always used in multimedia fate and transport modeling of contaminants and is aimed at documenting the information used in the Geographic Information System (GIS)-based MAPPE modeling strategy, developed within the FATE initiative and other projects involving the IES. However, the discussion broadens to include issues of concern for all currently used multimedia models, among which particularly the SIMPLEBOX/EUSES model endorsed by the European Commission in the context of risk assessment for new and existing substances. For this reason we hope that the material presented in this report will help supporting modelers in the choice of environmental parameters for their specific applications, and therefore contribute to better decisions in line with the Environment and Health Strategy of the European Commission.

Giovanni Bidoglio

Head,
Rural, Water and
Ecosystem Resources Unit
IES, EC DG JRC

Introduction

Landscape and climate variability is a key issue in multimedia environmental modeling. Predictions of chemicals fate and transport can be highly sensitive to some parameters, which in turn have high variability both across space and time. Hence it is important to characterize these parameters, in order to have appropriate information to supply to both spatially resolved and lumped models.
A broad body of literature exists on the effect of spatial and temporal variability of landscape parameters on chemical fate and transport model predictions. Although Hertwich et al., 1999, stress that landscape parameters variability may be of lesser importance than the uncertainty in emission and chemical properties, other studies using spatially resolved models indicated that spatial variability may be key under certain conditions (e.g. Pennington et al., 2005).
From these studies, it appears that evaluations using single default values for landscape parameters may be satisfactory when interested in small, homogeneous regions, while for continental or global scale predictions it would be more appropriate to refer to a whole range of the parameters, by performing e.g. calculations on a sufficiently representative set of unique combinations. An analysis of the effects of spatial variability when using the EUSES model (EC, 2004) has been performed with emphasis on the soil component (Verdelocco, 2004).
In the present contribution, we illustrate a set of landscape and climate parameter maps of Europe, aimed at providing input to models of both distributed and lumped type. The parameters are provided in the form of maps, with a conventional spatial resolution of 1 km, and with a temporal resolution of one month whenever applicable. Actual spatial resolution may be well coarser than 1 km, depending on the data sources; however, as a number of parameters can be estimated at such resolution, it has been chosen to keep it as a reference. In future improvements of the data set, data at coarser resolution will be gradually replaced with finer ones if deemed necessary to improve model predictions.

The data set is presented in the form of an atlas, i.e. a collection of reference maps easy to consult and to use for predictions with simple lumped models, when one is interested in making region-specific calculations. Also, the data sets are arranged as grids in the popular ArcInfo ASCII format, for import in most gridcell-based geographic information systems (GIS). This allows the use of information in more sophisticated modeling such as distributed models, and lumped models considering variations.

As an atlas, the data set reflects average conditions in time. Although different data may often refer to different averaging periods, we don't have at present consistent estimates for all parameters throughout.
Inherent in the approach is also the impossibility to provide actual time series of the parameters. This may be limiting in many applications, but for the fate and transport of chemicals at continental or global scale overall knowledge of the emissions is still so weak that often referring to an average intra-annual variation of the landscape and climate parameters is fully satisfactory.

Table 1 summarizes the parameters considered in the atlas. These parameters reflect the input needs of most multimedia environmental models with three compartments, namely surface water (freshwater and oceans), soil, and air, together with atmospheric aerosol and suspended sediments in water. Also, Leaf Area Index (LAI) is included as a representative parameter for vegetation. The parameters are specifically designed to cope with the GIS-based modeling strategy proposed by Pistocchi, 2005, but similar to the input required by most multimedia models.

After a general discussion on the use of landscape and climate parameters in fate and transport models, the variables listed in Table 1 are discussed with reference to the available data sets for estimation, and the recommended data sets are presented.

Parameter estimation for multimedia fate and transport models

Spatial and temporal variation of landscape and climate parameters is relevant for both lumped and distributed environmental models.
In the former case, spatial variation should be considered both for the choice of region-specific parameters, when modeling a particular spatial location, and the assessment of variability when considering large domains from continental to global.
In the latter, maps of parameters are inherently required as distributed input to the model.

The EUSES model (EC, 2004), which represents the lumped model endorsed by the European Commission, considers five steps for the evaluation of environmental distribution of substances:

1. Estimation of partition coefficients
2. Estimation of environmental degradation rates
3. Fate in sewage treatment
4. Regional environmental distribution
5. Local environmental distribution

For both regional and local distribution, in EUSES a nested boxes approach is used as implemented in the model SIMPLEBOX (Brandes et al., 1996).
Special consideration is reserved to process-specific phenomena such as the ones occurring in certain industrial production, and in sewage treatment.

Due to the finalities of a paneuropean spatially explicit multimedia environmental model, it has been chosen to consider only processes occurring once a chemical is released to the environment, and thus all intermediate passages from chemical industrial production, through consumption, to waste treatment and disposal are not considered and should be part of the process of emission estimation, for which results from the SIMPLEBOX / EUSES approaches can be in turn employed.

In other words, the parameters described in the following concern the processes affecting chemical substances only after their spread on soils and vegetation, or their release to water or air, disregarding the processes within industrial and wastewater treatment plants upstream of the release.

A number of spatially explicit (distributed) models also exist at present. These models use input landscape and climate parameters that can be updated on the basis of the analysis here presented.

Irrespective of the modeling strategy adopted, a common need is the determination of within-medium partitioning and subsequent mass balance calculation for control volumes in which emissions, advection (both inter- and intra-media) and degradation occur. The presently covered parameters allow a description of the processes summarized below. All parameters listed can be seen as relevantly varying over the landscape, and susceptible to be represented by a meaningful non-uniform spatial distribution following realistic geographic rules. A discussion of each individual parameter and its estimation follows.

1) Atmosphere

In this compartment, the following processes are considered:

- Gas/particle phase partitioning
- Degradation
- Air to ground diffusion of gases
- Air to ground dry deposition of particles
- Air to ground wet deposition (gas absorbed to rain droplets and particles scavenged by rain)
- Advection

Generally speaking, partitioning coefficients and degradation rate are assumed to be dependent on:

1. Temperature

According to an exponential law.

Degradation is often computed as the product of a reaction rate with OH radicals, and the concentration of OH radicals. This suggests that

2. OH concentration

Can be an important environmental parameter.

Gas-particle partitioning, or the fraction of chemical attached to aerosol, is usually computed in the form:

$$\phi = \frac{OC \;\; K_{oa} TSP}{1 + OC \;\; K_{oa} TSP}$$

where K_{oa} is the octanol-air partition coefficient, OC is the organic carbon content of aerosol and TSP its concentration. Therefore, important parameters are:

3. Aerosol concentration in air
4. Organic carbon content in aerosol

Air to ground diffusion of gases[1] is often predicted from regressions using substance physico-chemical properties (diffusivity or Schmidt number, in turn depending on molecular weight) and atmospheric turbulence as reflected by wind speed. For this reason,

5. 10 m height wind velocity

Represents a relevant parameter.

All removal processes from the atmosphere (wet and dry deposition of particles and gases) need to refer to a mixed zone volume to be compared with degradation rates. Usually we refer then to:

6. Atmospheric mixing height

as an important parameter.

Aerosol deposition velocity in the atmosphere depends on the size of the particles, on the conditions of the atmosphere and on the type of surface, the latter being linked to land use. Many methods have been proposed to compute particle deposition velocities in the atmosphere (e.g. Sehmel, 1980; Williams, 1982; Underwood, 1984; Erisman et al., 1994; Wesely and Hicks, 2000; Apsley, 2005). Usually, reference is made to the so-called "three resistances scheme" which accounts for a turbulent layer, a sub-laminar boundary layer near the surface, and the "surface resistance". Details are presented e.g. in Underwood, 1984.

The importance of surface roughness is generally acknowledged, but the parameterization of such effect is not well agreed upon. Wesely et al., 1985 (quoted in Erisman et al., 1994), under the assumption of neutral atmosphere propose a very simple relation of the type:

$$\mathrm{Vd} = \frac{u^*}{\alpha}$$

Where α is 500 for grassland and 100 for forest.
The friction velocity u* can be computed as:

$$u^* = k u_{10} \ln\left(\frac{10 - d}{z_0}\right)$$

where:
k : Von Karman constant = 0.4
z_0 : length of roughness [m]
d : "zero-plane displacement"
u_{10} : wind velocity [m/s] at 10 m height.

[1] Features of the ground surface affecting exchanges are discussed referring to the soil and water media

In turn, z_0 depends on the surface roughness and is normally estimated as one tenth of the height of the surface rough elements; also, d is assumed 0.5-0.7 times the height of the surface rough elements (e.g. Underwood, 1984). The choice of a parameterization for deposition velocities may be rather complex, however most of the schemes presently used refer to a reclassification of a map of:

7. Land cover characteristics

Together with atmospheric turbulence metrics such as u^* or u_{10}.

Wet deposition is controlled by:

8. Precipitation

and by the duration of the inter-storm period when atmospheric pollution builds up. The latter can be predicted by the:

9. Duration of the wet period

Advection in the atmosphere is intrinsically three-dimensional and schemes describing motion fields in bi-dimensional terms are now looked at as rather obsolete with respect to trajectory-based models. For continental scale analyses, a practical model to be used in place of trajectories is the ADEPT model that computes concentrations at a point (x,y) as:

$$C(x,y) = \sum_{i=1}^{n} E_i SR_i(x,y) \exp(-kT_i(x,y))$$

where n is the number of source regions, E_i is the emission from each source region, $SR_i(x,y)$ is the concentration of a conservative chemical reaching point (x,y) from a unit emission in region i, and T_i the time required for the pollutant to reach point (x,y) from region i. The model is appealing because of its simplicity, and requires providing:

10. Source-receptor relations
11. Source-receptor time of travel.

2) Freshwater

In this compartment, the following processes are considered:
- suspended solids/liquid partitioning
- degradation
- water to air volatilization
- advection.

Generally speaking, degradation rate is assumed to be dependent on temperature. Partitioning between water and sediments is generally affected to a limited extent by temperature. When no better information is available, freshwater temperature can be assumed to coincide with the maximum between air temperature and 1°C.

Suspended solids/liquid partitioning is computed according to the same logics as for the air-aerosol partitioning. This requires to define:

12. Suspended sediment concentration

Sediment organic matter content is also a relevant parameter. At present, however, it is not known out of a few local case studies, and a default value needs to be used. Pistocchi, 2006, shows that this parameter affects estimates less than suspended sediment concentration.

For lakes, according to most models, volatilization is assumed to depend on wind speed only as for the case of oceans. Volatilization from rivers is often computed as a function of the depth to velocity ratio according to O'Conner and Dobbins (see Schwarzenbach et al., 1993, for details). Therefore:

13. Water velocity
14. Water depth

are parameters of interest. Water depth allows defining the surface water control volume for mass balance calculations.

Advection processes involve dilution (controlled by discharges) and degradation along the stream pathways. Therefore the following:

15. Flow rate in surface water
16. Surface water residence time

represent analogous to atmospheric source-receptor and time of travel relations.

3) Soil

This compartment is assumed to coincide with topsoil. Indeed, this is the main part of the soil where chemical inputs occur, and from which fluxes of chemicals to the deeper layers and to water and air originate.
The following processes are considered:

- solid-liquid-gas partitioning of the chemicals
- degradation
- soil to air volatilization
- topsoil to vadose zone advection via infiltration
- soil to surface water advection via runoff and erosion.

Generally speaking, degradation rate and partitioning properties are assumed to depend on temperature, which is assumed to coincide with air temperature.

Partitioning of the chemical in the soil is given by the fractions dissolved in the soil water, in the soil gas phase and adsorbed to the soil solids, respectively:

$$FR\_DISS = \frac{M_l}{M_{soil}} = \frac{\vartheta}{\vartheta + K_d \cdot \rho + (\phi - \vartheta)K_{aw}}$$

$$FR\_GAS = \frac{M_g}{M_{soil}} = \frac{(\phi - \vartheta) \cdot K_{aw}}{\vartheta + K_d \cdot \rho + (\phi - \vartheta)K_{aw}}$$

$$FR\_SOL = \frac{M_s}{M_{soil}} = \frac{\rho \cdot K_d}{\vartheta + K_d \cdot \rho + (\phi - \vartheta)K_{aw}}$$

where:

M_i, i=l, g, s - mass in liquid, gas and solid phase of the soil [kg/m3] (for i=s units are [kg/kg])

$\rho = 2700\ (1- \phi\ )$ – Soil dry bulk density [kg/m3]

ϑ- soil water content [-]

ϕ - soil porosity [-]

M_s – mass in soil [kg]

K_d is the distribution coefficient given by:

$$K_d = fr_{OC} \cdot K_{OC}$$

where:

fr_{OC}– organic carbon fraction of suspended solids

K_{OC} – organic carbon-water partitioning coefficient [m3w/m3octanol]; Koc can be estimated from K_{ow}-type of quantitative structure-activity relations, e.g. the one developed by Karinckhoff $Koc = 0.4.K_{ow}$ (Mackay, 2001).

Therefore the following are relevant parameters:

17. Fraction of topsoil organic carbon
18. Soil texture

where soil texture allows parameterizing porosity, soil moisture and air content.
Volatilization from soil to the atmosphere is computed with reference to the gas phase chemical in soil and depends on soil water and air content. A common method used in these cases is the Millington-Quirk equation.

Advection to the vadose zone occurs through infiltration of soil water. Transport to the stream network and lakes occurs in liquid phase through runoff (and groundwater contribution to discharge) and water erosion of sediments. Runoff and infiltration are computed on the basis of land cover and soil texture, precipitation, and evapotranspiration.
Therefore, in addition to the other ones already mentioned, relevant parameters for this type of processes include in addition the following:

19. Erosion rate
20. Evapotranspiration

Sometimes, plant uptake of chemicals occurs in relation to water exchange. For this reason, also evapotranspiration is required. This is anyway a key parameter for the overall soil water budget. Also,

21. Leaf Area Index (LAI)

is a relevant parameter for both plant uptake and the deposition and absorption processes from the atmosphere.
Concerning the control volume definition in soils, although in principle a penetration depth can be defined for each contaminant based on its mobility in soils, often a homogeneous distribution in the soil surface layer is more realistic. In such case, it would be more correct to assume a default depth of the soil layer interested by contamination, if one is interested in screening level calculations. Anyway, penetration depth can be parameterized on the basis of soil type and land cover as well.

4) Oceans

In oceans, the following processes are considered:
- degradation
- solid-liquid partitioning
- particle sedimentation
- volatilization
- advection and dispersion

Degradation and partitioning depend on temperature and suspended solids as discussed for the atmosphere and freshwater compartments. Relevant parameters include:

22. Seawater temperature
23. Suspended solids concentration

Another parameter of importance is the fraction of organic carbon in suspended solids; this information is not available at present and needs to be taken as a default value.

Sedimentation depends on the sediment particle size distribution and ocean turbulence. However, for the removal of sediments the sinking flux of organic material is fundamental and it is parameterized sometimes using:

24. Chlorophyll concentration.

Volatilization is usually computed with the same algorithms of gas absorption to water surfaces, *mutatis mutandis*. A key parameter is therefore:

25. Wind speed at 10 m height on oceans

Advection and dispersion are controlled by:

26. Seawater velocity
27. Seawater mixing depth

Particularly, dispersion coefficients can be computed from the velocity of deformation field. Water depth allows defining the control volume for mass balance calculations.

Parameter	*intended use*	*spatial resolution*	*temporal resolution*	*source*	*web site*	*# of maps*	*Notes*
1. Air temperature	degradation, volatilization	10'	monthly climatology	CRU climatology (New et al., 2002)	http://www.cru.uea.ac.uk/cru/data/tmc.htm	12	
2. OH concentration	degradation in the atmosphere	0.25°	winter/summer	ADEPT model (Roemer et al., 2005)	http://ensure.jrc.it	2	
3. Aerosol concentration in air	partitioning and deposition	1°	annual average		http://ensure.jrc.it	1	
4. Organic matter content in Aerosol	partitioning and deposition	1°	annual average		http://ensure.jrc.it	1	
5. 10 m height wind velocity	Gas absorption and volatilisation, air/land or freshwater interface	10'	monthly climatology	CRU climatology (New et al., 2002)	http://www.cru.uea.ac.uk/cru/data/tmc.htm	12	
6. Atmospheric Mixing height	atmospheric control volume definition	0.25°	annual average	ADEPT model (Roemer et al., 2005)	http://ensure.jrc.it	1	Copy of the ADEPT model including data is to be asked to: arthur.baart@wldelft.nl
7. Land cover characteristics	Parameterization of atmospheric deposition, runoff/infiltration	0.25°	annual average		http://ensure.jrc.it	1	
8. Precipitation	Wet deposition, soil water budget	10'	monthly climatology	CRU climatology (New et al., 2002)	http://www.cru.uea.ac.uk/cru/data/tmc.htm	12	
9. duration of the wet period	Wet deposition	10'	monthly climatology	CRU climatology (New et al., 2002)	http://www.cru.uea.ac.uk/cru/data/tmc.htm	12	
10. atmospheric source-receptor relations	Atmospheric advection	0.25°	annual average	ADEPT model (Roemer et al., 2005)	http://ensure.jrc.it	1	Copy of the ADEPT model including data is to be asked to: arthur.baart@wldelft.nl
11. atmospheric source-receptor time of travel	Atmospheric advection	0.25°	annual average	ADEPT model (Roemer et al., 2005)	http://ensure.jrc.it	1	Copy of the ADEPT model including data is to be asked to: arthur.baart@wldelft.nl
12. suspended sediment concentration	partitioning of chemicals in freshwater	1 km	annual average	Pistocchi, 2006	http://ensure.jrc.it	1	
13. water velocity	Gas absorption to and Volatilization from rivers	1 km	monthly climatology	Pistocchi and Pennington, 2006	http://ensure.jrc.it	12	
14. water depth	Gas absorption to and Volatilization from rivers; surface water control volume definition	1 km	monthly climatology	Pistocchi and Pennington, 2006	http://ensure.jrc.it	12	

Parameter	*intended use*	*spatial resolution*	*temporal resolution*	*source*	*web site*	*# of maps*	*Notes*
15. river discharge	Surface water advection	1 km	monthly climatology	Pistocchi and Pennington, 2006	http://ensure.jrc.it	12	
16. surface water retention time	Surface water advection	1 km	annual average	Pistocchi and Pennington, 2006	http://ensure.jrc.it	1	
17. topsoil organic carbon content	partitioning	1 km	annual average	ESB - EC DG JRC (Jones et al., 2003)	http://eusoils.jrc.it/Website/octop/viewer.htm	1	
18. soil texture	Soil water, air content, porosity, runoff, infiltration	1 km	annual average	ESB - EC DG JRC, SGDBE	http://eusoils.jrc.it/ESDB_Archive/ESDBv2/index.htm	1	
19. Erosion Rate	Advection	1 km	annual average	ESB - EC DG JRC (Kirkby et al., 2004)	http://eusoils.jrc.it/ESDB_Archive/pesera/pesera_cd/index.htm	1	
20. Evapotranspiration	Infiltration; plant uptake	1 km	monthly climatology	Pistocchi et al., 2006	http://ensure.jrc.it	12	results from model calculations, input data included in the ALPaCA
21. leaf area index	Vegetation	2 km	monthly climatology	Pinty and Gobron, personal communication (see refs. in text)	http://ensure.jrc.it	12	
22. seawater mixing layer temperature	Ocean degradation/volatilization	20 km	monthly climatology	Stips, personal communication (see refs. in text)	http://ensure.jrc.it	12	
23. seawater total suspended solids concentration	Ocean partitioning	2 km	monthly climatology	Melin, personal communication (see refs. in text)	http://ensure.jrc.it	12	
24. chlorophyll	Organic matter sinking flux	2 km	monthly climatology	Melin, personal communication (see refs. in text)	http://ensure.jrc.it	12	
25. 10 m height wind velocity on oceans	Ocean volatilisation; gas absorption	1°	monthly climatology	ICOADS	http://www.cdc.noaa.gov/cdc/data.coads.1deg.html	12	
26. seawater mixing layer average speed	Ocean advection	20 km	monthly climatology	Stips, personal communication (see refs. in text)	http://ensure.jrc.it	12	

Parameter	*intended use*	*spatial resolution*	*temporal resolution*	*source*	*web site*	*# of maps*	*Notes*
27. Seawater mixing depth	Ocean control volume definition	20 km	monthly climatology	Stips, personal communication (see refs. in text)	http://ensure.jrc.it	12	

Table 1 - summary of the environmental parameters considered in the present report

Atmospheric parameters[2]

Temperature

Temperature represents a well-studied variable, and many databases are available. Among others, the one of the European Commission derived from the MARS system and contained in the GISCO database can be used. The latter provides values at 50 km resolution based on data from national meteorological services in Europe.

The climatology of New et al., 2002, provides monthly values with a higher spatial resolution (10' latitude/longitude) and is therefore recommended when climatologically averaged values are accepted.
Map 1shows the annual average temperature obtained from New et al, 2002 data, available through the Climatic Research Unit, (http://www.cru.uea.ac.uk).

The coefficient of variation of monthly values has been plotted in Map 2 to identify areas of significant variability in temperatures. It is noticed that values of variation are smaller than 4%, so often it is appropriate to consider the annual average for certain calculations. However, there are phenomena that show an exponential dependence on temperature also in the limited range of ambient values (approximately -5 to 25 ^{o}C on average).
Atmospheric temperature can be also used as a proxy for temperature in surface water and soil whenever more refined information is not available.

OH concentration

OH concentration is used to compute atmospheric degradation rate. The ADEPT model (Roemer et al., 2005) brings estimates of averaged values of OH concentration for Continental Europe as shown in Map 3.
It is worth noting that the map provides a pattern of variation of the parameter, tending to be higher in Southern Europe. However, for the sake of modeling ADEPT uses a representative continental average.
Alternative estimates of OH concentration come from the application of the TM5 model, available at the EC JRC (Krol et al., 2005).
Modeled OH concentrations are available with spatial resolution of 1 degree x 1 degree in the horizontal plane, at heights of 52, 80, 135, 246, 435, 716, 1103, 1606, 2236, 3006, 3929, 5022, 6308, 7816, 9588, 11689 and 14160 meters, and have been poled to yearly averages in order to investigate vertical variability.
For reference, we present in Map 4 the average concentration together with the coefficient of vertical variation relative to the first 1000 m of height (Map 5). The pattern is somehow consistent with the one of Map 3: OH is strongly dependent on latitude as it

[2] **F.Gigante** has collaborated in the writing of this chapter and the processing of the data presented here, during his internship at EC, DG JRC, September 2005-april 2006. **F.Dentener** of EC, DG JRC, IES, has provided suggestions and data from the output of the TM5 model.

is related to solar radiation. The vertical variation tends to be significant in the belt of Central Europe and particularly in the western area.
Referring to a three dimensional model allows to investigate the vertical distribution of the parameters. For the sake of illustration, we refer to the 15 points indicated in Figure 1.

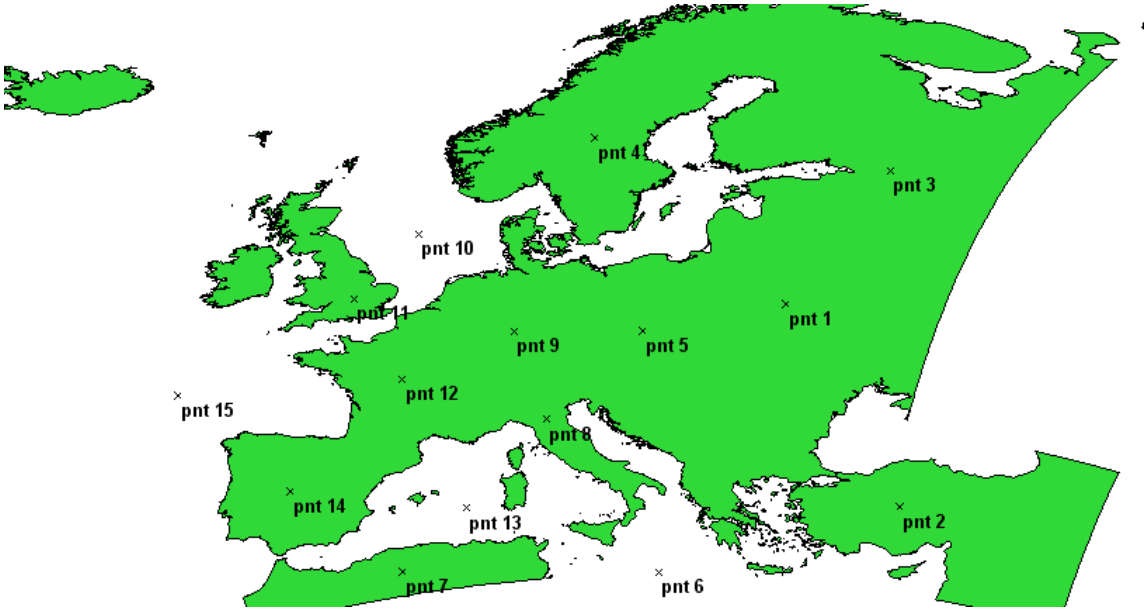

Figure 1– example locations for the vertical distribution of OH, aerosol, and OC content of aerosol.

As one can observe in Figure 2, the vertical profiles show a general trend to decrease with elevation, although a clear peak at approximately 100- 1000 m (the order of magnitude of the mixing height) is sometimes observed.

Another issue is the temporal variability of this parameter: as it is temperature-dependent, OH concentration shows a clear seasonal pattern. In the ADEPT model dataset, additional maps of OH concentration for winter and summer separately are provided. In the literature, reported values of OH concentration in summer are generally 1.5 to 2 times higher during summer than winter (e.g. Wang et al., 1998). This systematic variation suggests that whenever using temporally varying patterns of emissions and a temporally resolved model, monthly values of the parameter are by far more appropriate.

Aerosol concentration in air

Data for the years 1980-2000 on PM10 concentration are available at the EMEP web site: http://www.emep.int/aerosol/aerosol_descr.html. Map 5 – coefficient of vertical variation of OH concentration relative to the first 1000 m of height (TM5 model)
Map 6 reports a linear kriging interpolation of the average values over that period, highlighting some hotspots of high concentration.
The PM_{10} distribution is representative of overall aerosol concentration in the sense that concentration ranges are similar, and the spatial pattern compares reasonably with more

specific model estimates such as the ones of the TM5 model model (Vignati et al., 2004; Kinne et al., 2005; Textor et al., 2005).

Data worth using for multimedia modeling at the continental scale are « climatological » averages at monthly step, and in this form estimates of the TM5 model were imported. Data are available with spatial resolution of 1 degree x 1 degree in the horizontal plane, at heights of 52, 80, 135, 246, 435, 716, 1103, 1606, 2236, 3006, 3929, 5022, 6308, 7816, 9588, 11689 and 14160 meters.

For reference, we present in Map 7 and Map 8 the average concentration and the coefficient of variation relative to the first 1000 m of height. Indeed, this proves to be the layer were the largest portion of variation of the parameter occurs, as shown by the graphs of concentration (Figure 3) at the 15 representative points of Figure 1.

The main part of the aerosol is in generally dust (around 90 %) and sea salt (around a few % above the sea).

Also in the case of aerosol, concentrations tend generally to decrease with elevation.

Sometimes a peak concentration is observed at the level of the atmospheric mixing layer (100- 1000 m).

Organic carbon content in aerosol

From the same TM5 model estimates come concerning the organic carbon (OC) content of aerosol.

Data are available with spatial resolution of 1 degree x 1 degree in the horizontal plane, at heights of 52, 80, 135, 246, 435, 716, 1103, 1606, 2236, 3006, 3929, 5022, 6308, 7816, 9588, 11689 and 14160 meters

For reference, we present in Map 9 and Map 10 the average OC content together with the coefficient of variation relative to the first 1000 m of height. Also, vertical profiles at the same locations as before are presented in Figure 4.

10 m height wind velocity

This parameter has been taken from the climatology developed by New et al., 2002. This climatology represents at present the most complete and spatially resolved data set available, with global coverage, over the continents. The same parameter is presented for ocean areas in a following section.

Map 11 and Map 12 show the annual average wind speed at 10 m and coefficient of variation of monthly values.

Atmospheric mixing height

This parameter is available within the data set of the ADEPT model (Roemer et al., 2005), as shown in Map 13. The pattern of atmospheric mixing height shows low values on the west coast, and higher values in the interior. This is not consistent with the patterns of wind speed, which should be an indicator of atmospheric turbulence, hence mixing height. These considerations shed light on the inconsistency of the mixing height

map of Map 13 and the wind speed distribution of, both being a measure of atmospheric turbulence. For this reason, one should select these parameters critically.
However, ADEPT uses a representative continental average for the sake of modeling. Values of mixing height are about a half of the ones reported as default in the literature (around 1000 m). During night time, often mixing height reduces to near zero; as an average, it is likely that this map reflects the relative variation.
For the goal of more refined time dependent modeling, this map should not be used.

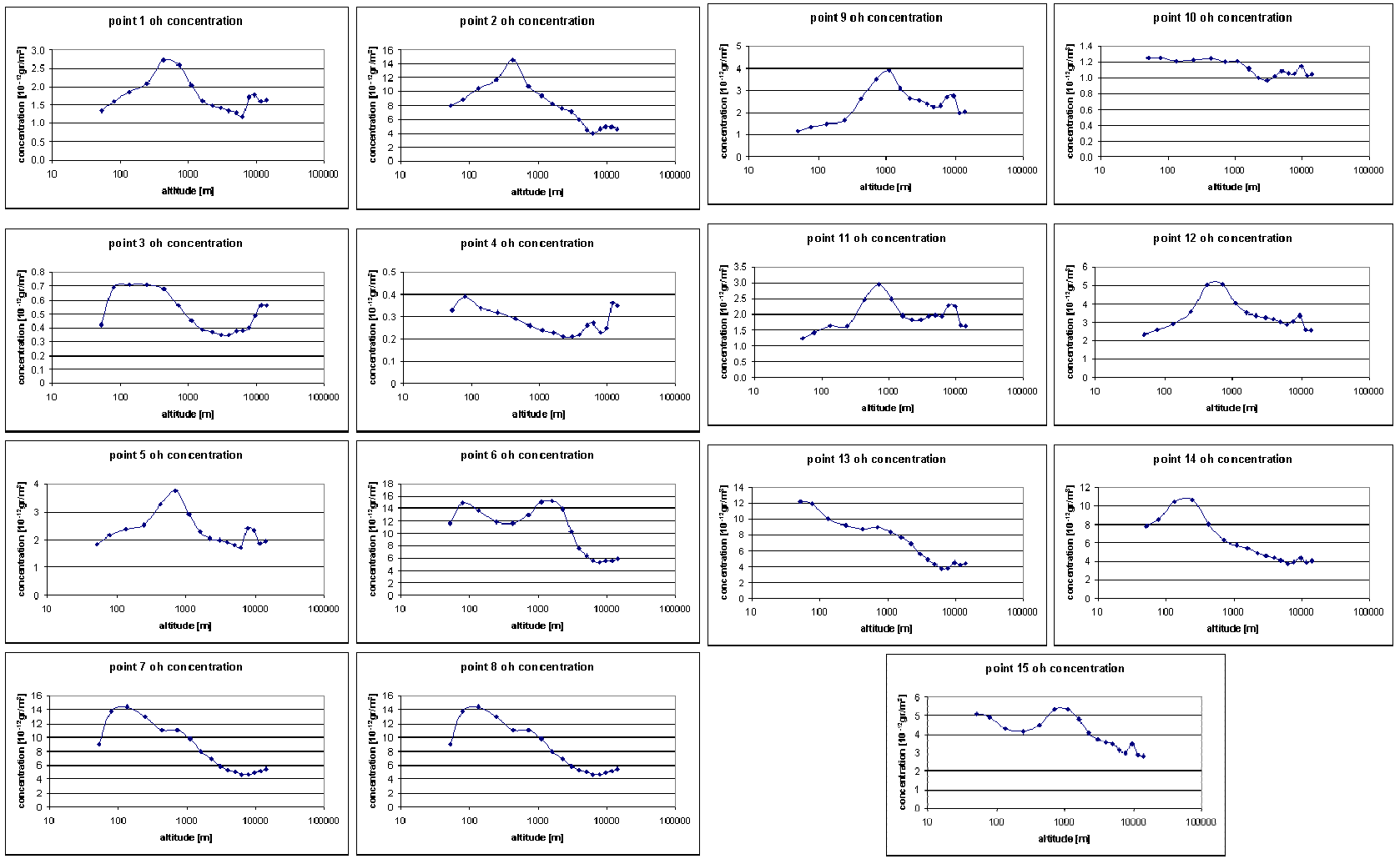

Figure 2– vertical profiles of OH concentration at a few selected locations.

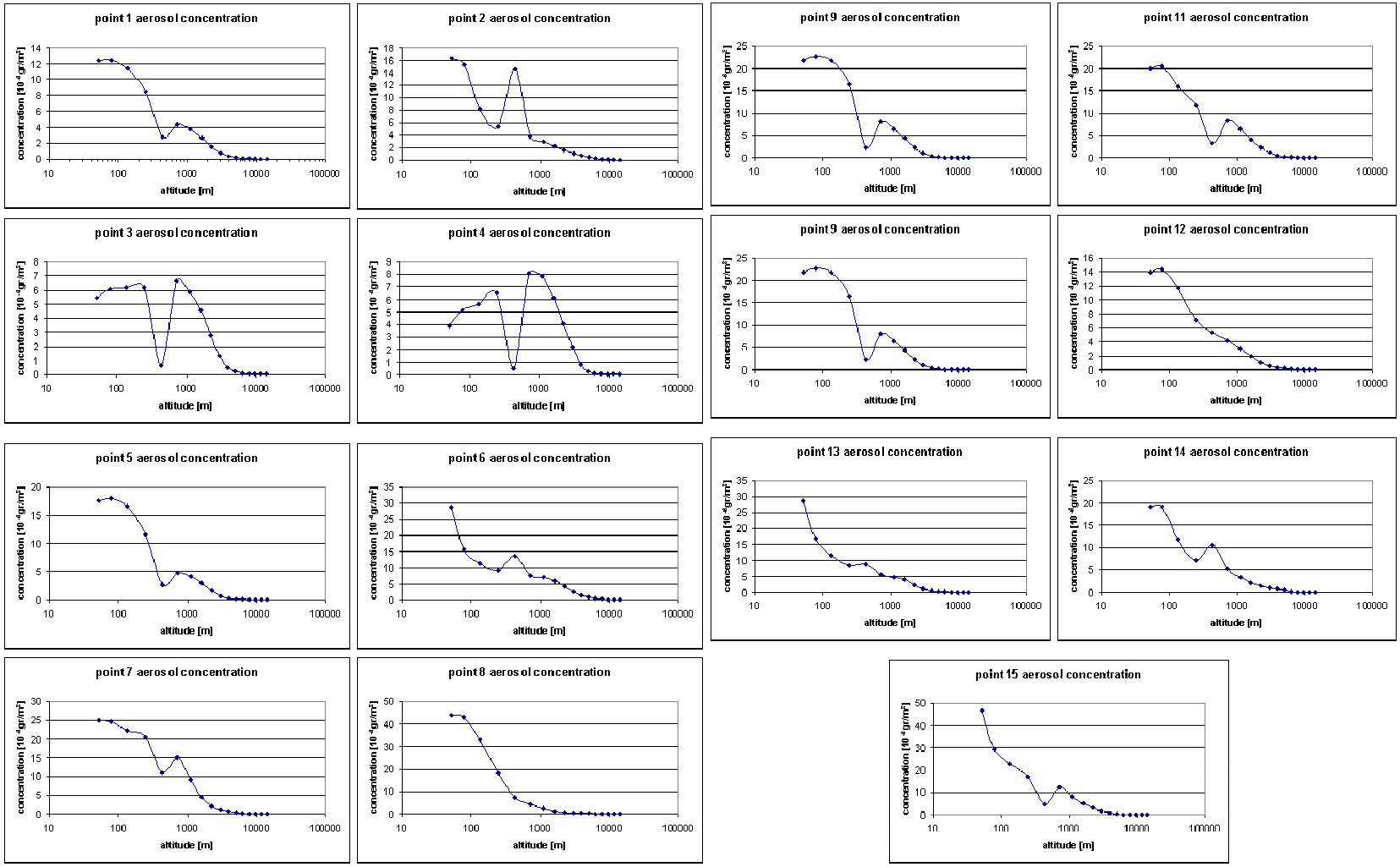

Figure 3. Vertical profiles of aerosol concentration at a few selected locations.

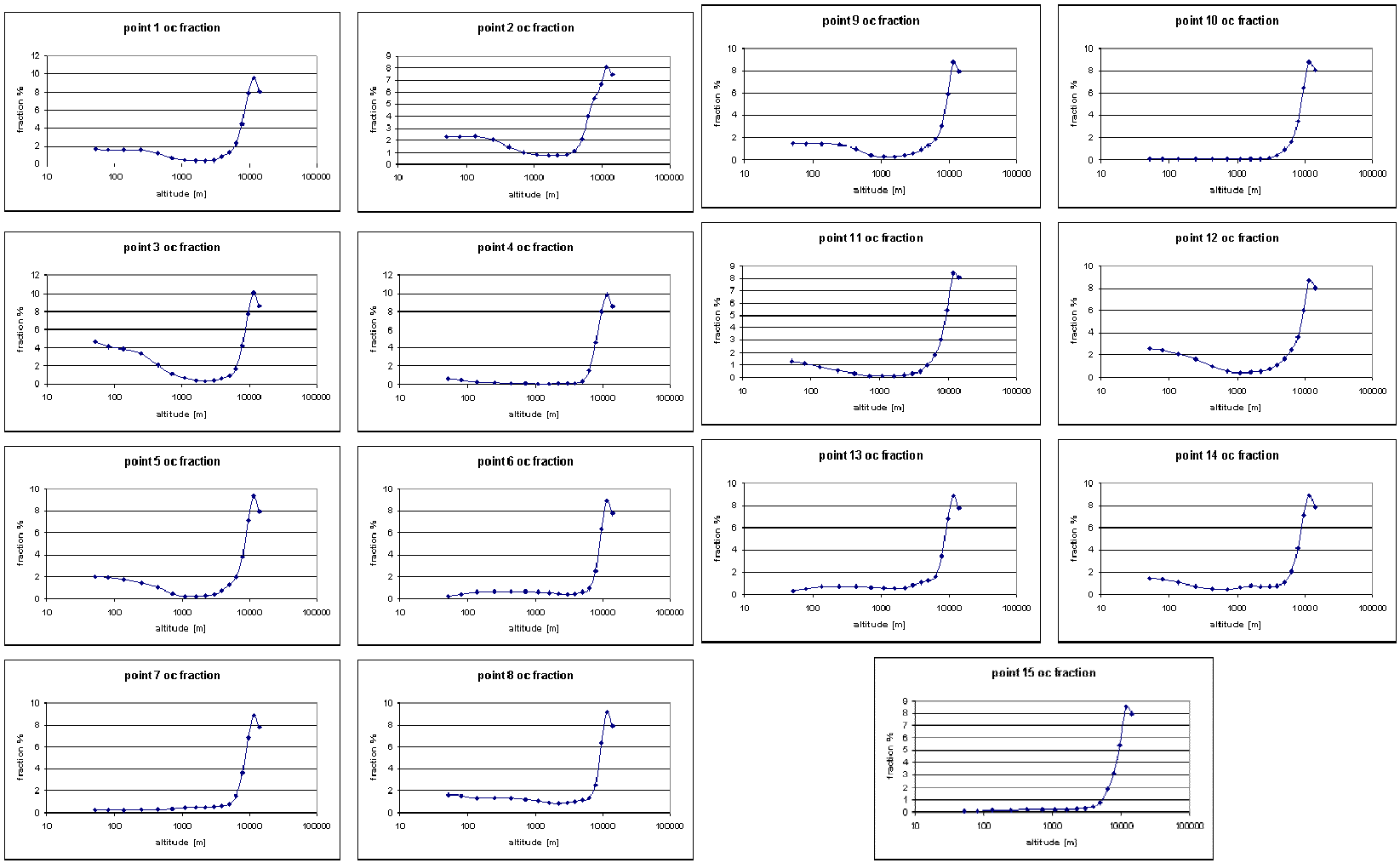

Figure 4– vertical profiles of OC fraction in aerosol at a few selected locations.

Land cover characteristics for particle dry deposition velocity

Land use shows being of significant importance for the deposition velocity. The following data were used to compute the relative importance of deposition velocity. Marner and Harrison, 2004, provide the following mean values for deposition velocity of nitrogen as aerosol in the UK.

Component	Urban	Forest	Arable	Grassland	Water
Aerosol NO_3	1.78	1.78	0.26	0.15	0.23
Aerosol NH_4	1.02	1.02	0.10	0.06	0.11

Table 2– atmospheric deposition velocities in cm/ s (after Marner and Harrison, 2004)

We can take the mean between NO_3 and NH_4 as typical values for the different types of land use. Their range is between 0.105 for grassland, and 1.4 for urban and forest areas. These values of typical deposition velocities were mapped using the PELCOM grid (http://www.geo-informatie.nl/projects/pelcom/public/index.htm), reclassified according to the following lookup table. The figures are not significant in absolute terms, as they refer to a specific case study, but provide an estimate of the relative rank of the land use classes.

Class_name	deprate_cm
Coniferous forest	1.400
Deciduous forest	1.400
Mixed forest	1.400
Grassland	0.105
Rainfed arable land	0.180
Irrigated arable land	0.180
Permanent crops	0.180
Shrubland	0.180
Barren land	0.105
Permanent Ice&Snow	0.170
Wetlands	0.170
Inland waters	0.170
Sea	0.170
Urban areas	1.400

Table 3

Map 14 shows the reclassified PELCOM map. There are many other sources of land use or land cover characteristics. The one presented here provides only an example of parameterization of the land surface. Other schemes can be retrieved e.g. from Erisman et al., 1994, or from the EMEP MSCE-POP model (www.emep.int). In general, deposition velocity appears to be quite a difficult term to predict in environmental modeling, it is often substance-specific and requires further investigation.

Precipitation, Duration of the wet period

Rainfall and duration of the wet period (expressed as an average of wet days per month) can be taken from the data set of New et al., 2002. Both datasets are monthly climatologies. An average and coefficient of variation for monthly values are reported in Map 15 and Map 16

At the European Commission's DG Joint Research Centre, also the MARS project (Monitoring Agriculture from Remote Sensing - http://agrifish.jrc.it/marsstat/Crop_Yield_Forecasting/cgms.htm) started in 1988 an activity of crop growth modeling based on input meteorological data interpolated from points in European national monitoring networks. Such data are interpolated with resolution of 50 km, and are available in time series of daily values which should reflect the available European national meteorological information.

An apparent problem with these data is the annual total of precipitation is often lower than the runoff reported by e.g. GRDC (Fekete et al., 2000). This problem has been observed both with the New et al., 2002, data, and with the MARS data set (see Figure 5 below). The areas where such discrepancies occur coincide fairly with mountainous regions. In those regions, it is likely that part of the precipitation occurs either as snowfall or "invisible precipitation" (air moisture condensation); also, it is possible that gauging is insufficient in those areas to capture the spatial variability of the phenomena. his phenomenon appears more patently using the coarser MARS data set, but is basically the same with the New et al., 2002, climatology. The inconsistency can be removed by applying appropriate constraints to the soil water budget as discussed in Pistocchi, 2005.

The number of wet days, which is a proxy to the duration of the wet period, is obtained from the New et al., 2002, global climatology. The average and coefficient of temporal variation of the parameter are reported in Map 17 and Map 18 respectively.

For fate and transport modeling of chemicals, snow is an extremely important factor. At present, the Wilmott and Matsuura (2000) archive (http://climate.geog.udel.edu/~climate/html_pages/README.wb_ts.html) has been retrieved which provides the snow water equivalent (SWE) in mm, and snow melt, in mm also, at monthly steps in climatological form. While SWE seems correct, an apparent underestimation of snowmelt is present across the whole Europe, with an average snowmelt of less than 1 mm/ month (12 mm/year) for most of Europe. The data are shown in Map 19 and Map 20 respectively. In the future, snow water equivalent retrieval from remote sensing is expected to provide standard products which will make the ones presented here obsolete.

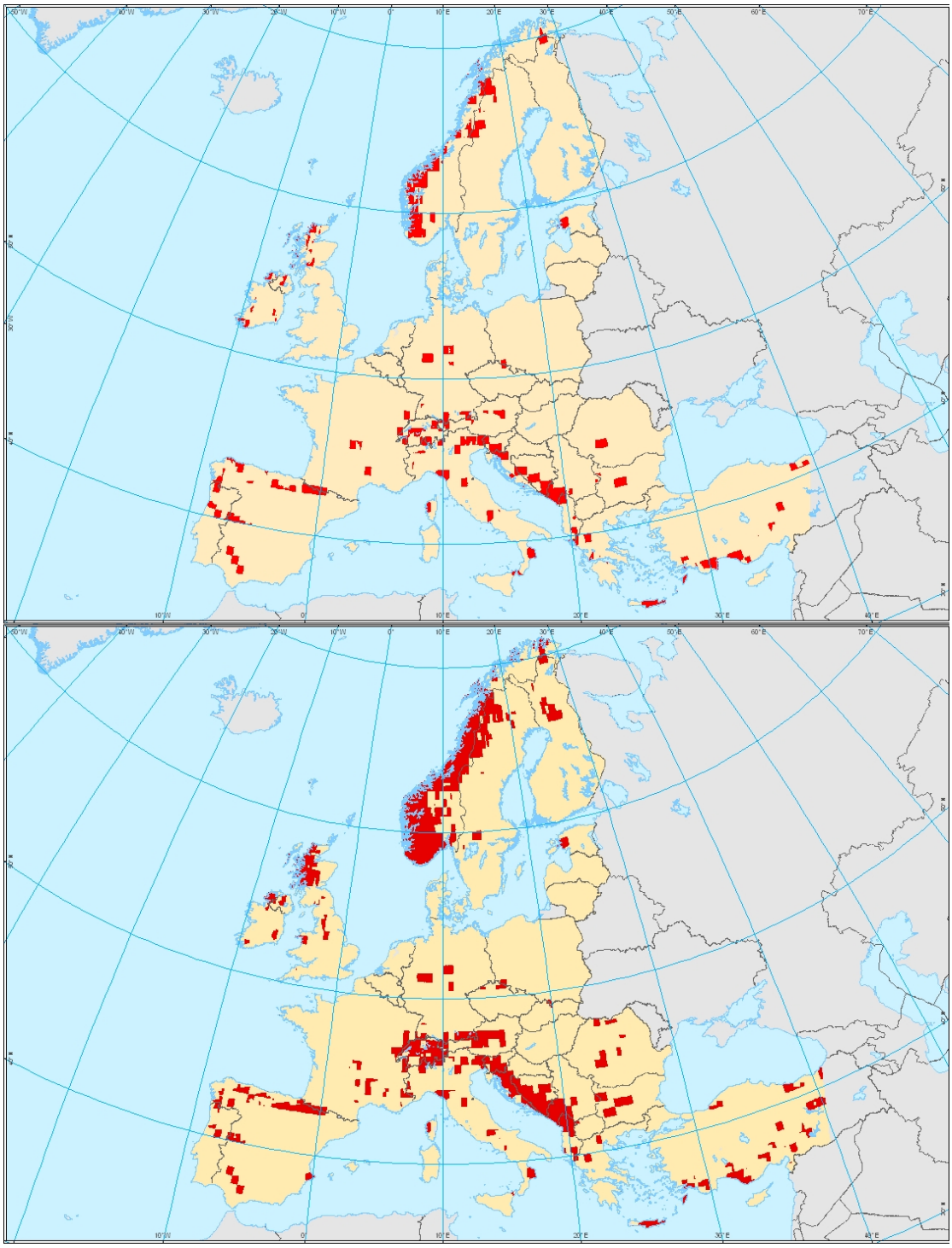

Figure 5- Areas with precipitation less than runoff: above, New et al., 2002; below: MARS dataset

Atmospheric transport: Source-receptor relations, Source-receptor time of travel.

A source-receptor relation is a map providing for each point in the computation domain a value of concentration that would result from a unit emission from a give source. A source-receptor map is required for each emission source to be considered. At present, source-receptor relations have been developed within the context of the ADEPT model (Roemer et al., 2005) and are available for emissions represented as national totals for all European Countries. The resolution of these maps is 0.25° (approximately 30 km) and these can be used under the assumption that emissions are distributed according to population density. This assumption can be limiting for the region near the source, as many emissions (such as pesticides) actually follow other emission patterns. However, at a sufficient distance from the source the differences tend to attenuate.

Another limitation in the annual averaged source-receptor approach of the ADEPT model appears neglecting the sub-monthly variability of atmospheric processes, which have a time scale of a few days as a maximum in continental Europe.

As an example, Figure 6 and Figure 7 provide maps of the source-receptor relation and time of travel for France and Italy. The same type of data is available for all European countries through the ADEPT model.

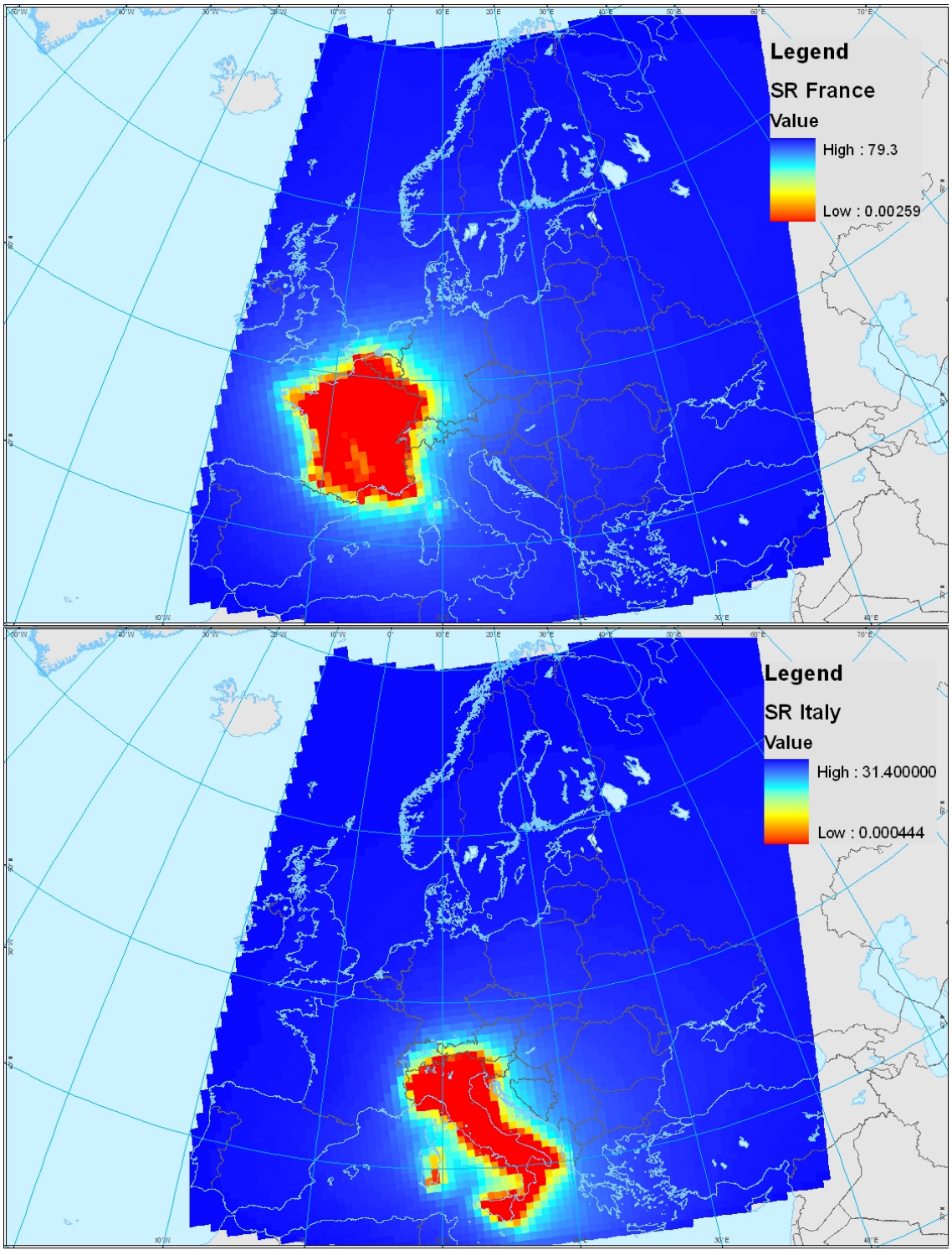

Figure 6– example source-receptor maps for France and Italy.

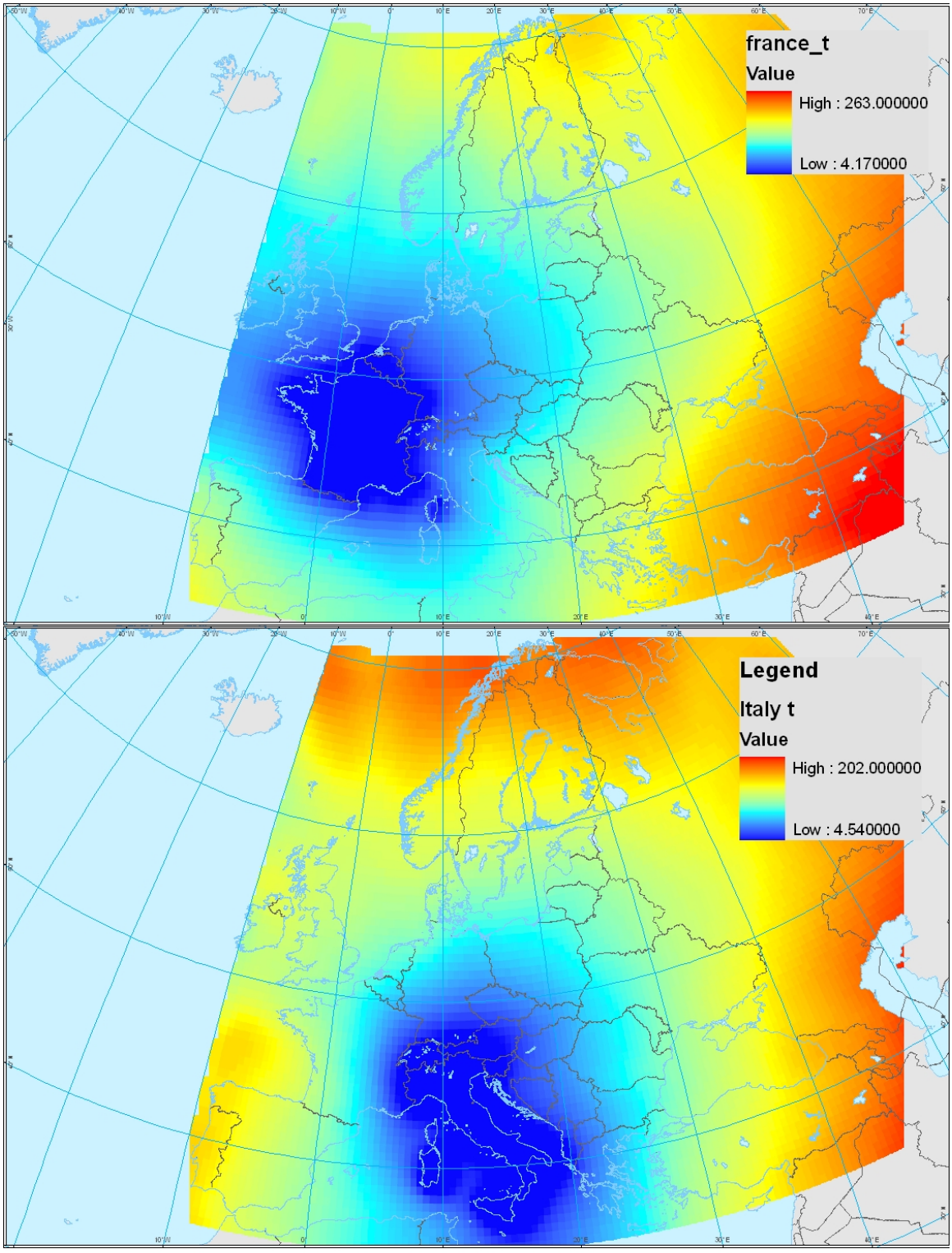

Figure 7– example time of travel maps for France and Italy.

Surface water parameters

River discharge Q

The Global Runoff Data Center (GRDC) estimates total runoff values at monthly time step (Fekete et al., 2000). These can be used to estimate river discharge Q virtually at any point, using a flow accumulation function. This way to estimate river discharge is robust with respect to spatial scale and to the size of the rivers, as shown in Pistocchi and Pennington, 2006.

Reported and computed values of discharge at selected locations, following the European Environmental Agency (EEA) Waterbase, and GRDC station data are normally within a factor of 2 (Pistocchi and Pennington, 2006).

It is helpful to notice that a rigorous comparison of GRDC point discharges with a flow accumulation computed on the Hydro1k grid is not possible due to the coarse scale georeferencing of the gauging stations. So, an interpretation of the results has been necessary.

Also, the river network considered for the evaluation of computed discharges was obtained from hydrologic processing of the digital terrain model, which leads to inaccuracies in the location of the channels.

Both factors induce the need to perform a careful interpretation of the data, while comparing computed and reported values.

The following figures show examples of the kind of interpretation required in a few cases, and highlight how the whole analysis is oriented to the mere capturing of large-scale trends, while for local or regional model applications a better insight from more refined sources can be looked for.

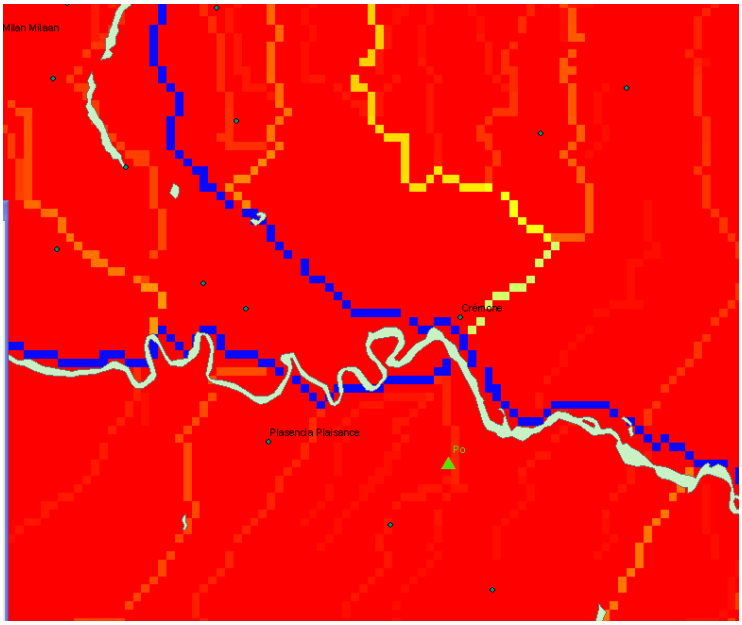

Figure 8– overlaying of the drainage network derived from hydrologic processing of the Hydro1k data set, with a vector map of water bodies obtained from Lehner and Doell, 2004. The example refers to the Po river between Milano and Piacenza, Italy.

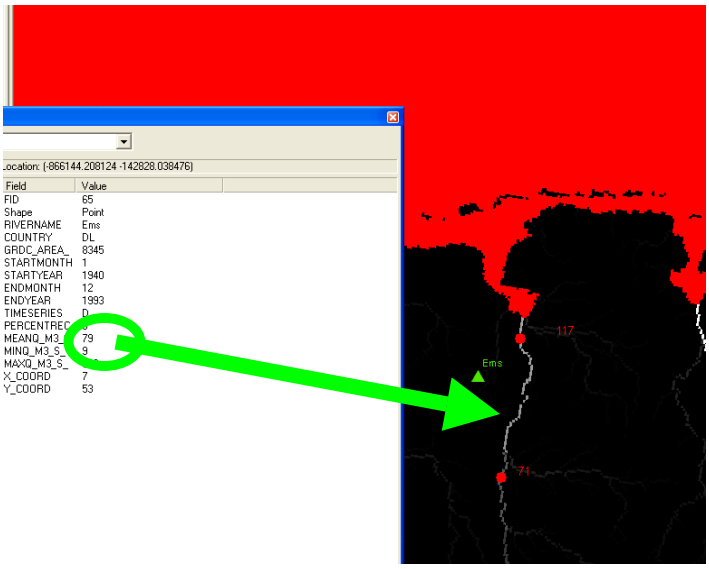

Figure 9 – in the example, the Ems river station (Germany) reported by GRDC has average discharge of 79 m^3/s. Although the location is imprecise, the value compares favourably with the computed values of 71 and 117 m^3/s, upstream and downstream of the gauging station respectively.

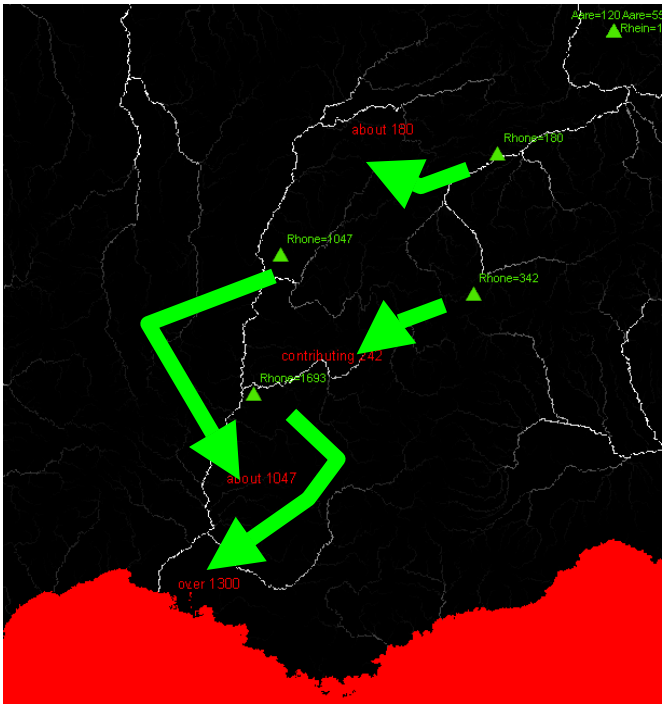

Figure 10– Comparison of GRDC-reported and computed values for the Rhone, France. It is apparent that the locations of the gauging stations are shifted northward, while considering stretches of the river network more to the South would substantially improve the match of the values.

The mean monthly runoff reported by GRDC is represented in Map 20, while Map 21 shows their coefficient of variation. As it can be observed, the pattern is in good

agreement with the one reported by the EEA Atlas http://dataservice.eea.eu.int/atlas (Rees et al., 1997) as shown in Figure 11.

In comparison with EEA-reported values, GRDC underestimates runoff in low runoff regions such as the eastern Iberian peninsula, and part of the Balkans (where it assigns zero runoff).

It must be said that the GRDC estimates represent at present the best available figures of total water fluxes eventually reaching the stream network. For this reason, they are to be seen as fixed points for the setup of a continental scale water budget. The coefficient of variation of monthly values of runoff identifies areas where significant temporal variability appears. One can observe that discharge variability tends to be higher in Northern and Eastern Europe, where seasonal patters such as snowmelt appear, and in arid regions of southern Europe. Also, larger rivers tend to show lower variability apparently because of the modulating effects of large watersheds, while the patchy appearance of Map 21 reflects the spatial resolution of runoff estimates. In general, variation is about 10 to 300 % of annual mean and it is appropriate to consider monthly values.

An example of discharge map is provided in Figure 12. This parameter is also represented at monthly levels.

River slope

River slope can be in principle estimated from digital elevation data nowadays increasingly available with finer and finer resolution, but this would require intensive processing of large amounts of data. At present, it has been preferred to estimate slopes based on large-scale topography as derived from the GTOPO30 digital elevation model (DEM) (http://edcdaac.usgs.gov/gtopo30/gtopo30.asp). This allows to compute generic slope that can be used to assign guess values of river channel slope through linear stretching. Assuming that slope adjusts to a negative exponential equation, it has been chosen to compute channel slope in every point of a certain basin as:

$$slope = k \times z_0 \times e^{(-k \times x)}$$

Where z_0 is maximum altitude for this basin, x is the length of the flow upstream to each point, and k is a topographic constant that depends on the maximum difference of altitudes within the basin and the maximum length of the flow according to the formula:

$$k = \frac{\ln\left(\frac{z_{max}}{z_{min}}\right)}{L}$$

where z_{max}, z_{min} and L are the maximum and minimum elevation and maximum flow length of the catchment, respectively. Figure 13 provides an example of river slope in the Po river basin for rivers.

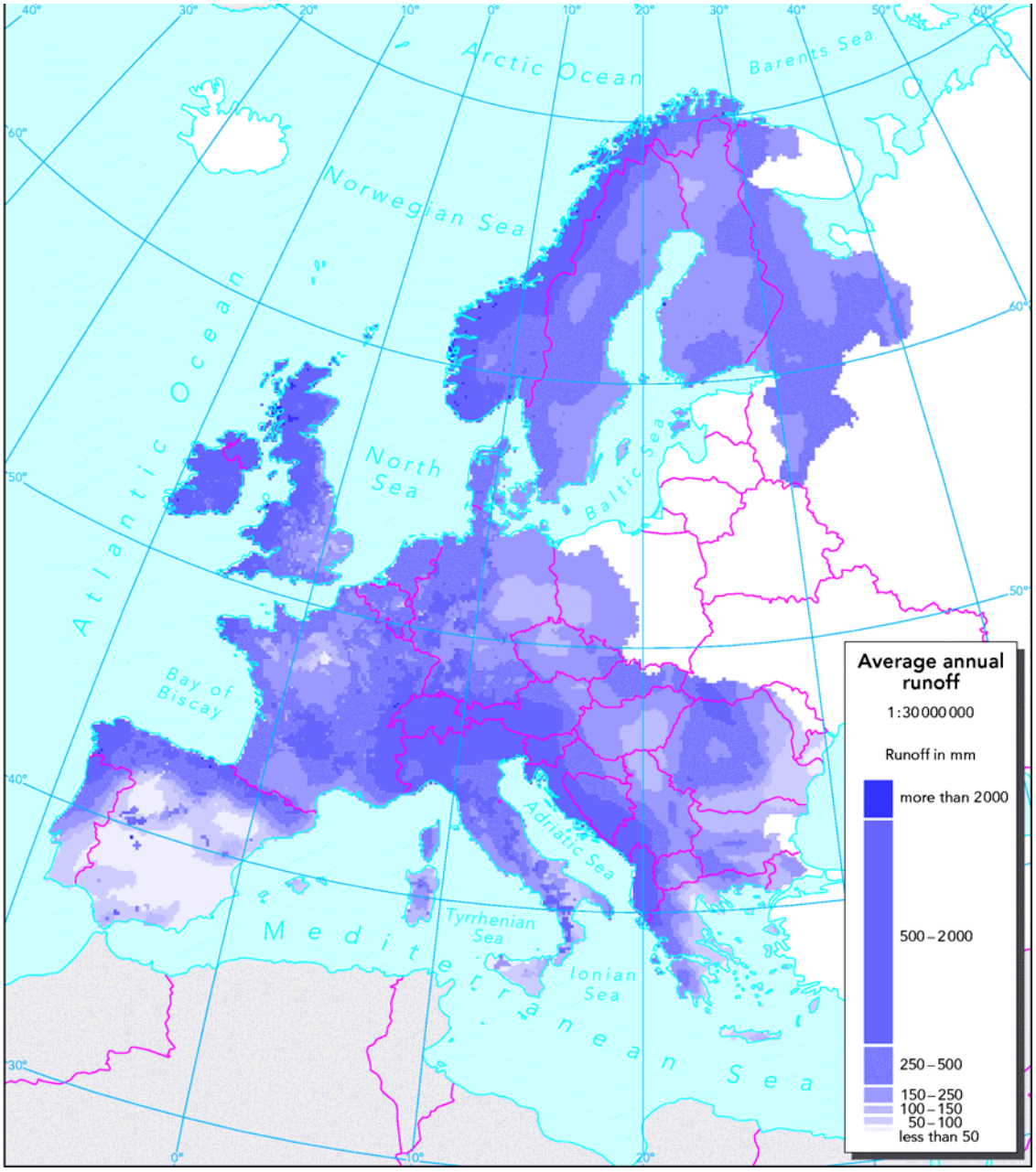

Figure 11– runoff distribution from the EEA Atlas: http://dataservice.eea.eu.int/atlas (Rees, 1997)

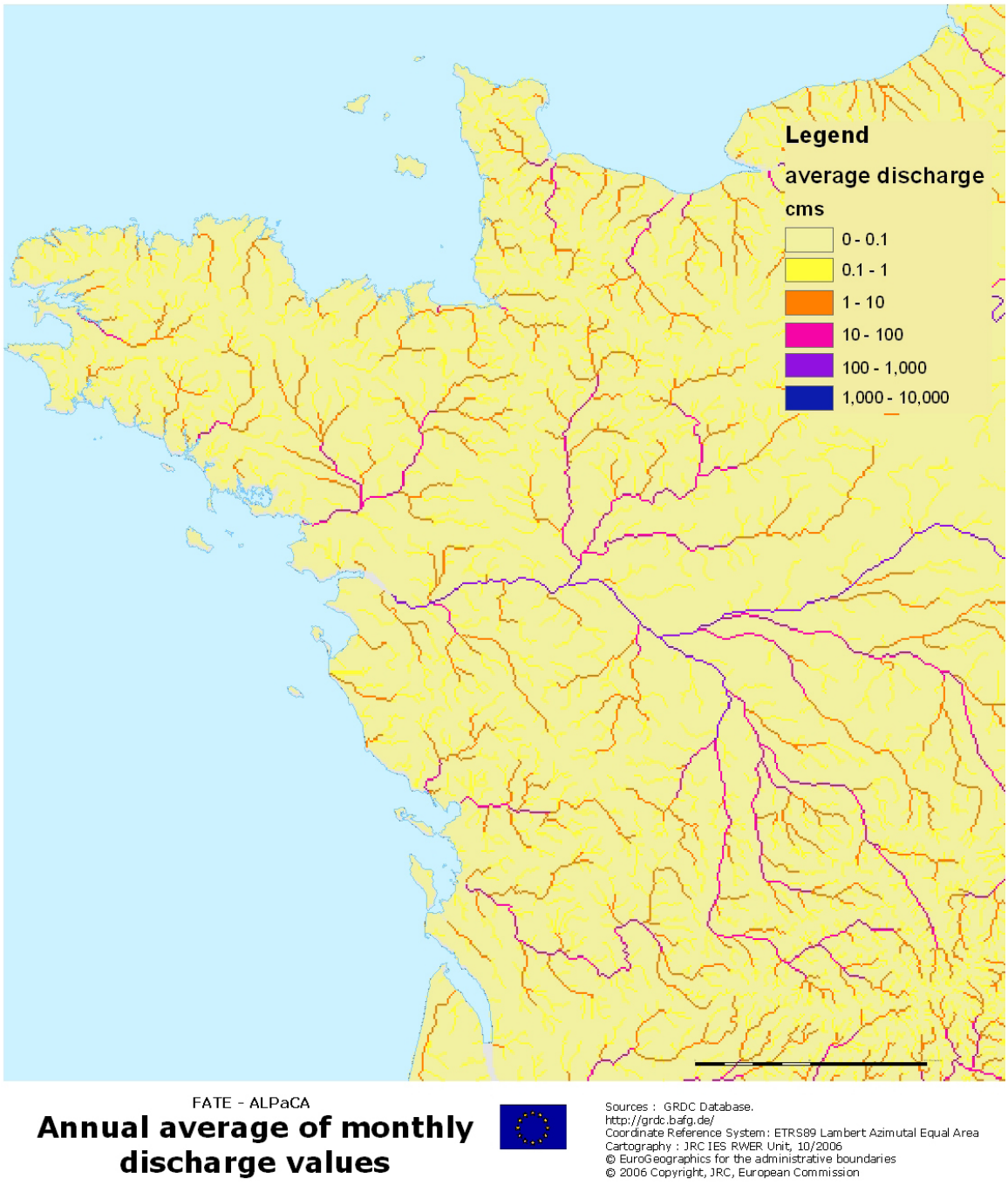

Figure 12– example map of discharge in rivers for rivers in France

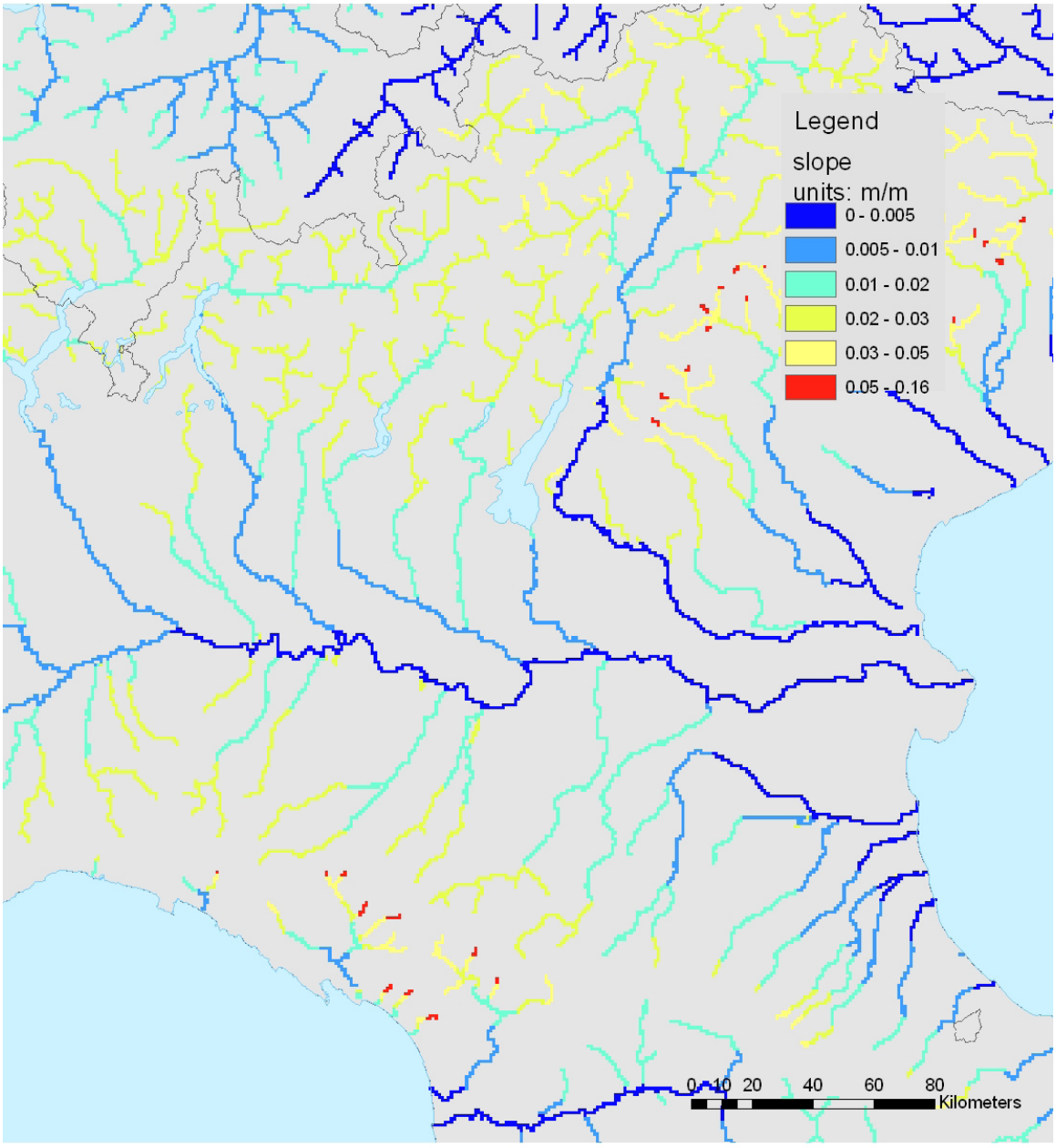

Figure 13– example map of slope in rivers in Italy

River width

Based on annual average river discharge Q, Pistocchi and Pennington, 2006, propose an estimate of river cross section width W according to the formula:

$$W = 7.1\ Q^{0.539}.$$

An example of map of width computed with this formula, for rivers, is provided in Figure 14.

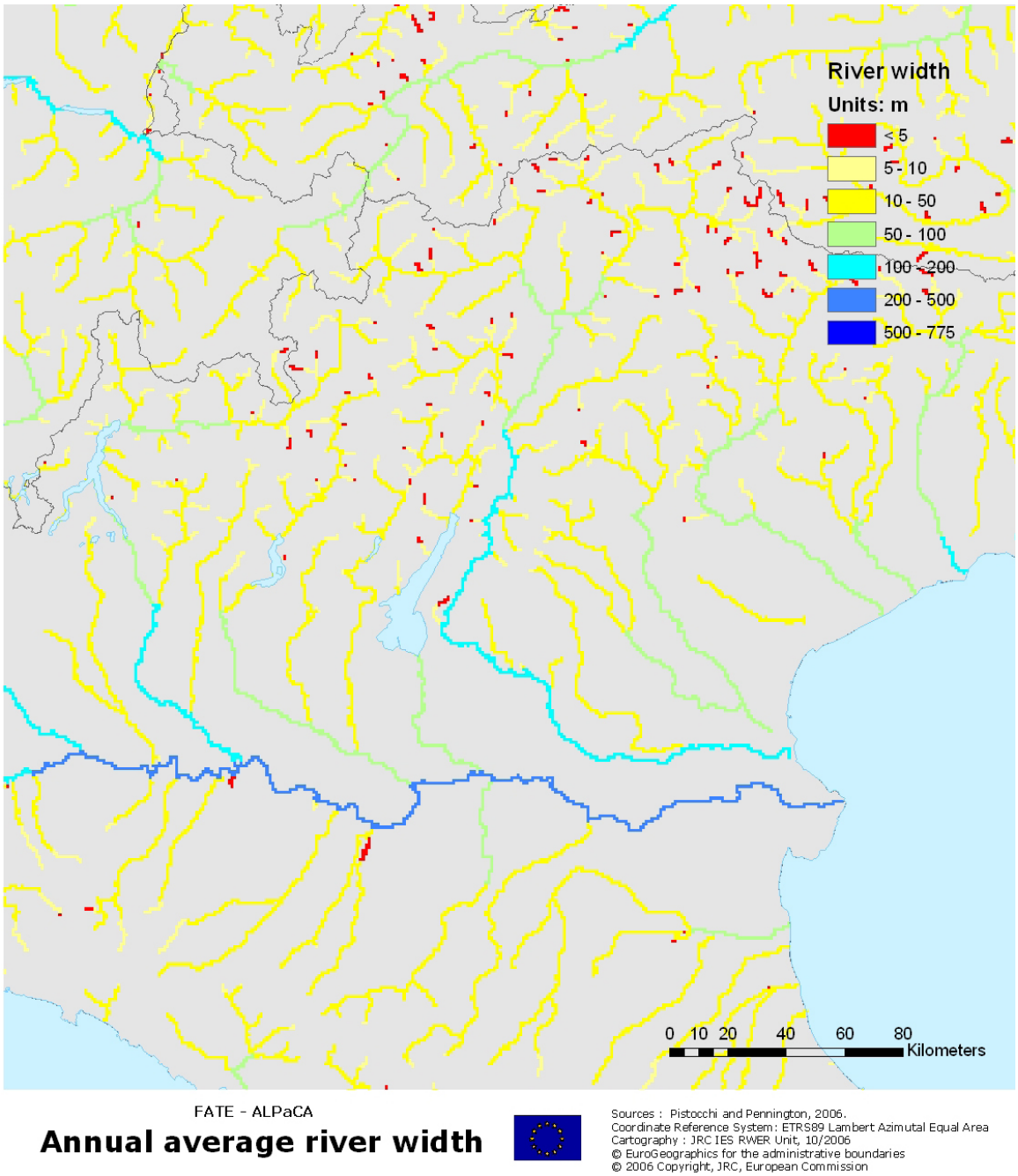

Figure 14– example map of width in rivers

The process of computing width from discharge is comfortable and provides a generic trend across the continent. However, better estimates can be obtained using the information sources on the Internet, such as the MapMachine of National Geographic, or Google Earth. The following picture shows a screenshot of the National Geographic MapMachine (http://mapmachine.nationalgeographic.com) that allows to display aerial and satellite imagery of the Earth, and take measurements. The example is referred to the Po river, Italy, at Piacenza.

The co-referencing of river width and annual average discharge cannot be done in a rigorous way, as the information sources on the Internet cannot be overlaid to other data. For this reason, a qualitative identification of precipuous points is required and can be done by referring to the peculiar points of the river network, such as junctions or large scale river meanders that are preserved by the 1-km grid of the flow accumulation computed on the GTOPO30 DEM.
The following picture provides an example of how a stretch of the river network in the UK is identified.

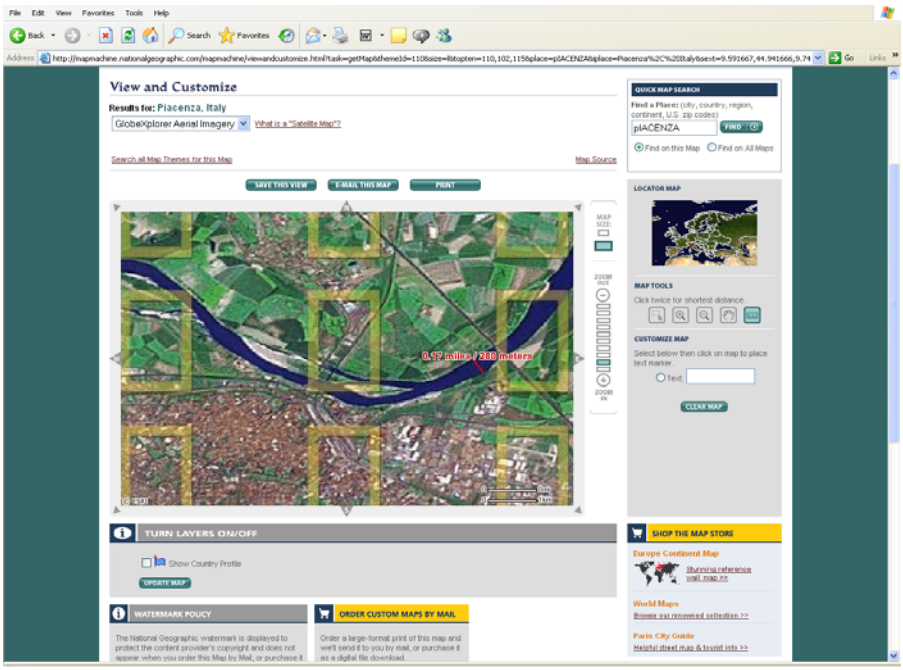

Figure 15- Satellite imaginery of the Po river at Piacenza.

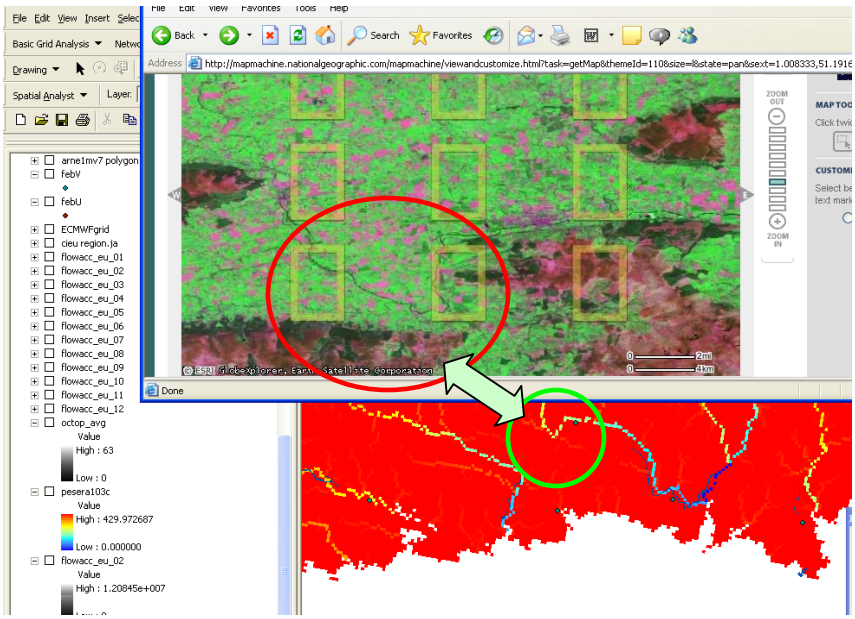

Figure 16- Example of identification of stretchs in river network

Water velocity, Water depth

Water velocity V and depth h for running waters can be described on the basis of river discharge Q, river cross section width W and slope J according to Manning's equation where n=0.045 s $m^{-1/3}$ (Pistocchi and Pennington, 2006):

$$V = 6.43\ W^{-2/5} Q^{2/5} J^{3/10}$$

$$h = 0.16\ W^{-3/5} Q^{3/5} J^{-3/10}$$

Using this estimate of J, W, and Q, one can compute annual average river depth.
An example of this calculation is given in Figure 17.

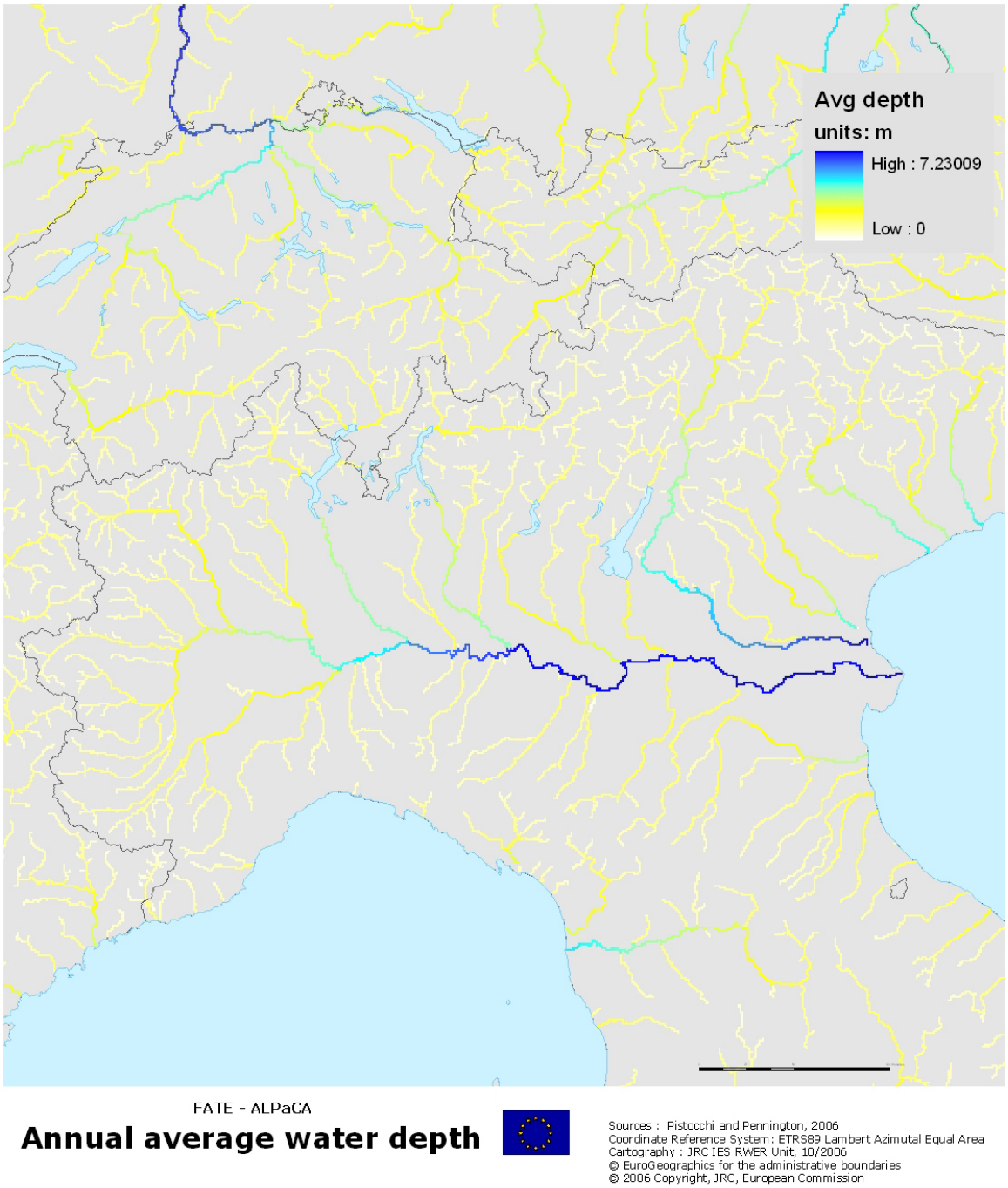

Figure 17– example map of depth in rivers

Velocity can be estimate in the same way. The pattern coming from our calculation shows an increase in velocity with slope, that is a weak trend in decrease in the downstream direction. This is not fully realistic according to Leopold and Maddock, 1953, and subsequent observations, but it is intrinsic in the theoretical assumptions made in Pistocchi and Pennington, 2006. In general, however, the trend is weak and velocity tends to assume a rather constant value, unlike depth which is more variable
Depth can be estimated at a monthly step using the discharges obtained from GRDC.
Examples of maps of velocity for rivers are provided in Figure 18.

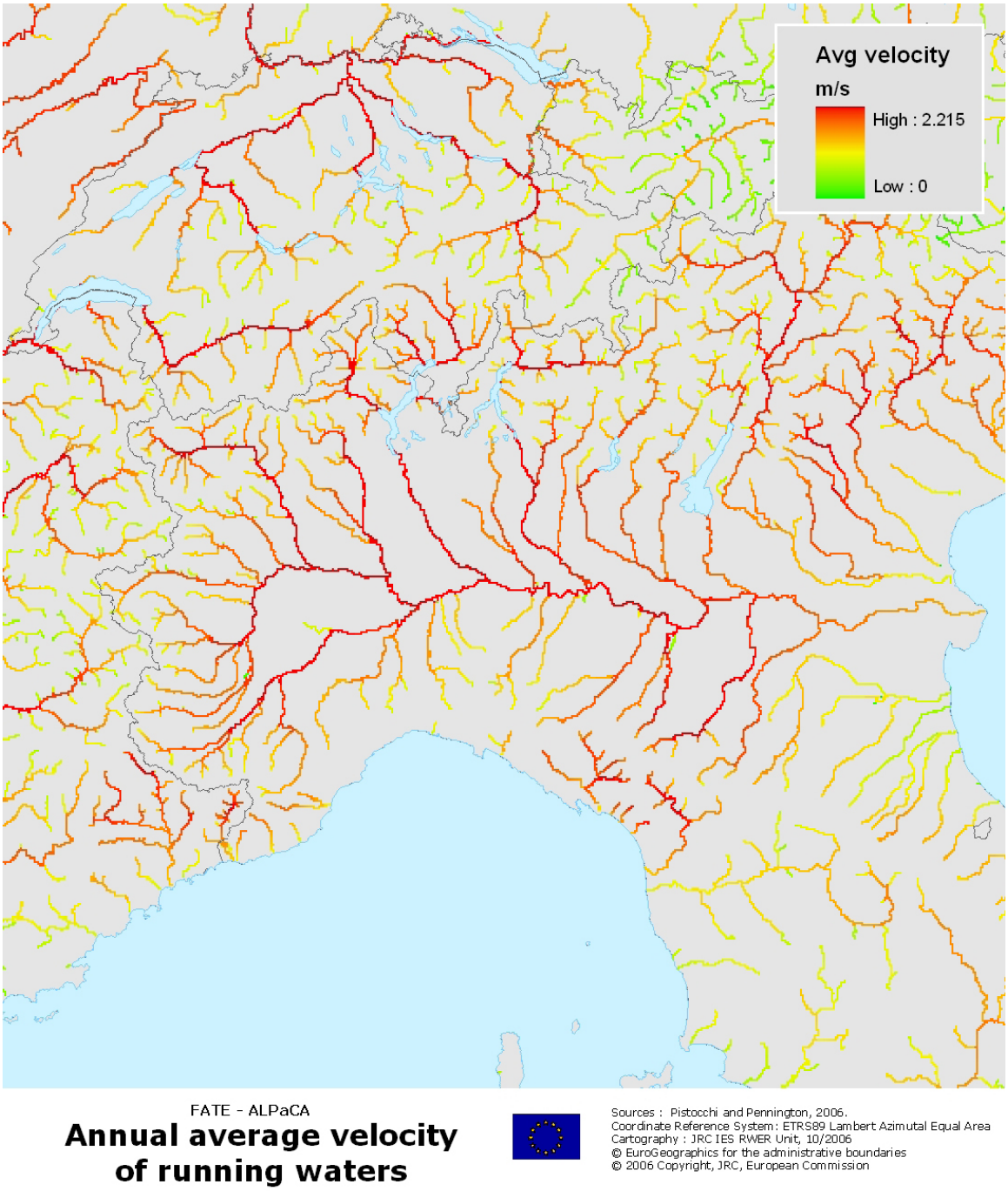

Figure 18– example map of velocity in rivers

Suspended sediment concentration

At present, suspended sediments are not mapped in a consistent way throughout the continent. Also, this parameter has high inherent variability. So far, the only possibility that has been tested is the technique outlined in Pistocchi, 2005, p. 38, based on a published work by Hakanson et al., 2005. the results are plotted in Map 22.
Although further testing is required, it can be observed that the pattern follows reasonably the one of soil loss risk for water erosion as discussed in a following section. Also, the method allows distinguishing between shallow and deep lakes across the continent.

Sediment organic matter content

This variable cannot be described at present through a spatial distribution due to a substantial lack of data. However, as it represents a relevant parameter for the fate and transport of chemicals, it is worth considering future research on the topic.

Surface water residence time

Surface water residence time can be computed once the geometry of water bodies and throughflow are known.
In general, average hydraulic retention time is defined as the volume to throughflow ratio.
In the case of rivers, it coincides with the length to mean velocity ratio. From what outlined above, storage volume in running waters and retention time can be also computed directly as the product of river width W and depth h.
For lakes, an estimate of mean depth, hence storage volume, can be drawn from existing reported values.
These values can be retrieved from the ILEC database (http://www.ilec.or.jp/) and from the EEA Waterbase related to lakes (www.eea.eu.int). However, Pistocchi and Pennington, 2006, point out that this description may be incomplete for many regions of the continent, where small lakes build up altogether relevant storage volumes. The Authors propose then an estimate based on topographic features.
From the following figures, it is apparent how much a more detailed representation of lakes adds to the overall understanding of surface waters retention time. Although the main lakes are represented in reported sources, there is a massive presence of lakes in certain areas, such as Northern Germany and Poland, Spain, Scotland, and Scandinavia (Figure 20), which is not captured by bibliographic sources. Its role in defining retention time needs an assessment that can be performed at the screening level using the proposed approach.

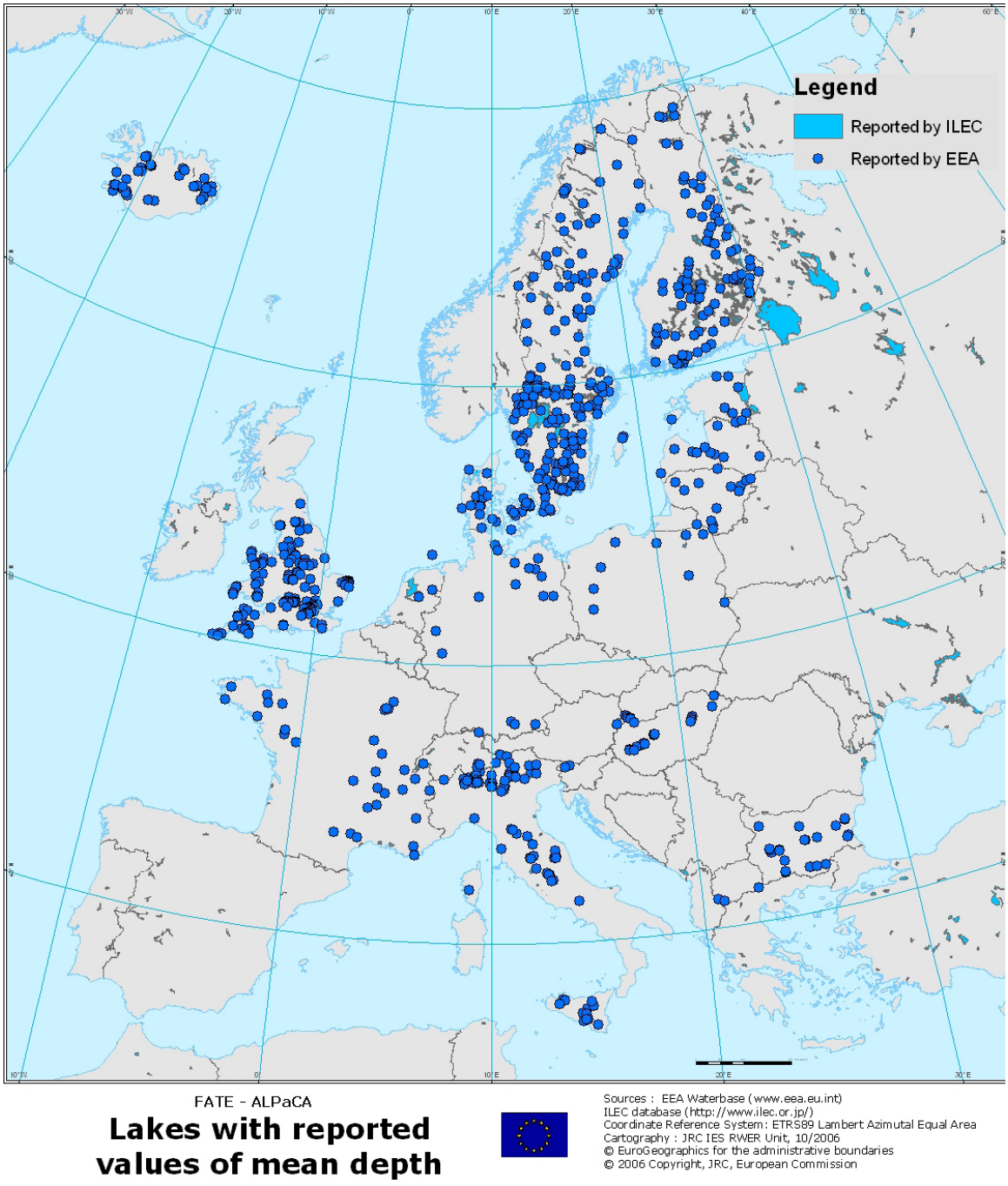

Figure 19 – lakes for which a mean depth is reported by EEA (dots) or ILEC (polygons)

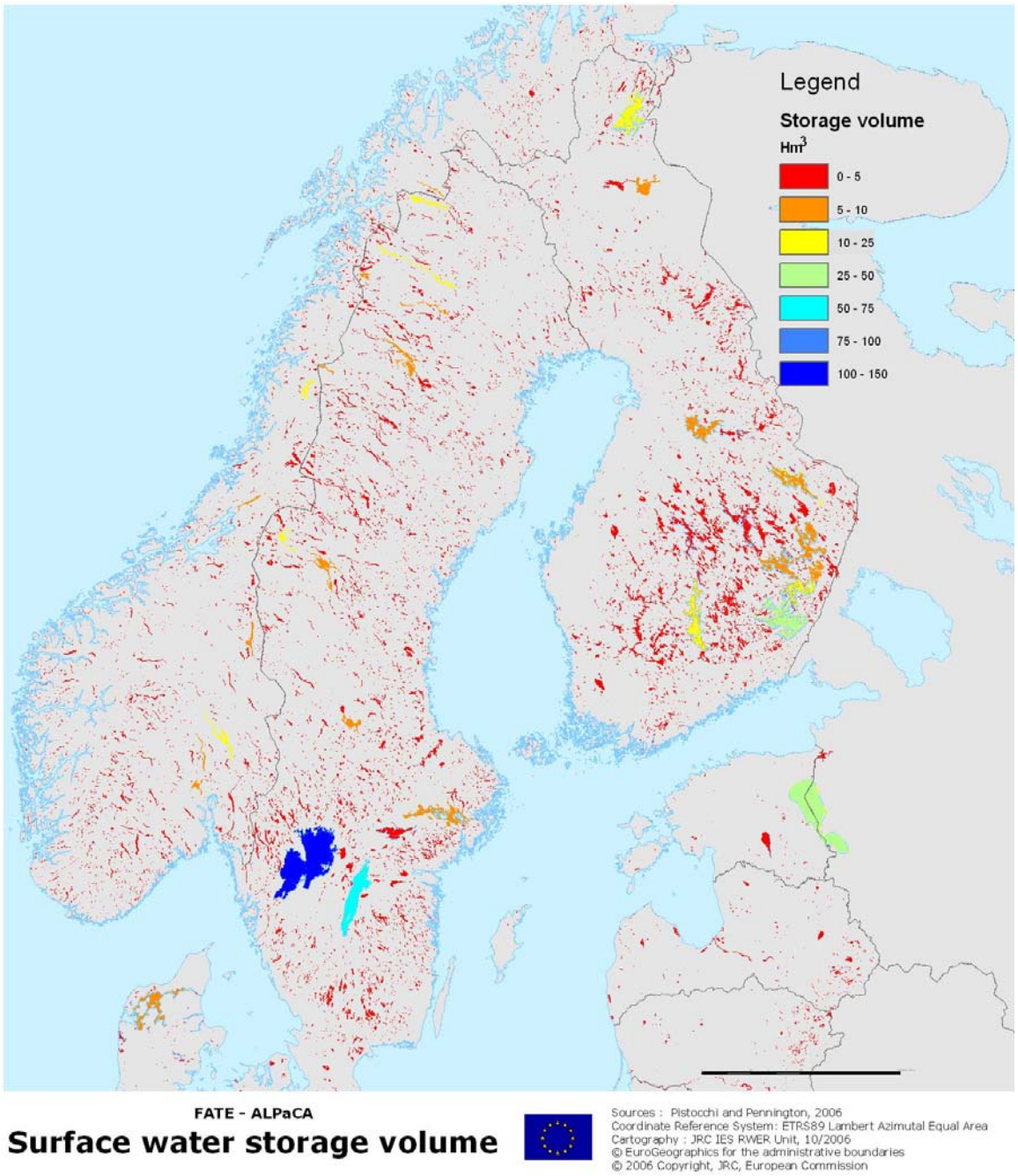

Figure 20 – computed lake volume for lakes in Scandinavian peninsula, according to Pistocchi and Pennington, 2006.

Reservoirs also play a relevant role in the definition of surface water residence time. Estimates of reservoir volumes can be taken from the GLWD data set (Lehner and Doell, 2004; http://www.worldwildlife.org/science/data/globallakes.cfm) that reports values given by the ICOLD (International Commission on large Dams). Reservoirs play a role in the Iberian peninsula, Scandinavia and Finland (Figure 21).

Figure 21 – ICOLD reservoirs with volume in Scandinavian (above) and Iberian (below) peninsula

Throughflow can be computed as the zonal maximum value of annual average discharge, evaluated across the lake area. This is equivalent to assuming that the lake has a single outflow section. The approach has proved to work reasonably in comparison with reported hydraulic retention times (see Pistocchi and Pennington, 2006). Map 23 shows the result for Europe.
The above data allow to compute the surface water retention time for continental Europe.
In principle, this can be done at the monthly time step, but given the uncertainties it seems preferable, as a first approximation, to refer to the average annual conditions. This is particularly appropriate for the case of lakes, where, in case of large compensation volumes, seasonal variations can be regularised.
The strategy to estimate surface water retention times includes the following steps:

1) Compute lake retention time

Reported values of lake mean depth were collected from ILEC and EEA. When both sources were reporting a value, ILEC was preferred, as from the sample considered EEA data appeared less correct.
Reported values of reservoir mean depth, from ICOLD, were taken from the Lehner and Doell, 2004, data set. All other lakes included in the Lehner and Doell data set, when not associated with a mean depth, received a value estimated using the algorithm by Pistocchi and Pennington, 2006.
Lake surface area was measured directly from GIS. The product of surface area and mean depth provides the volume. The ratio of volume on throughflow provides the mean hydraulic retention time of lakes.

2) Compute river retention time

The retention time of rivers is given by the cell length divided by mean river velocity. In this case, no effort has been spent in separating the case of diagonal or straight flow (the former being approximately 40% longer than the latter) as tortuosity within the grid cell was not included. Grid cell size was set to 1 km.

3) Compute a combined retention time map

In order to have a map with the retention time referred to a single grid cell, a lake mean velocity is required. This involves the estimation of water path lengths within the lake. Although this can be done in principle, the uncertainty associated with such operation is rather high and the principle of Occam's razor suggests to assign each lake a single mean pathway length. This has been accomplished as follows:

a. Compute the distance, whithin the lake, to the outlet, hence the lake length

Lake length D is computed as the diameter of a circumference *having the same area as the lake (A)*.

$$D = \sqrt{\frac{4A}{\pi}}$$

b. Compute the lake mean velocity

The lake mean velocity is assumed to be the ratio of lake length divided by lake retention time. Each cell within a lake is thus assigned a constant velocity value.

c. Combine the velocity values of lakes and rivers

In principle, this operation should be done trivially taking the lake velocity within the lakes, and the river velocity outside. However, a strategy has been needed to cope with geometric inaccuracies and inconsistencies of the data set. For instance, grid cells classified as lakes actually lay on rivers, and should be correctly classified as such. This type of error may derive from misclassification of e.g. remotely sensed images in the original data set.
A first criterion has been set in order to establish wether a lake should be considered as such or as a river: this has been identified in the ratio of lake surface area over contributing catchment area. Indeed, lakes with too high contributing catchment area with respect to surface area are likely to be river stretches. From inspection of the data, it has been decided to set a threshold for "lakeship" at the surface/contributing area ratio R ual to 0.01. A fuzzy membership function "being a lake" has thus been defined as:

$$\mu_L = \begin{cases} 1, & R \geq 0.01 \\ \dfrac{R}{0.01}, & R < 0.01 \end{cases}$$

Cases where $\mu_L = 1$ are thus assigned the lake velocity, while for cases where $\mu_L < 1$ the value of velocity assigned is:

$$v = \mu_L v_L + (1 - \mu_L) v_R$$

Using these rules allows to combine in a reasonable way the estimates of lake velocities and river velocities, by forcing misclassified cells laying on rivers to receive the underlying river velocity value, if their likelyhood to be a lake, i.e. membership function, is low.
Having river and lake velocities combined in a map allows to use them as a weight for downstream flow length. Indeed, the weight represents the time required to cross the cell; so dividing the cell length by velocity provides the cell crossing time.
It's worth stressing here that it has been assumed that lake velocities are obtained dividing lake length along the dominant flow direction, by lake retention time.
This assumption implies that for "long" lakes the residence of water particles entering the downstream part of the lake are shorter than the ones upstream. This is in conflict with the assumption of perfectly mixed lake, with uniform retention time. For this reason, the terming "mean lake retention time" must be well understood.

4) time required to sea outflow

As a good indicator for natural attenuation processes of pollutants released to surface water, a map of the time required for discharge to the sea can be drawn based on the above integrated retention time map. The time to sea discharge map, or flowpath retention time, is shown in the following figures and can be calculated either in total terms or for rivers and lakes separately. As one can notice, most of the continent has flowpath retention time in the orders of magnitude 10^{-2} to 10^{-1} years (3 days to 1 month). However, there are regions with much higher flowpath retention time (the Alpine region, Scandinavia and Finland). Also, smaller regions upstream of reservoirs and lakes with high retention time have long retention times. These are scattered through the continent but particularly in the Iberian peninsula, and Greece. Also, many regions are "quick flow path" ones, all along the Continent shoreline.

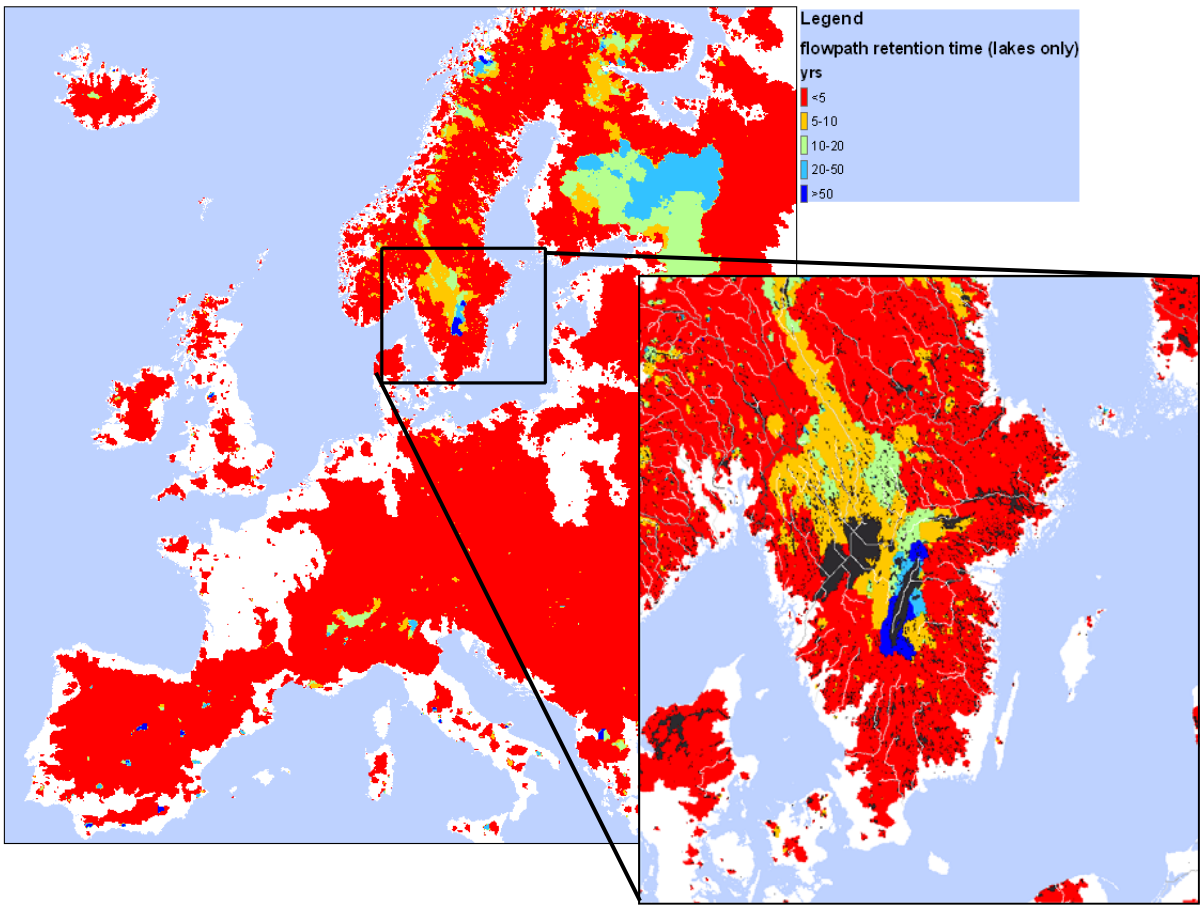

Figure 22 – flowpath retention time, considering only time spent in lakes along flowpaths.

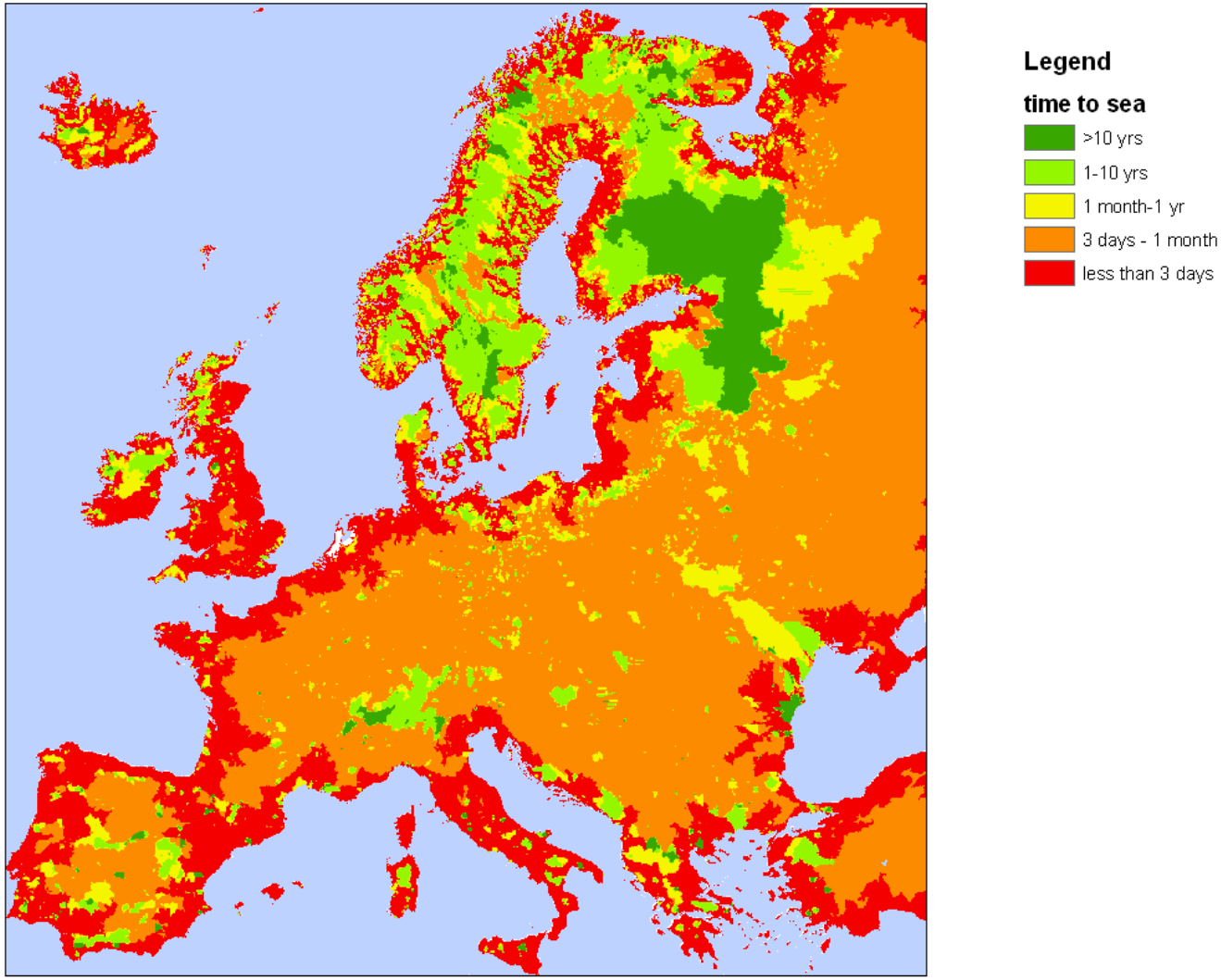

Figure 23 – time to discharge to the sea for Europe.

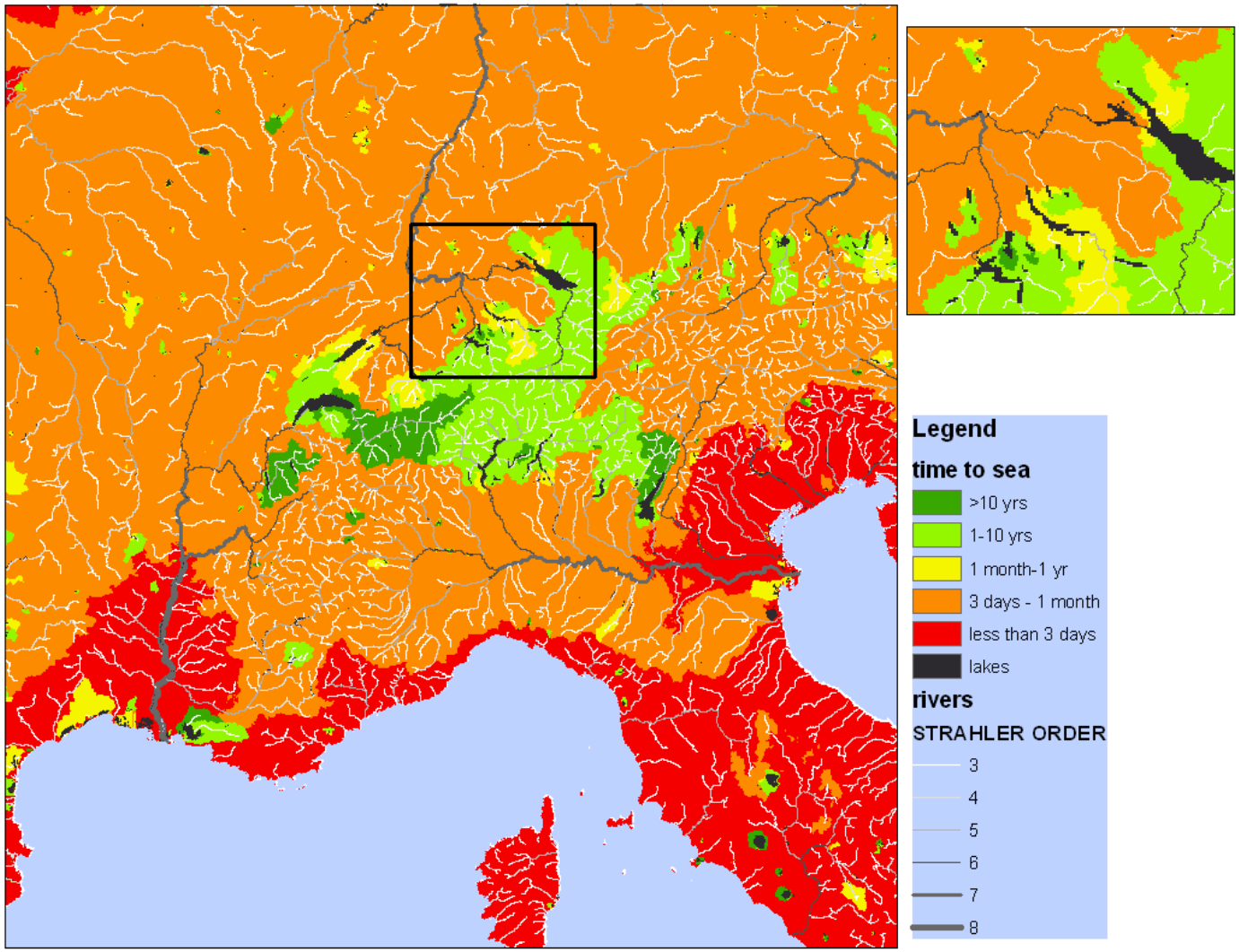

Figure 24 – details on the arrangement of the river network inclusive of lakes, based on the CCM database and Hydro1K digital elevation data.

The reported values provided by the sources considered show frequent errors, and cannot be considered as an "absolutely true" reference. The computed and reported values of retention time are rather dispersed than correlated, but the distribution of errors is unbiased and the average values at the continental scale should be correctly reflected, although no formal proof can be provided at present. The following graph shows the dispersion of the values.

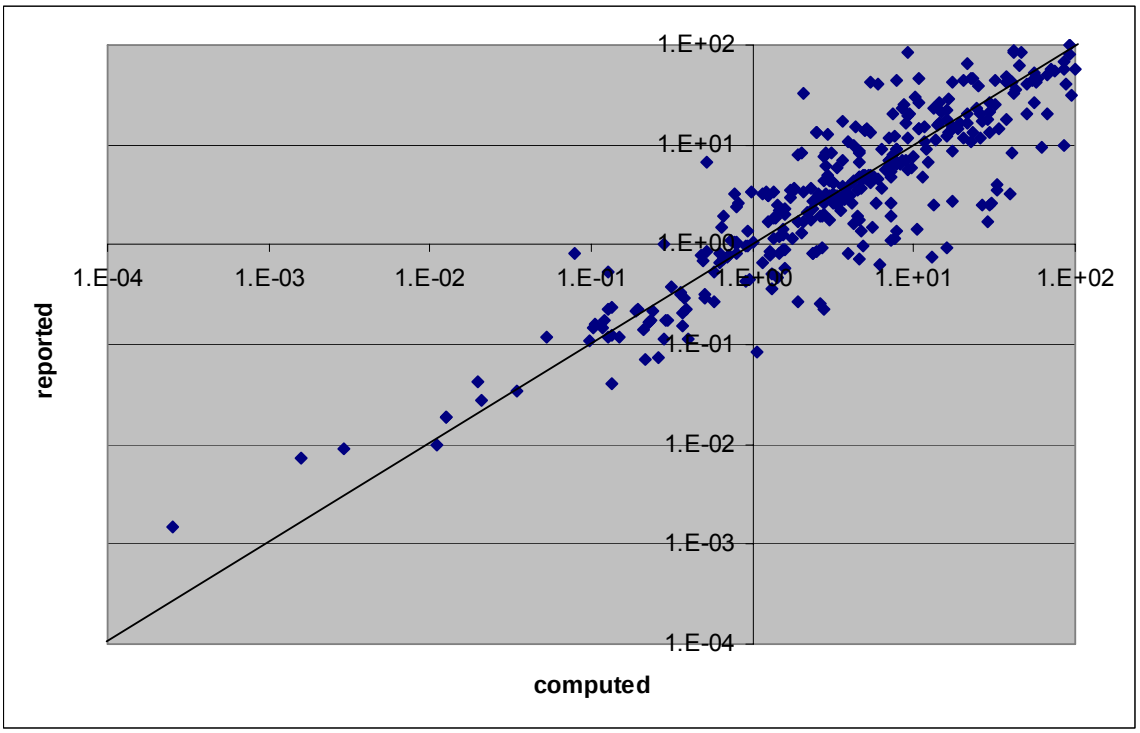

Figure 25 – scatter diagram of the lake retention time values reported from ILEC and EEA, as a function of computed values according to Pistocchi and Pennington, 2006 (values in years).

Soil parameters

Soil properties for Europe are currently best parameterized on the basis of textural data and other categoral information available through the Soil Geographic Database of Eurasia (SGDBE) and associated Pedotransfer Rule Database (PTRDB) (European Soil Bureau, 2004). The two are publicly available tools (http://eusoils.jrc.it) that allow to derive soil parameter values over grid cells of the size of 1 km x 1 km, although it is considered in general that 10 km be the finest resolution at which categoral indications contained in the database maintain a physical meaning (Tiktak et al., 2004).

Although in the SGDBE information is available for both subsoil and topsoil, in the context of chemical modeling it is preferable to refer to the topsoil in that it represents the part actually interacting with the atmosphere and surface waters. Indeed, although the importance of surface-groundwater exchanges is out of discussion, at present no sufficient information is available for continental scale representation of the subsoil and groundwater processes that affect the fate and transport of chemicals, so the principle of Occam's razor favors referring only to the upper part of the soil, assuming precautionarily that water in the subsoil has the same features as infiltrating water. The issue is discussed more in detail in Pistocchi, 2005. In the following, we will refer to the first 30 cm of soil that normally coincide with topsoil.

The degree of saturation of soil porosity in water and, consequently, its air content can be obtained from a soil water balance as a function of soil characteristics (porosity and pore-size distribution, saturated hydraulic conductivity, evapotranspiration and precipitation).
Soil moisture is connected to the soil recharge or dry-up conditions, and the state and flux variables of soil moisture, precipitation, evapotranspiration, and infiltration or runoff are tightly interlinked. Although laminar soil processes are reasonably described by partial differential equations such as Richards' one, and many methods have been proposed to embed into the latter correction terms to account for turbulent or otherwise complex phenomena such as preferential flow in macropores, the local description requires detailed data that are not available at the continental scale.

Traditionally, in large scale climatological studies the Thornthwaite-Mather bookkeeping procedure is often used (Thornthwaite and Mather, 1955). This method consists in the calculation of the water balance for a control volume of soil assumed to retain water up to a "soil water holding capacity", and leaving the excess water through. Inputs to the calculation are precipitation and potential evapotranspiration that can be calculated on the basis of temperature and radiation parameters. This method has the drawback of requiring specifying a water holding capacity of the soil, which is sometimes not free from subjectivity. In addition, the method neglects infiltration excess mechanisms. However, it has been widely implemented in many contexts with reasonable results and represents therefore a standard method.

Lettau, 1969, has proposed a different approach, based on the methods of "evapo-climatonomy", i.e. consistency constraints between energy budget and water budget. Eagleson, 1978, has developed a method based on a simplified probabilistic assessment of the annual aggregated magnitudes of the main physical processes occurring in soils.

In some modeling applications, soil moisture is predicted on the basis of the recharge rate using a soil moisture redistribution model; the approach is found e.g. in the USEPA HSSM model (Charbeneau et al., 1995); see also Chen et al., 1994. For continental scale multimedia modeling, Pistocchi et al., 2006 have developed a simplified method to predict mean monthly soil moisture, based on soil wilting point and field capacity, pore size distribution index, and net precipitation (i.e. precipitation net of actual evapotranspiration and direct runoff). Average monthly soil water content is predicted as a function of net average monthly water input to the topsoil (net precipitation or evapotranspiration); soil matrix pore-size index; saturated, residual, wilting point and field capacity soil moisture.
The necessary input to compute soil moisture includes textural classes, for which average parameters have been developed within the European Soils Database (ESDB) (IES JRC, 2006). Although the variability of properties with texture is rather high, a number of 5 textural classes have been defined. The European soil database contains data on soil mapping units as categoral classes. The aim of the database is primarily descriptive and not oriented to provide crude single values to feed mechanistic models. Hence indications provided concern a range of variation of soils present in the mapping units either as dominant or secondary ones, with no resolution within mapping units about local properties. The textural classes are represented in the following textural triangle.

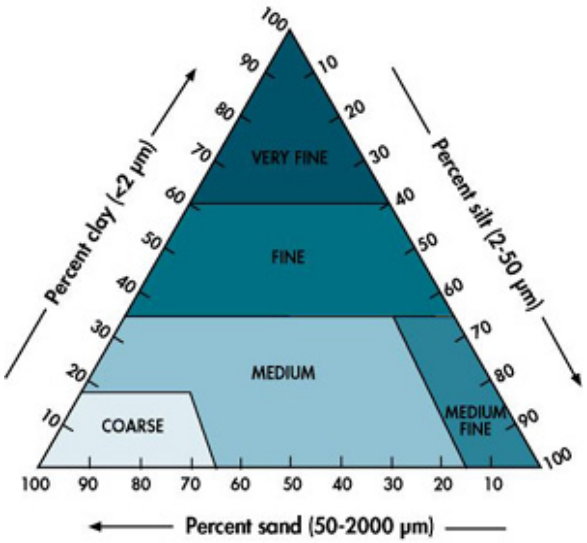

Figure 26 – textural triangle of the European Soil Database
(http://www.mluri.sari.ac.uk/hypres/hypressoil.html)

Map 24 presents the textural classes of Europe. Estimates of representative values of soil hydraulic properties have been derived from the HyPRES database (Wosten et al, 1999) according to textural classes, as shown in the following table.

Although it is more appropriate to refer to site specific information on soil texture in order to get more refined estimates, for continental scale applications it can be argued that using class average parameters instead of pointwise estimates is more robust and better corresponds to the currently available knowledge. In another context, Starks et al., 2002, already pointed out that when knowledge of soil is limited, using textural class-averaged values of soil properties instead of pointwise estimates proves better in simulation models.

Textural class	θ_r	θ_s	α	n	m	l	K_s	*Bulk density* [3]
Coarse	0.025	0.403	0.0383	1.3774	0.2740	1.2500	60.000	1.6119
Medium	0.010	0.439	0.0314	1.1804	0.1528	-2.3421	12.061	1.5147
Mediumfine	0.010	0.430	0.0083	1.2539	0.2025	-0.5884	2.272	1.539
Fine	0.010	0.520	0.0367	1.1012	0.0919	-1.9772	24.800	1.296
Very Fine	0.010	0.614	0.0265	1.1033	0.0936	2.5000	15.000	1.0422

Table 4- soil textural class average hydraulic parameters for the topsoil: θ_r= residual saturation, θ_s= maximum saturation, α, n, m , l parameters of the Van Genuchten model, Ks = saturated hydraulic conductivity

The parameters of the previous table allow to represent water retention curves according to the van Genuchten (VG) model; a pore-size distribution index for equivalent Brooks-Corey (BC) model can be estimated by fitting a power law representing the BC model to the VG one, as shown in the following figure.

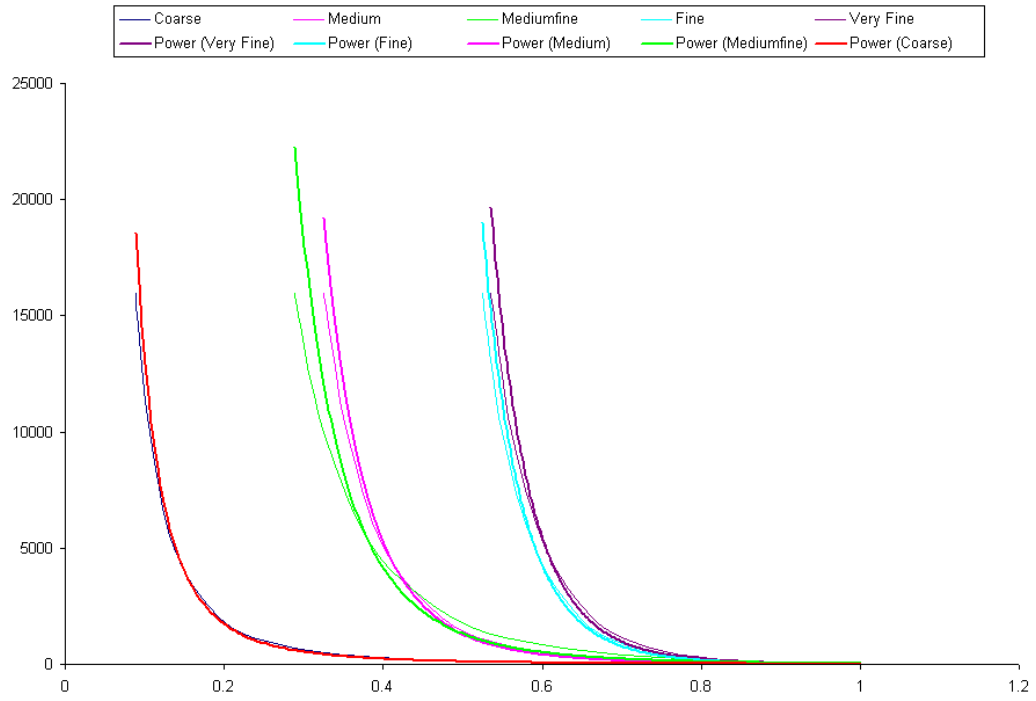

Figure 27 – VG and BC (power) models for suction head (cm) as a function of saturation (-), for the 5 textural classes.

In order to give an idea of the soil moisture distribution in Europe, as can be derived from the above mentioned data, Map 25 reports the average value between field capacity and wilting point for European soils, as computed using the HyPRES database. As this is a quantity depending only on soil texture, it is not representative of climate as the same saturation is not reached uniformly across Europe at the same

[3] Bulk density values are computed here from saturation water content assuming a grain density of 2.7 t/m^3.

time. However, it provides an idea of the spatial variability of the phenomenon under the ergodic hypothesis. The following table summarizes the parameters required to compute soil moisture according to the formula proposed above.

Texture:	#1 Coarse	#2 Medium	#3 Mediumfine	#4 Fine	#5 Very Fine
θ_{FC}	0.294	0.379	0.406	0.472	0.567
θ_{WP}	0.059	0.151	0.133	0.279	0.335
λ	2.92	5.15	6.28	11.12	11.21
η	36.9	33.9	33.2	31.8	31.8

Table 5- soil textural class hydraulic parameters for the topsoil, derived in order to implement the soil moisture model proposed by Pistocchi et al., 2006.

Fraction of topsoil organic carbon

The organic carbon content of soils is also part of the information with SGDBE and PTRDB, in a categoral form. However, for this specific parameter a map for topsoil in the whole Europe has been developed (Jones et al., 2004) and is shown in the following figure.

Soil Bulk density of soils can be parameterized on the basis of textural data and other categoral information available through the Soil Geographic Database of Eurasia (SGDBE) and associated Pedotransfer Rule Database (PTRDB).

However, the information available is rather coarse, as density is classified into 3 classes only, of which 2 cover 99% of soils. For this reason, bulk density is better estimated for the textural classes of Table 4, assuming a grain density of 2.7 t/m^3, as shown in Table 4.

Using soil texture and land cover to predict Runoff, Evapotranspiration, Infiltration

These parameters derive from a soil water balance calculation. For the purposes of continental scale multimedia modeling, the fluxes through soils are distinguished here between runoff, which is the amount of water immediately leaving the topsoil as a response to precipitation ("direct runoff") and the infiltration to the vadose zone. In general, the latter builds up the delayed response of a catchment to precipitation, partly as interflow and partly as groundwater return flow. As it has not been possible to collect sufficient information to build a model for this delayed response, the fluxes in soil deeper than 30 cm are not considered explicitly.

Pistocchi et al., 2006, argue that the variability in runoff within a soil textural class, depending on antecedent moisture conditions and precipitation intensity, is comparable with the variability arising from different land uses on a certain soil textural class. Based on this consideration, they propose a base model reflecting average runoff as a function of precipitation at the monthly step, and a correction factor for reducing or increasing runoff depending on land use. In their approach,

monthly runoff is predicted from monthly precipitation on the basis of the soil texture class, and land use characteristics using a fuzzy logic model combining a linear response with a Curve Number – type model involving a "retention coefficient" to be linked to the capacity of a given land use type to absorb precipitation, a runoff coefficient and storage potential, equal to 0.47 and 400 mm for coarse soil texture, and 0.59 and 250 mm for other textures respectively. The retention coefficient γ is a measure of fuzzy membership (in the sense of Zadeh, 1965) of a given land use type to the class of land uses having high capacity to retain precipitation rather than originating direct runoff. This retention coefficient can be assigned to land use classes based on expert judgment, or considered as a calibration parameter.

There are at least three representations of the land use variability across Europe, that can be considered as patterns for runoff response, namely the CORINE Land Cover 2000 (EEA, www.eea.eu.int), the Global Land Cover (GLC) 2000 map (http://www-gvm.jrc.it/glc2000/), and the PELCOM data set (http://www.geo-informatie.nl/projects/pelcom/public/index.htm).

The GLC2000 represents a reasonable compromise between the very high detail of the recent CORINE 2000 release, and the information in PELCOM which is rather old.

The following figure shows a distribution of the correction factors that allow distinguishing the runoff response between land use types. The two graphs represent Europe and Northern Europe, as available from the GLC 2000 project web site. The two areas differ from each other as long as the classification is concerned. It is important to stress that the aim of this representation of runoff is to reproduce in a sensible way the variability of runoff responses in space, but not necessarily at a location. For this reason, local accuracy of the land use map is not so relevant.

Using these correction factors allows obtaining variability in runoff response that spans the full range one would predict based on a physically based daily time step model, as shown in Figure 29.

Actual evapotranspiration (ET) can be computed as a yearly total according to Turc's formula (Turc, 1953):

$$ET = \frac{P}{\sqrt{\alpha + (\frac{P}{PET})^2}}$$

where:

P = total annual precipitation [mm]

PET = annual potential evapotranspiration [mm];

in most applications, reference is made to the Langbein formula, PET = 300 + 25 T + 0.05 T^3, where T = mean annual temperature [C]. Parameter α is set to 0.9.

Map 26 represents the value of AET computed according to Turc, using P and T as from the MARS data set.

In the future, other strategies can be implemented. For instance, a correction factor to the map of New et al., 2002, can be applied.

As an alternative, Pistocchi et al., 2006 propose a modified form of the Turc's equation, that better reproduces monthly values of actual evapotranspiration.

Both methods have the advantage that they relate this parameter to precipitation and temperature or, in the latter case, potential evapotranspiration. The following figure shows the evapotranspiration map computed according to Turc's formula.

Once computed runoff from precipitation, and evapotranspiration, infiltration to the vadose zone is estimated as the difference between precipitation and the other terms.

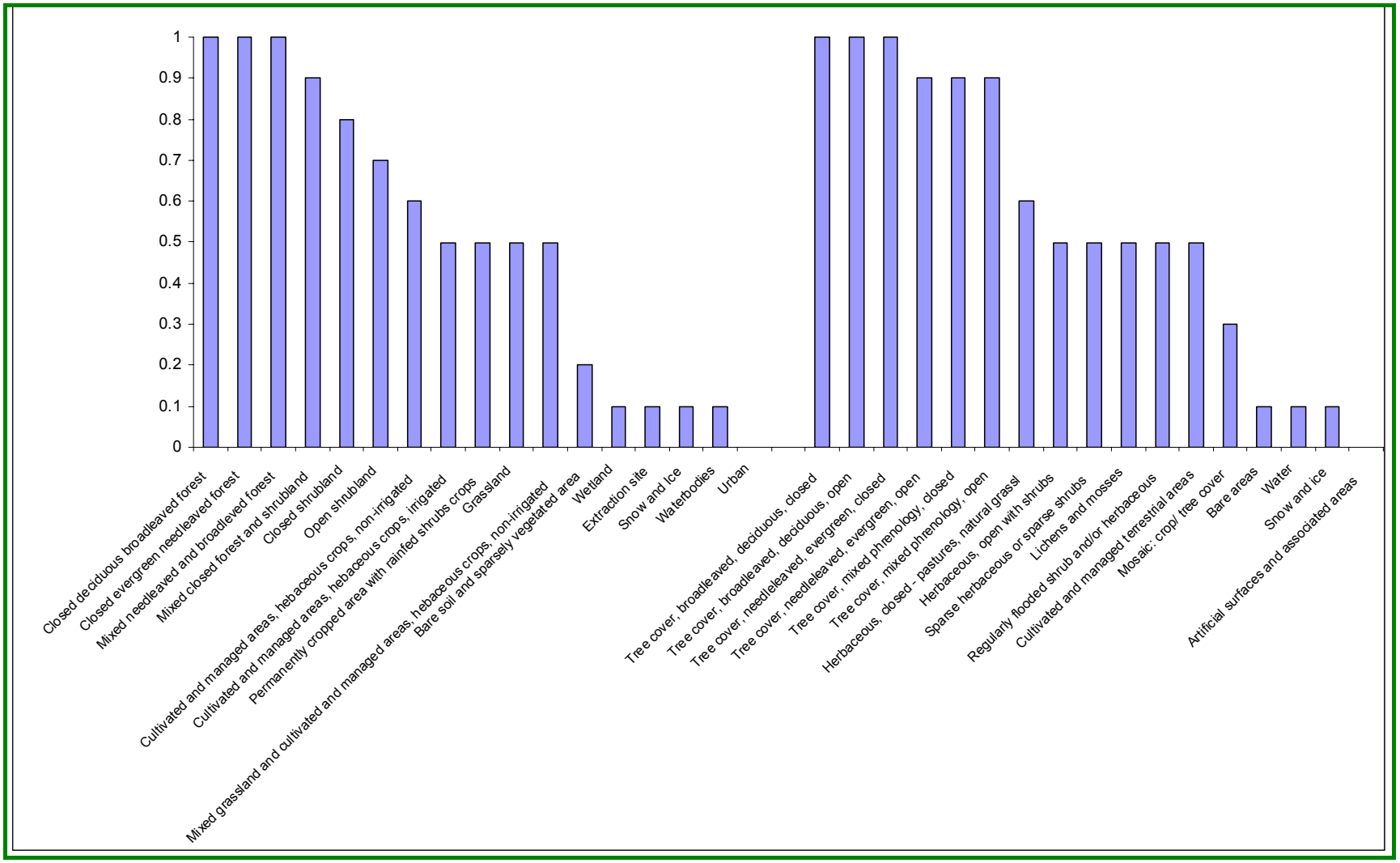

Figure 28– runoff correction terms for NE Europe (right) and Europe (left) according to the GLC 2000 classification.

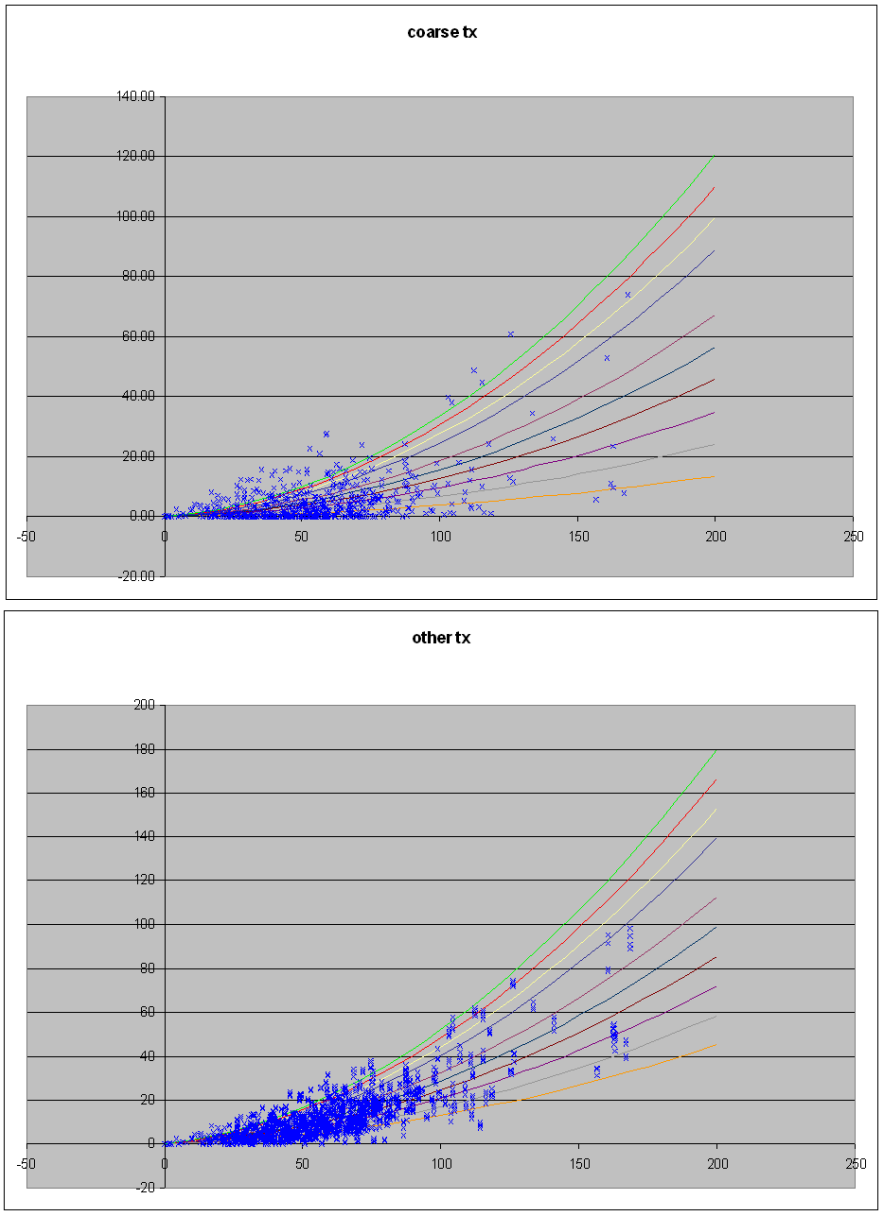

Figure 29– monthly runoff as predicted from a daily step physically based model, for coarse texture and for the other soil textures, as a function of precipitation (data points). The lines represent theoretical runoff response curves proposed for different land use classes, as in Figure 28

Erosion rate

Soil erosion estimates (t/ha/yr) have been made for Europe by applying the PESERA GRID model at 1km, using the European Soil Database, CORINE land cover, climate data from the MARS Project and a Digital Elevation Model. The resulting estimates of sediment loss are from erosion by water. The PESERA model produces results that depend crucially on land cover as identified by CORINE and the accuracy of the interpolated meteorological data.

Soil erosion has proved to be rather difficult to predict at the continental scale, although a map of soil erosion risk for Europe according to the PESERA model has been published officially by the European Commission (Kirkby et al., 2004). Although this map is not always significant locally, nevertheless it provides a reasonable general trend and allows to capture the variability of the phenomenon.

Map 26 – Annual Evapotranspiration according to Turc's formula

Map 27 displays the PESERA model results.

The map is not covering Scandinavia and Finland, nor Switzerland and former Yugoslavian countries outside EU.

Regions outside the covered area can be modeled using a simplified USLE-type approach as shown e.g. by Van der Knijff et al., 2000. The parameters of the USLE model developed by Van der Knijff et al., 2000, are computed on the basis of annual or seasonal rainfall depth, land cover, slope inferred from Hydro1k DEM, and soil texture. Erodibility is also represented by the PTRDB in categoral form as shown in Figure 30.

However, the quantitative estimate of Van der Knijff et al., 2000, which is based on averaged textural parameters, is to be seen as more appropriate for the purpose. The erodibility values estimated by van der Knijff et al., 2000, are reported in Table 6.

Textural class	*USLE Erodibility K (t ha^{-1} yr^{-1} MJ^{-1} mm^{-1})*
Coarse	0.0115
Medium	0.0311
Mediumfine	0.0438
Fine	0.0339
Very Fine	0.0170

Table 6 – erodibility parameters

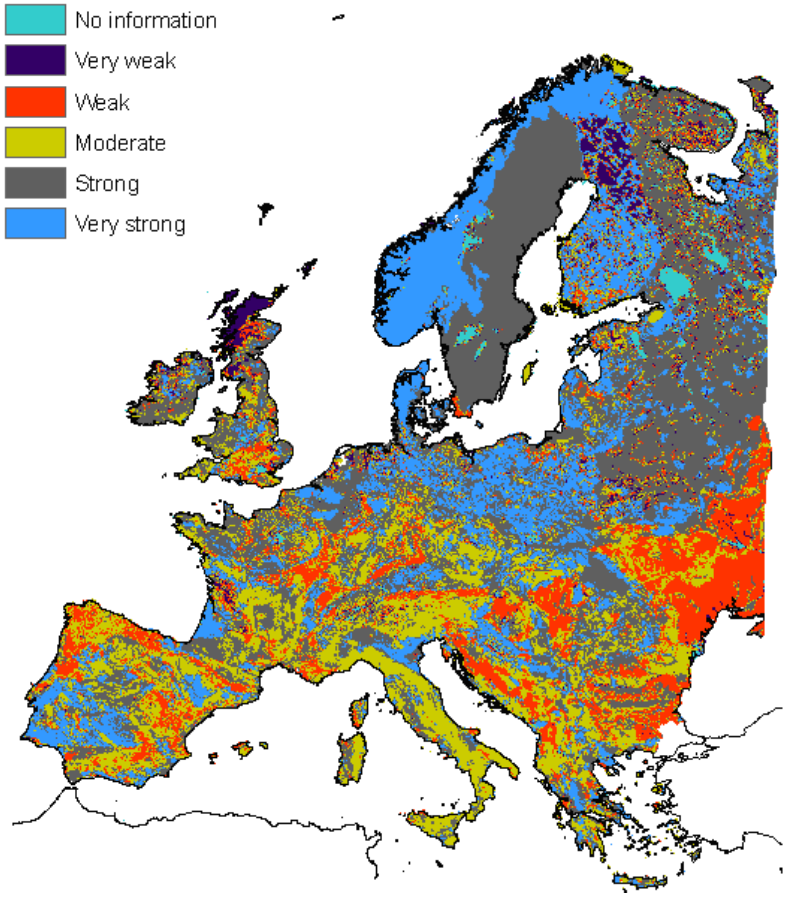

Figure 30 – soil erodibility classes for Europe, according to the PTRDB

Leaf Area Index (LAI)

Leaf Area Index (LAI) is an environmental indicator increasingly used in spatially distributed environmental models to parameterize vegetation. Although a vegetation module is not included explicitly in the fate and transport model conceptualisation by

Pistocchi, 2005, and the vegetation component included in the SIMPLEBOX model is not very influential on the fate results, it is worth nevertheless discussing this parameter here for the sake of completeness. Research on the role of vegetation in the fate and transport of chemicals is ongoing and the availability of parameters for vegetation patterns may be of help in future generations of models. Here we present LAI derived from remotely sensed images. The estimation of accurate allometric LAI values (that is, as they would be measured in situ)is not yet done operationnally in a reliable manner. To bypass a number of difficult issues, the averaged LAI values used here are simply obtained from the SeaWiFS FAPAR JRC product (http://fapar.jrc.it/) as follows (Pinty et al., 2006). An effective LAI, LAI' is given by :

LAI ' = -2. * cos (Sun zenith angle) * Ln [1-FAPAR].

These values are estimated on a monthly basis and then averaged month by month over a six year period. The LAI is called effective in the sense that it refers to a radiative balance. It was shown in Pinty et al., 2006, that these effective LAI values differ from the allometric values by a factor depending on the vegetation structure and spatial heterogeneity inside a given domain.
LAI was processed considering the maximum value of the parameter along the year. The results for Europe are displayed in Map 38. LAI was not defined for winter months in Northerly areas (e.g. Scandinavia) due to the lack of information (snow cover or low radiation).
The ratio of average to peak LAI over the year is about 0.65, with a coefficient of variation of about 10% (ELDAS data sets: http://www.knmi.nl/samenw/eldas/).

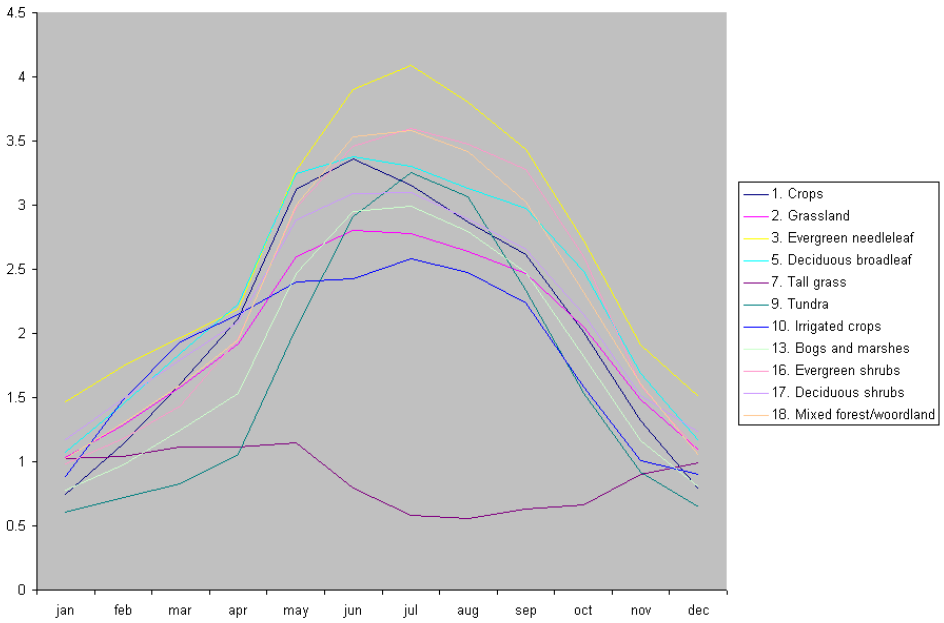

Figure 31 – annual behaviour of the LAI (after ELDAS: http://www.knmi.nl/samenw/eldas/)

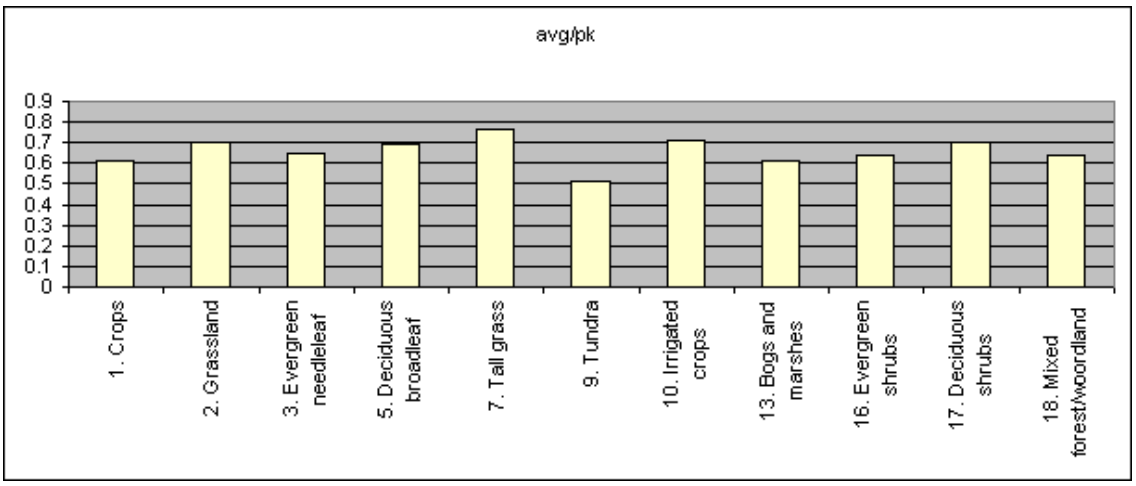

Figure 32 – average to peak ratio of LAI (after ELDAS: http://www.knmi.nl/samenw/eldas/)

Ocean parameters[4]

Seawater mixing depth

This parameter is relevant as it defines the effective mixing volume of chemicals in oceans (Map 28, Map 29). An estimate of monthly average mixing depths has been done for the Mediterranean, Baltic, North and Black seas using the results of the GETM model. For the Atlantic, data from the Monterey and Levitus (1997; http://www.cdc.noaa.gov/cdc/data.nodc.woa94.html) global dataset have been used. These come with a much coarser resolution (1 degree). From inspection of Map 28, coastal areas show lower mixing depths. What is important, however, is the thermohaline stratification that generates coefficients of variation often around 1 and not infrequently as high as 2.

Seawater velocity

Hydrodynamics of European seas has been described by a physically based hydraulic model implemented in the GETM software for the Northern and Baltic Sea (Stips et al., 2005), the Black Sea (Peneva and Stips, 2005) and the Mediterranean (Stips, 2005: personal communication).
The three simulations were performed during different years, with different spatial resolution and input data, but lead to a rather consistent description of the hydrodynamic patterns thanks to the robust physically based model used.
The results of the simulations were averaged at a monthly step to provide an annual climatology of hydrodynamics. The following figure shows the average velocity map of the three European internal seas. For the Atlantic, not covered by the available models, data form the Mariano dataset (http://oceancurrents.rsmas.miami.edu/data.html; Mariano et al., 1995; Ryan et al., 1996) are used. The latter show clearly a much coarser resolution and derive from the processing of observations of surface velocity. For this reason, the two data sets are not fully comparable and further analysis with the GETM model is required to obtain a homogeneous coverage (Map 30, Map 31).

Seawater temperature

Temperature is also part of the GETM model output. For the Atlantic, not covered by the model, the dataset of Monterey and Levitus has been used.
This parameter affects the degradation rate of chemicals. Its value follows grossly latitude. Higher variation is found across the year in the shallow seas subject to high air temperature variations (Baltic and Northern Black seas) (Map 32, Map 33).

Suspended solids concentration

This parameter is important as it affects partitioning of the chemicals between suspended solids and the dissolved phase. It is possible to provide an estimate of total suspended solids by processing remotely sensed images The maps of total suspended matter (TSM) have been obtained from the ocean color sensor Sea-viewing Wide Field-of-View Sensor (SeaWiFS). The raw imagery over Europe has been processed

[4] Data and suggestions about this compartment have been provided by **F.Melin** and **A.Stips** from EC, DG JRC, IES.

using an atmospheric correction scheme described and validated by Sturm and Zibordi (2002) and Mélin et al. (2003), and the final products are created as illustrated by Mélin et al. (2002). The calculation of near-surface TSM concentration is based on a bio-optical algorithm presented in Berthon et al. (2002). A set of monthly averaged values over the time series available have been computed. These allow an estimate within less than an order of magnitude pointwise, but most importantly provide a spatial pattern of the parameter, with a resolution of approximately 2 km. One limitation of the method is its dependence on sunlight, which is not sufficient to inspect the northern part of the continent during winter months.

Map 34 and Map 35 provide an insight in the spatial patterns of total suspended matter (TSM) in january and july. As one can see, higher values of TSM are in coastal areas where significant contributions from inland waters are present. The variation of the parameter is quite high depending seasonally on discharges from land.

Another parameter of importance is the fraction of organic carbon in suspended solids. Although this parameter is as important as TSM in controlling solid-water partitioning of chemicals, it is not possible at present to estimate it from available data at spatially distributed level. Further research is required to link it e.g. to chlorophyll or other parameters retrieved from remotely sensed images.

Wind speed at 10 m height on oceans

The climatology produced by New et al., 2002, only covers land. For what concerns oceans, data exist in spatially distributed form from the processing of SSM/I remotely sensed images. Dachs et al., 2002, used these data to provide estimates of volatilization fluxes at the air-ocean interface. The data come as time series with 5 days or monthly steps. For the purposes of continental scale modeling of chemicals, however, a climatology of wind speed has been preferred for simplicity. Data from ICOADS (http://www.cdc.noaa.gov/cdc/data.coads.1deg.html) with 2 degrees resolution have been then selected for the purpose. The ocean wind speed has a rather low coefficient of temporal variation when compared to other parameters, as shown in Map 36and Map 37. Velocities are highest on the Atlantic and lowest in the Mediterranean (Northern Adriatic and East) and Eastern Black sea.

Chlorophyll

Chlorophyll concentration represents an indicator of organic matter concentration in sea water. As such, it has been used to parameterize the sinking flux of organic matter in sea water, among others, by by Dachs et al., 2002. As an example and Fig. 33 presents average results for monthly values in the Black Sea with the data obtained from the cholorophyll dataset of the EU (http://marine.jrc.ec.europa.eu/data_portal/oc_portal/main.php).

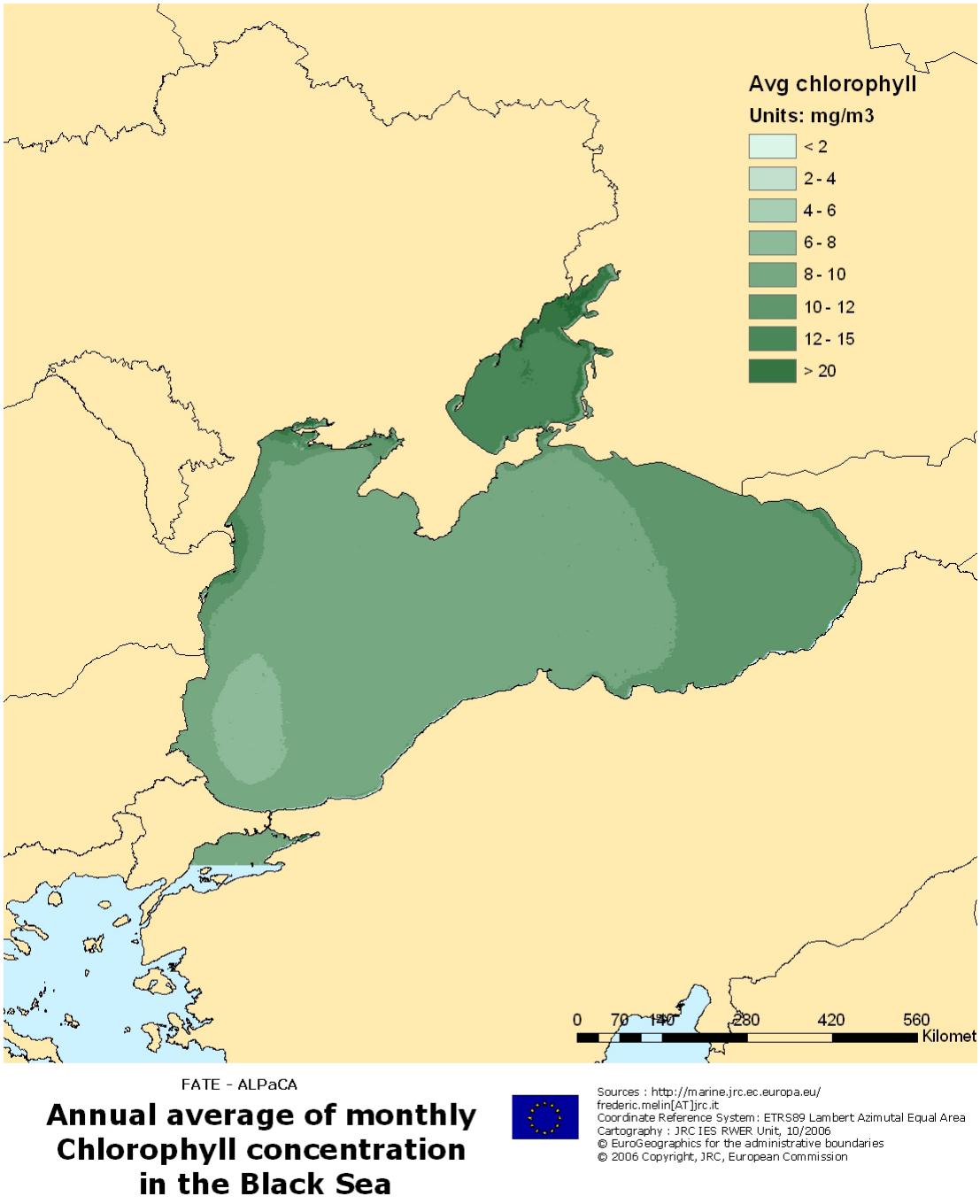

Figure 33. Example of average values of chlorophylls.

Acknowledgements

Dr Frank Dentener of JRC-IES – Climate Change Unit, Ispra, provided the TM5 estimates in the form of monthly average values of Aerosol concentration and chemistry, and OH concentration. Dr B.Pinty and Dr N.Gobron of JRC-IES – Global Vegetation Monitoring Unit, Ispra, provided the estimates of LAI from the FAPAR. Dr A.Stips and Dr F.Melin of JRC-IES – Inland and marine Waters Unit, Ispra, provided the hydrodynamics, Chlorophyll and TSM data for the European seas in the form of monthly averaged parameters. All above mentioned colleagues, together with Dr Stefano Galmarini, Dr Claudio Carlon, Dr Luca Montanarella, Dr Faycal Bouraoui of JRC, were also kindly available to get involved in many helpful discussions on the approaches and data here presented. This research was financially partly supported by

the European Union within the project NoMiracle (European Commission, FP6 Contract No. 003956).

References

1. Apsley, D.D., Dyster, S.J., McHugh, C., Modeling dry deposition, ADMS 3 P 17/13E/05, july 2005. http://www.cerc.co.uk/software/pubs/ADMS3-1TechSpec/P17_13.pdf
2. Berthon, J.-F., G. Zibordi, J.P. Doyle, S. Grossi, D. van der Linde, C. Targa: "Coastal Atmosphere and Sea Time Series (CoASTS): Data analysis." NASA Goddard Space Flight Center, Greenbelt, MD, SeaWiFS Tech. Rep., NASA Tech. Memo. 206892, vol. 20, 2002.
3. Brandes, L.J., den Hollander, H., van de Meent, D., Simplebox 2.0: a nested multimedia fate model for evaluating the environmental fate of chemicals, RIVM Report no. 719101029, Bilthoven, december 1996
4. Charbeneau, R.J., et al., 1995:The Hydrocarbon Spill Screening Model (HSSM). Volume 2: Theoretical Background and Source Codes, EPA/600/R-94/039b
5. Chen,Z.Q., R.S.Govindaraju, M.L.Kavvas, (1994a,b). Spatial averaging of unsaturated flow equations under infiltration conditions over areally heterogeneous soils; Parts I and II, Wat Res Research, 30(2), 523-548.
6. Dachs, J., Lohmann, R., Ockenden, W.A., Mejanelle, L., Eisenreich, S.J., and Jones, K.C., Oceanic Biogeochemical Controls on Global Dynamics of Persistent Organic Pollutants. Environ. Sci. Technol., 36, 20, 4229 - 4237, 2002, 10.1021/es025724k
7. Eagleson, P.S., Climate, soil and vegetation – 1. Introduction to water balance dynamics, Wat. Res. Res., vol. 14, no. 5, pp 705-712, 1978
8. EC (2004) European Union System for the Evaluation of Substances 2.0 (EUSES 2.0). Prepared for the European Chemicals Bureau by the National Institute of Public Health andthe Environment (RIVM), Bilthoven, The Netherlands (RIVM Report no. 01900005). Available via the European Chemicals Bureau, http://ecb.jrc.it
9. Erisman, J.W., Van Pul, A., Wyers, P., Parametrization of surface resistance for the quantification of atmospheric deposition of acidifying pollutants and ozone, Atm. Env., vol. 28, n. 16, pp 2595-2607, 1994
10. European Soil Bureau, ESDBv2 Raster Archive - a set of rasters derived from the European Soil Database distribution version 2 (published by the European Commission and the European Soil Bureau Network, CD-ROM, EUR 19945 EN)
11. Fekete, B.M., Vorosmarty, C.J., Grabs, W., Global Composite Runoff Fields Based on Observed River Discharge And Simulated Water Balances, Global Runoff Data Center Report No. 22, 2000
12. Håkanson, L., Mikrenska, M., Petrov, K., Foster, I., Suspended particulate matter (SPM) in rivers: empirical data and models, Ecological Modelling, Volume 183, Issues 2-3, 25 Pages 251-267, 2005
13. Hertwich, E.G., McKone, T.E. , Pease, W.S., Parameter Uncertainty and Variability In Evaluative Fate and Exposure Models, Risk Analysis, Vol. 19, No. 6, pp 1193-1204, 1999
14. Jones, R.J.A. , Hiederer, R., Rusco, E., Loveland, P.J. , Montanarella, L., THE MAP OF ORGANIC CARBON IN TOPSOILS IN EUROPE: VERSION 1.2 SEPTEMBER 2003 Explanation of: Special Publication Ispra

2004 No.72 S.P.I.04.72
http://eusoils.jrc.it/ESDB_Archive/octop/octop_data.html

15. Jurado, E., Jaward, F.M., Lohmann, R., Jones, K.C., Simo, R., and Dachs,J., Atmospheric Dry Deposition of Persistent Organic Pollutants to the Atlantic and Inferences for the Global Oceans. Environ. Sci. Technol., 38, 21, 5505 - 5513, 2004, 10.1021/es049240v
16. Kinne, S.; Schulz, M.; Textor, C.; Guibert, S.; Balkanski, Y.; Bauer, S. E.; Berntsen, T.; Berglen, T. F.; Boucher, O.; Chin, M.; Collins, W.; Dentener, F.; Diehl, T.; Easter, R.; Feichter, J.; Fillmore, D.; Ghan, S.; Ginoux, P.; Gong, S.; Grini, A.; Hendricks, J.; Herzog, M.; Horowitz, L.; Isaksen, I.; Iversen, T.; Kirkevåg, A.; Kloster, S.; Koch, D.; Kristjansson, J. E.; Krol, M.; Lauer, A.; Lamarque, J. F.; Lesins, G.; Liu, X.; Lohmann, U.; Montanaro, V.; Myhre, G.; Penner, J.; Pitari, G.; Reddy, S.; Seland, O.; Stier, P.; Takemura, T.; Tie, X. An AeroCom initial assessment – optical properties in aerosol component modules of global models. Atmos. Chem. Phys. Discuss. 2005, 5, 8285-8330.
17. Kirkby, M.J., Jones, R.J.A., Irvine, B., Gobin, A, Govers, G., Cerdan, O., Van Rompaey, A.J.J., Le Bissonnais, Y., Daroussin, J., King, D., Montanarella, L., Grimm, M., Vieillefont, V., Puigdefabregas, J., Boer, M., Kosmas, C., Yassoglou, N., Tsara, M., Mantel, S., Van Lynden, G. (2004). Pan-European Soil Erosion Risk Assessment: The PESERA Map, Version 1 October 2003. Explanation of Special Publication Ispra 2004 No.73 (S.P.I.04.73). European Soil Bureau Research Report No.16, EUR 21176, 18pp. and 1 map in ISO B1 format. Office for Official Publications of the European Communities, Luxembourg.
18. Krol, M., Houweling, S., Bregman, B., van den Broek, M., Segers, A., van Velthoven, P., Peters, W., Dentener F., Bergamaschi P., The two-way nested global chemistry-transport zoom model TM5: algorithm and application. Atmos. Chem. Phys. 4, 3975-4018 – 2005
19. Langbein, W.B. ,The Water Supply of Arid Valleys in Intermountain Regions, in Relation to Climate. IAHS Bull. Vol. 7, No.1, 1962.
20. Lehner, B. and Döll, P., Development and validation of a global database of lakes, reservoirs and wetlands. Journal of Hydrology 296/1-4: 1-22; 2004
21. Leopold, L.B., Maddock, T., The Hydraulic geometry of stream channels and some physiographic implications, US Geol. Survey prof. Paper 252, 1953, 56 pp
22. Lettau, H., Evapotranspiration climatonomy 1. – A new approach to numerical prediction of monthly evapotranspiration, runoff, and soil moisture storage, Monthly Weather Review, vol. 97, n.10, pp 691-699, 1969
23. Mackay, D., Multimedia Environmental models: the fugacity approach, 2nd ed., Lewis Publishers, New York, 2001, 261 pp
24. Mariano, A.J., E.H. Ryan, B.D. Perkins, S. Smithers.The Mariano Global Surface Velocity Analysis 1.0, U.S. Coast Guard Technical Report, CG-D-34-95, 1995.
25. Marner, B.B., Harrison, R.M., A spatially refined monitoring based study of atmospheric nitrogen deposition, Atm. Env., 38, pp 5045-5056, 2004
26. Mélin, F., C. Steinich, N. Gobron, B. Pinty, M.M. Verstraete: "Optimal merging of LAC and GAC data from SeaWiFS." Int. J. Remote Sens., 23, 801-807, 2002.
27. Mélin, F., G. Zibordi, J.-F. Berthon: "Assessment of SeaWiFS atmospheric and marine products for the Northern Adriatic Sea." IEEE Trans. Geosci. Remote Sens., 41, 548-558, 2003.
28. Monterey, G. I., and S. Levitus, 1997: Climatological cycle of mixed layer depth in the world ocean. U.S. Gov. Printing Office, NOAA NESDIS, 5pp.

29. New, M., Lister, D., Hulme, M., Makin, I., A high resolution data set of surface climate over global land areas, Climate Research, 21, 1-25, 2002
30. Pennington, D.W., Margni, M., Ammann, C., Jolliet, O., Multimedia fate and human intake modeling: spatial versus non spatial insights for chemical emissions in western Europe. Environ.Sci.Technol., 2005, 39, 1119-1128
31. Pinty, B., T. Lavergne, R. E. Dickinson, J.-L.Widlowski, N. Gobron and M. M. Verstraete (2006) 'Simplifying the interaction of land surfaces with radiation for relating remote sensing products to climate models', Journal of Geophysical Research, 111, doi:1029/2005JD005952
32. Pistocchi, A., Bouraoui, F., Pennington, D.W., A simplified parameterization of the monthly topsoil water budget for continental scale modeling of pollutants, submitted, 2006
33. Pistocchi, A., Pennington, D.W., European hydraulic geometries for continental scale environmental modeling, Journal of Hydrology (2006) 329, 553– 567
34. Pistocchi, A., Report on multimedia fate and exposure model with various spatial resolutions at the European level, NoMiracle project Deliverable 2.4.1, 2005. http://nomiracle.jrc.it
35. Rees, H.G., Croker, K.M., Reynard, N.S. & Gustard, A. (1997): Estimating therenewable water resource. In Estimation of renewable water resources in the European Union. Eds: H.G. Rees and G.A. Cole, 1997. Institute of Hydrology, Wallingford, UK. Final Report to Eurostat (SUP-COM95, 95/5-441931EN).
36. Roemer, M., Baart, A., Libre, J.M., ADEPT: development of an Atmospheric Deposition and Transport model for risk assessment, TNO report B&O- A R 2005-208, Apeldoorn, 2005
37. Ryan, E.H., A.J. Mariano, D.B. Olson, R.H. Evans, Global Sea Surface Temperature and Currents, 1996 Fall AGU Meeting Eos, Transactions, AGU, Vol 77, No 46, November 12, 1996 (OP22A-16).
38. Schwarzenbach, R. P.; Gschwend, P. M.; Imboden, D. M. Environmental Organic Chemistry; Wiley: New York, 1993
39. Sehmel, G., Particle and dry deposition: a review. Atm. Env., vol. 14, pp 983-1011, 1980
40. Starks, P. J., G. C. Heathman, L. R. Ahuja, and L. Ma, Use of limited soil property data and modeling to estimate root zone soil water content, J. Hydrol. (Amsterdam), 272, 646 131–147, 2003.
41. Sturm, B. and G. Zibordi: "SeaWiFS atmospheric correction by an approximate model and vicarious calibration." Int. J. Remote Sens., 23, 489-501, 2002.
42. Textor, C.; Schulz, M.; Guibert, S.; Kinne, S.; Balkanski, Y.; Bauer, S.; Berntsen, T.; Berglen, T.; Boucher, O.; Chin, M.; Dentener, F.; Diehl, T.; Easter, R.; Feichter, H.; Fillmore, D.; Ghan, S.; Ginoux, P.; Gong, S.; Grini, A.; Hendricks, J.; Horowitz, L.; Huang, P.; Isaksen, I.; Iversen, T.; Kloster, S.; Koch, D.; Kirkevåg, A.; Kristjansson, J. E.; Krol, M.; Lauer, A.; Lamarque, J. F.; Liu, X.; Montanaro, V.; Myhre, G.; Penner, J.; Pitari, G.; Reddy, S.; Seland, Ø.; Stier, P.; Takemura, T.; Tie, X. Analysis and quantification of the diversities of aerosol life cycles within AeroCom. Atmos. Chem. Phys. Discuss. , 5, 8331-8420, 2005
43. Thornthwaite, C. W. , Mather, J. R., The Water Balance. Publications in Climatology Volume VIII, Number 1, Centerton, New Jersey – 1955
44. Tiktak, A., de Nie, D.S., Pineros Garcet, J.D., Jones, A., Vanclooster, M., Assessment of the pesticide leaching risk at the Pan-European level. The EuroPEARL approach. Journal of Hydrology 289 (2004) 222–238

45. Turc, L., Le bilan d'eau des sols: relations entre les precipitations, l'evaporation et l'ecoulement. Institut national de la recherche agronomique. Paris: 252 pp, 1953
46. Underwood, B.Y., Chapter 2 – Dry deposition, in Review of specific effects in atmospheric dispersion calculations, Euratom Report EUR 8935 EN, 1984
47. Van der Knijff, J.M., Jones, R.J.A., Montanarella, L., Soil erosion risk assessment in Europe, EUR 19044 EN, 44 pp, Office for Official Publications of the European Communities, Luxembourg, 2000
48. Verdelocco, S., Modelling Potential Vulnerability of Soils at European and Regional Scale: Linking EUSES to Geo-Referenced Data. A thesis presented for the degree of Doctor of Philosophy at the University of Aberdeen, 2004
49. Vignati E., Krol M.C., Dentener,F., Global and regional Aerosol modeling: a picture over Europe, NATO ARW series, in: Advances in Air Pollution Modeling for Environmental Security, I. Farago (eds), Springer, the Netherlands, 2005
50. Wang, Y., J.A. Logan, and D.J. Jacob, Global simulation of tropospheric O3-NOx-hydrocarbon chemistry, 2. Model evaluation and global ozone budget, J. Geophys. Res., 103, 10,727-10,756, 1998.
51. Wesely, M.L., Hicks, B.B., A review of the current status of knowledge on dry deposition, Atm. Env., vol. 34, pp 2261-2282, 2000
52. Williams, R., M., A odel for the dry deposition of particles to natural water surfaces, Atm. Env., vol. 16, n. 8, pp 1933-1938, 1982
53. Wosten, J.H.M., Lilly, A., Nemes, A., Le Bas, C., Development and use of a database of hydraulic properties of European Soils, Geoderma, 90, 169-185, 1999
54. Zadeh, L.A., 1965. Fuzzy sets, IEEE Informatics and Control, n.8, pp. 338-353

List of the maps of ALPaCA-Fate

Map 1 - annual average temperature
Map 2 - coefficient of variation of monthly temperature values
Map 3 - OH concentration (ADEPT model)
Map 4 - average OH concentration relative to the first 1000 m of height (TM5 model)
Map 5 – coefficient of vertical variation of OH concentration relative to the first 1000 m of height (TM5 model)
Map 6 – concentration of PM_{10} according to EMEP
Map 7 – aerosol average concentration relative to the first 1000 m of height (TM5 model)
Map 8 – aerosol concentration coefficient of variation relative to the first 1000 m of height (TM5 model)
Map 9 - average OC relative to the first 1000 m of height (TM5 model)
Map 10 – coefficient of variation of OC content relative to the first 1000 m of height (TM5 model)
Map 11 - annual average wind speed at 10 m obtained from New et al, 2002 data
Map 12 - coefficient of variation of monthly values of wind speed at 10 m obtained from New et al, 2002 data
Map 13 – atmospheric mixing height from the ADEPT model
Map 14 - PELCOM map reclassified to account for relative deposition velocity depending on the surface roughness
Map 15 –monthly average precipitation according to New et al., 2002
Map 16 – coefficient of variation of the monthly values of precipitation according to New et al., 2002
Map 17 - monthly average wet days according to New et al., 2002
Map 18 - coefficient of variation of the monthly number of wet days according to New et al., 2002
Map 19 – snowpack according to Wilmott et al.,
Map 20 –average monthly runoff (GRDC)
Map 21 – coefficient of variation of variation of the monthly values of runoff (GRDC)
Map 22 – suspended sediment concentration according to Hakanson et al., 2005
Map 23 – Retention time of European lakes
Map 24 – soil textural classes of Europe
Map 25 – soil moisture computed as the average between field capacity and wilting point.
Map 26 – Annual Evapotranspiration according to Turc's formula
Map 27 – PESERA model results for soil erosion.
Map 28 -Seawater mixing depth (mean)
Map 29 - Seawater mixing depth (coefficient of variation)
Map 30 - Seawater velocity (mean)
Map 31 - Seawater velocity(coefficient of variation)
Map 32 - Seawater temperature(mean)
Map 33 - Seawater temperature(coefficient of variation)
Map 34 - Seawater total suspended solids(january)
Map 35 - Seawater total suspended solids(july)
Map 36 - Wind speed on sea surfaces(mean)
Map 37 - Wind speed on sea surfaces(coefficient of variation)
Map 38 - Maximum values of LAI for Europe.

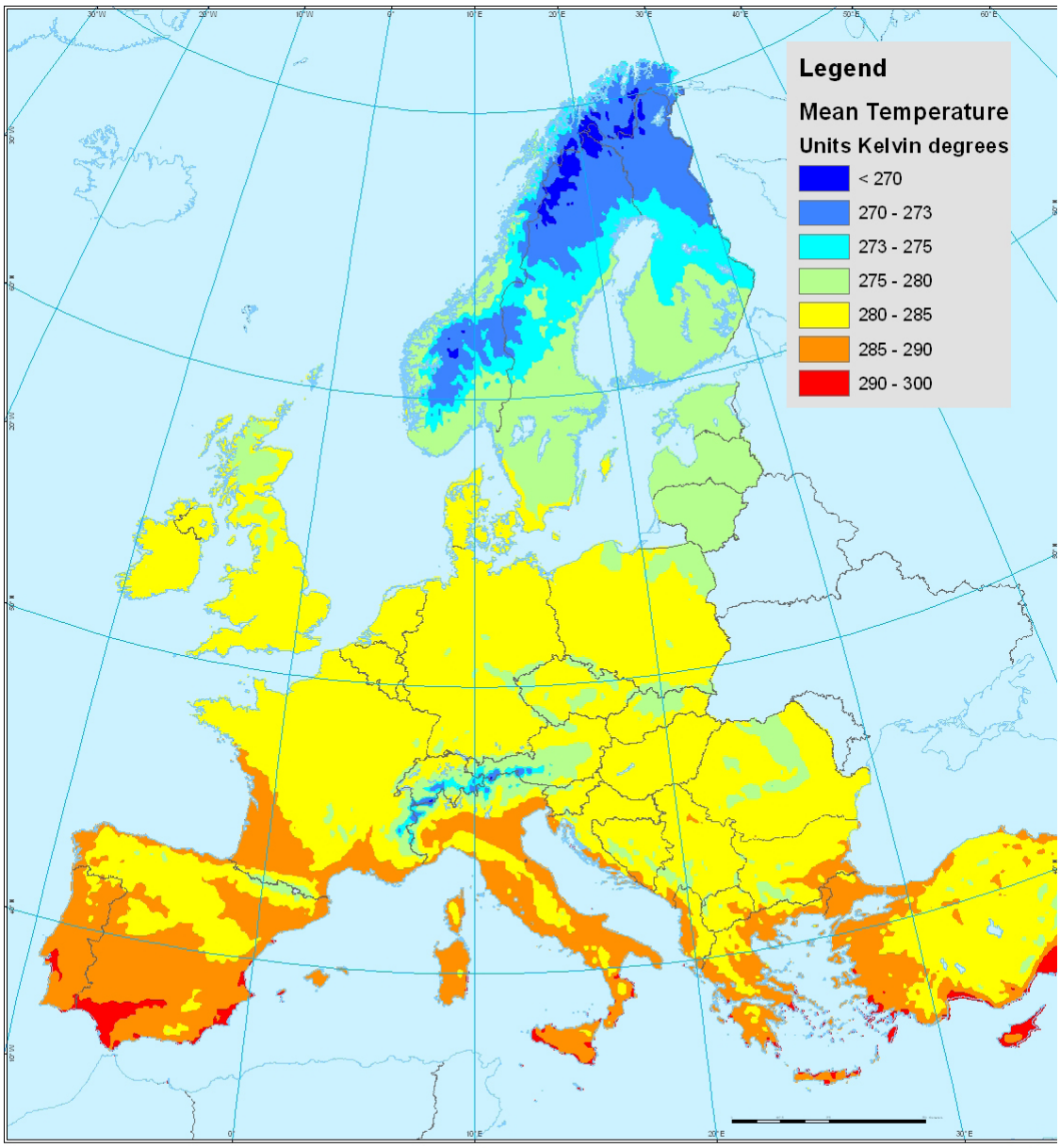

Map 1 - annual average temperature

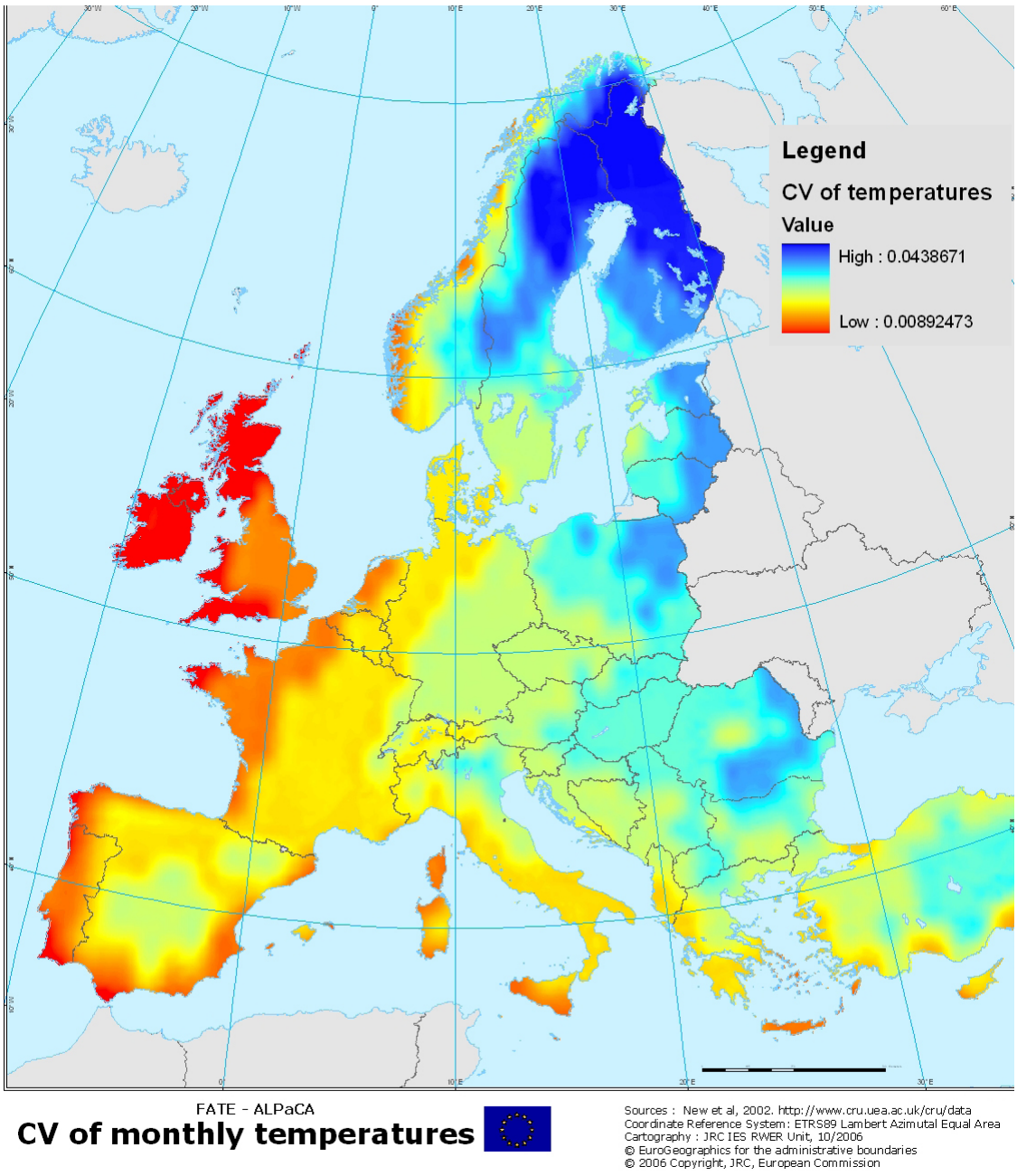

Map 2 - coefficient of variation of monthly temperature values

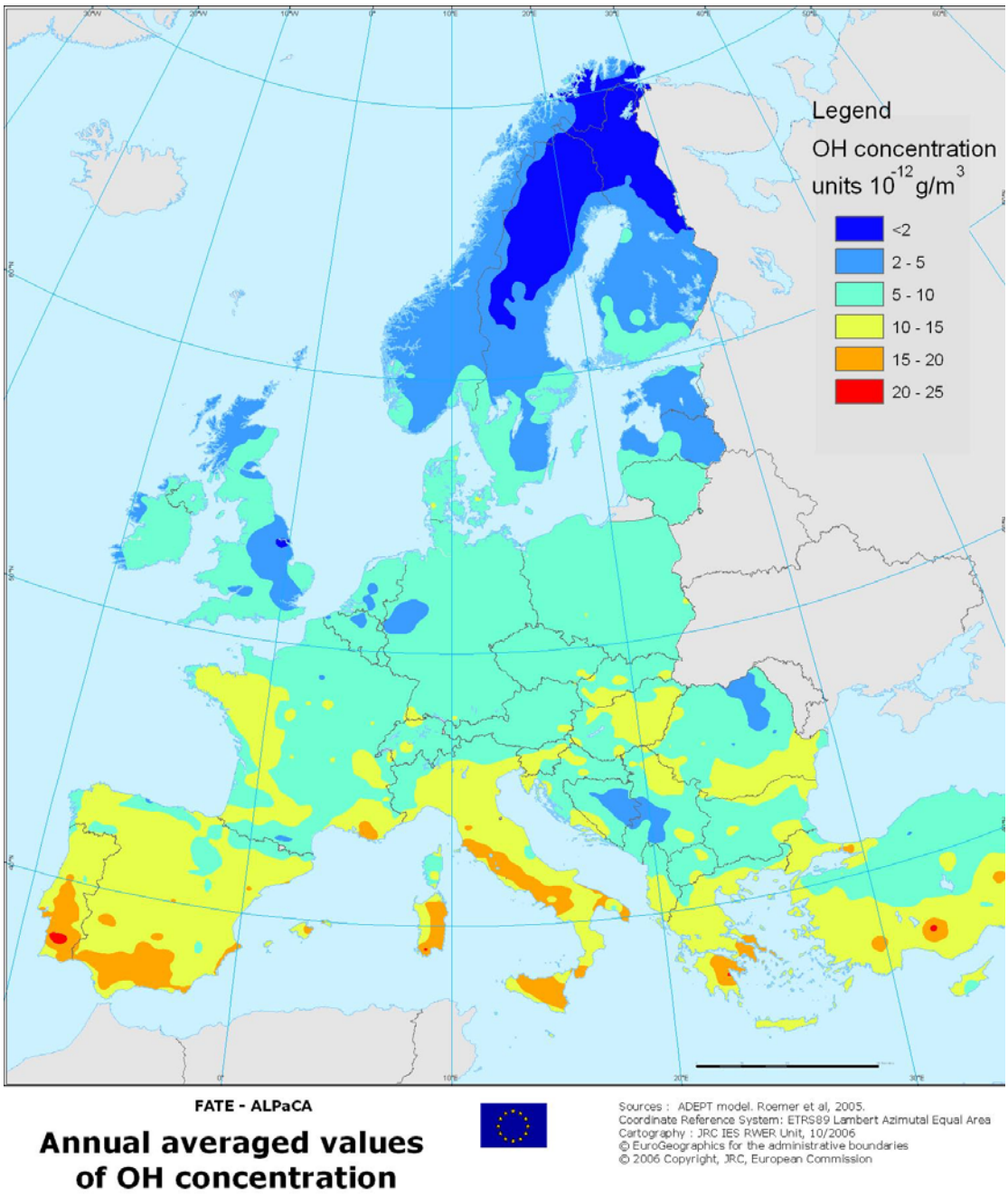

Map 3 - OH concentration (ADEPT model)

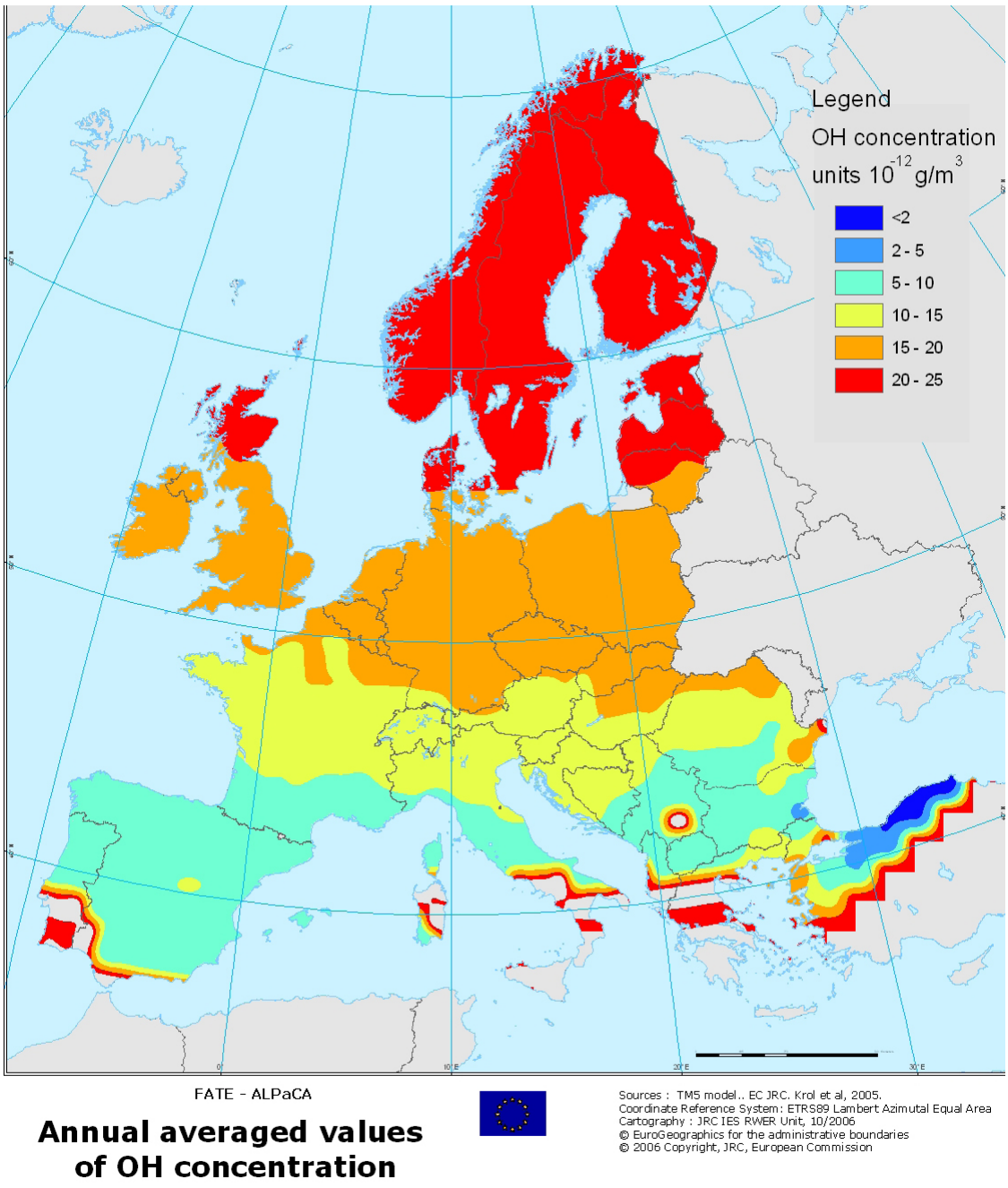

Map 4 - average OH concentration relative to the first 1000 m of height (TM5 model)

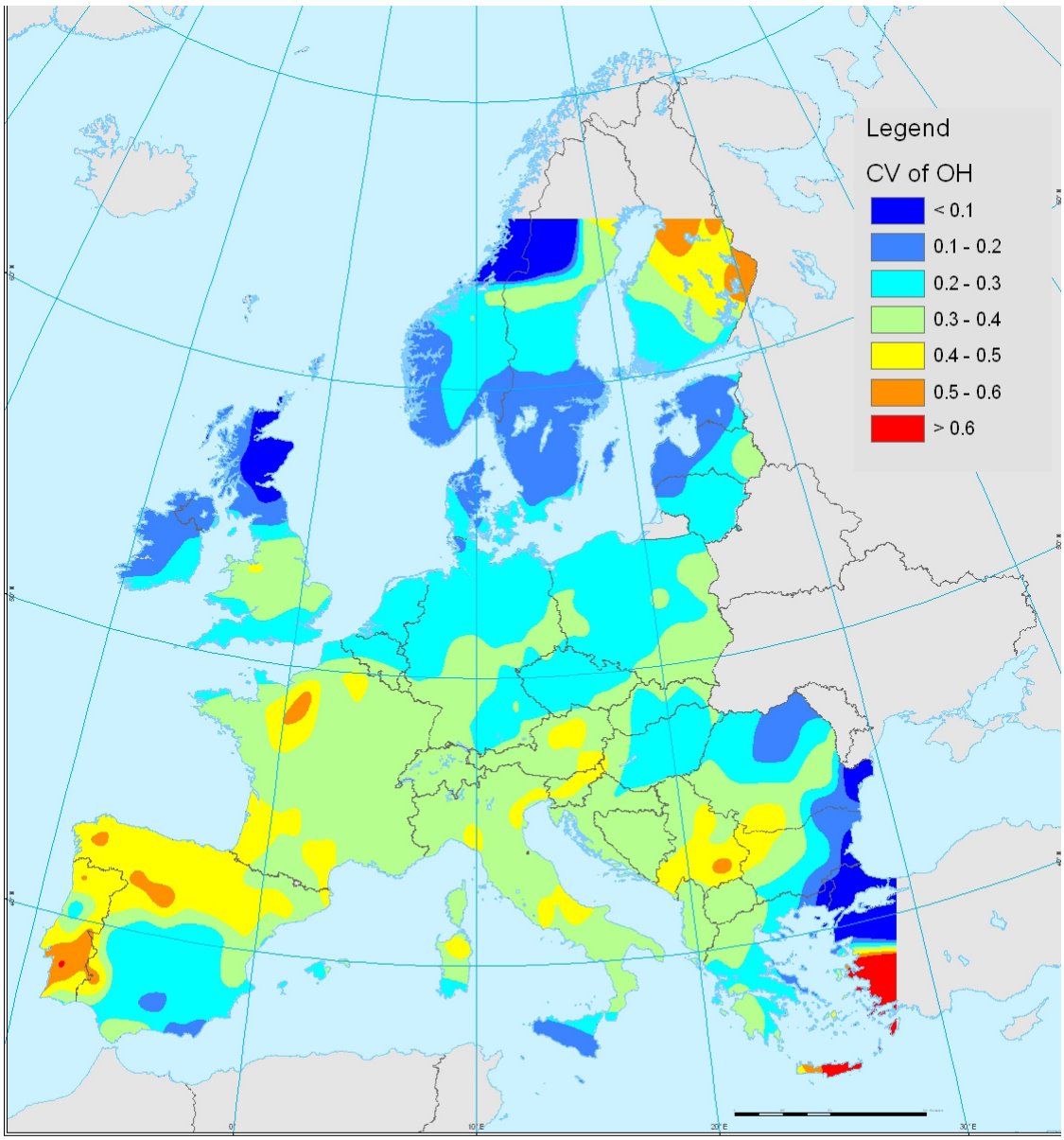

Map 5 – coefficient of vertical variation of OH concentration relative to the first 1000 m of height (TM5 model)

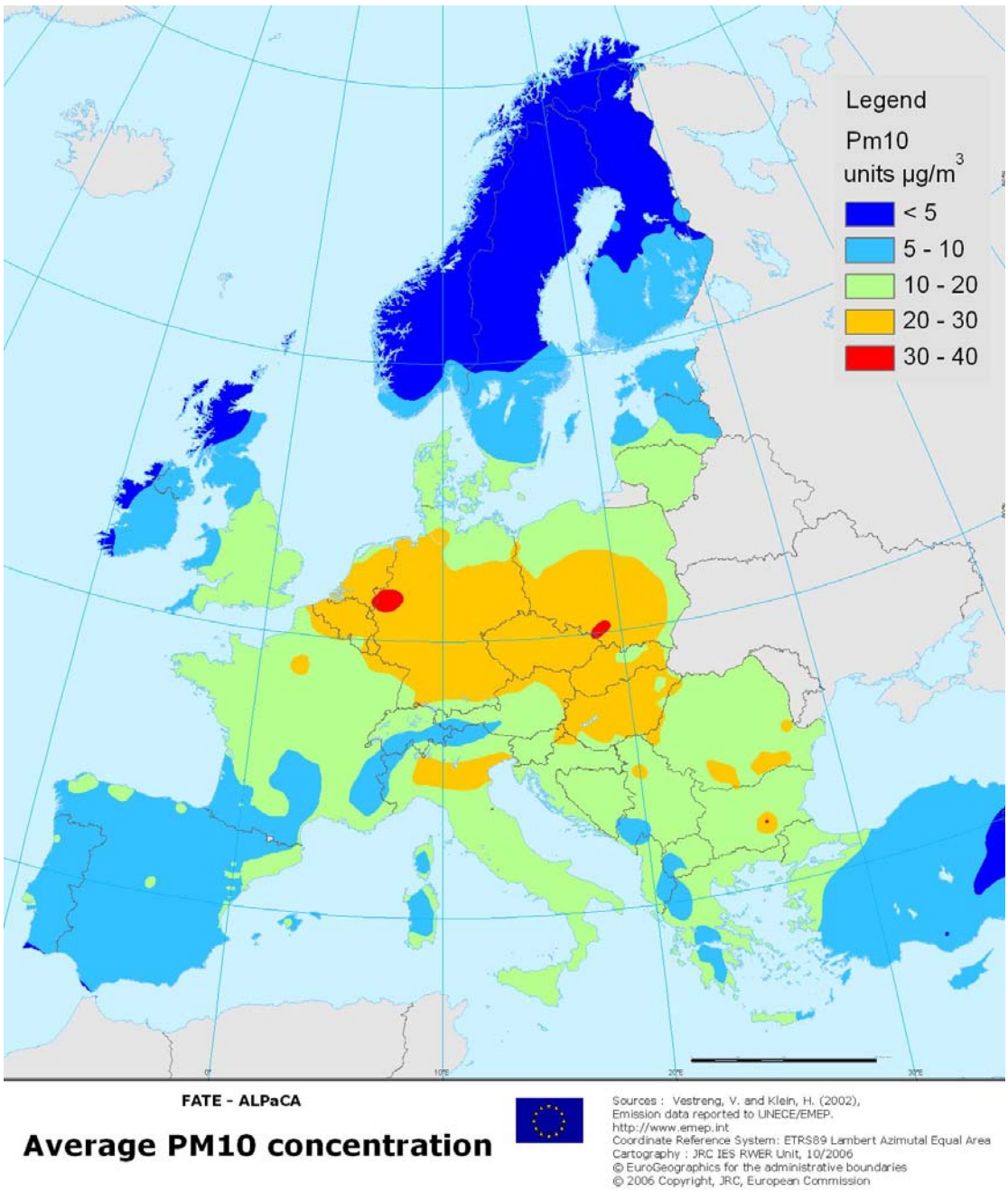

Map 6 – concentration of PM_{10} according to EMEP

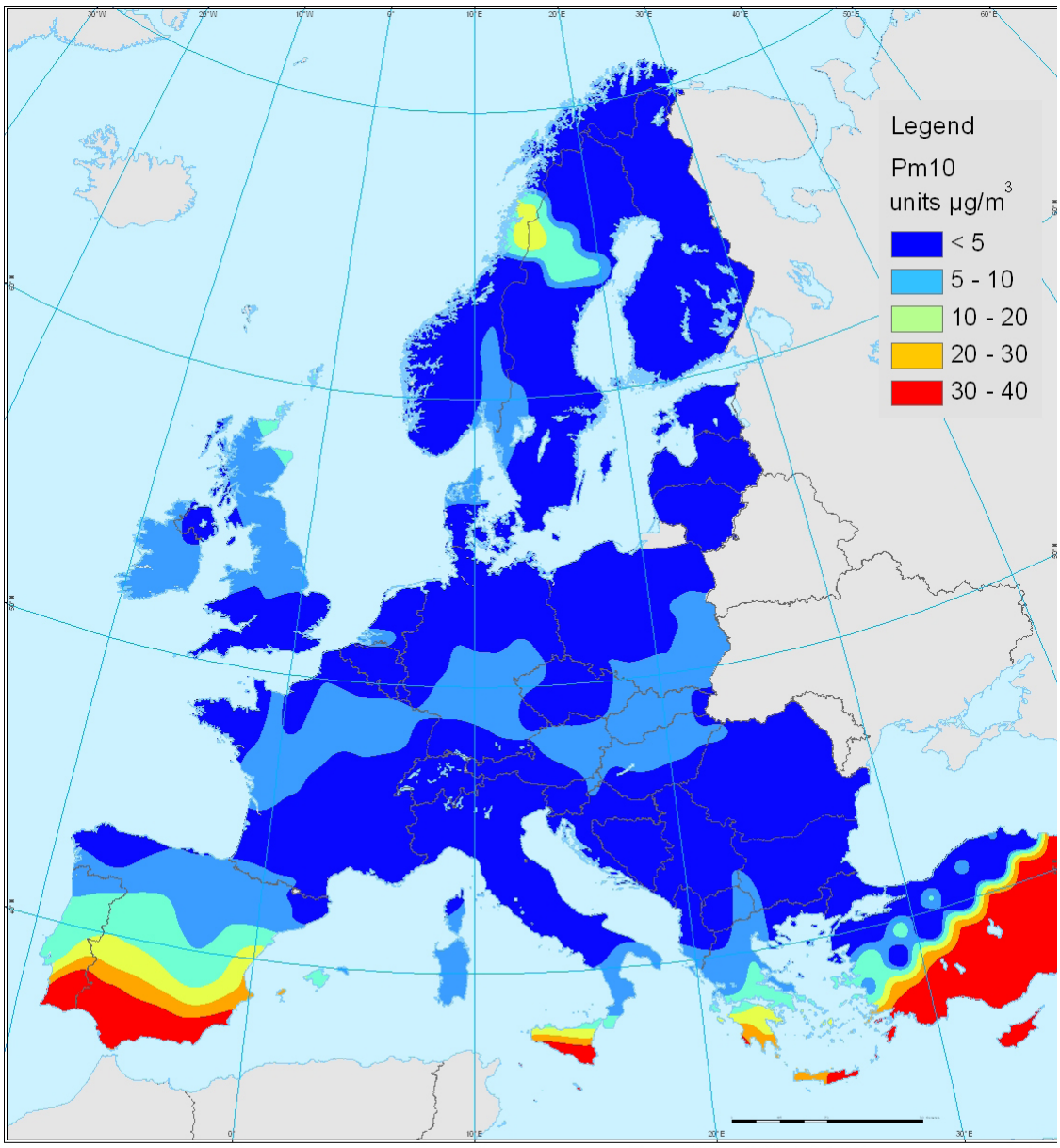

Map 7 – aerosol average concentration relative to the first 1000 m of height (TM5 model)

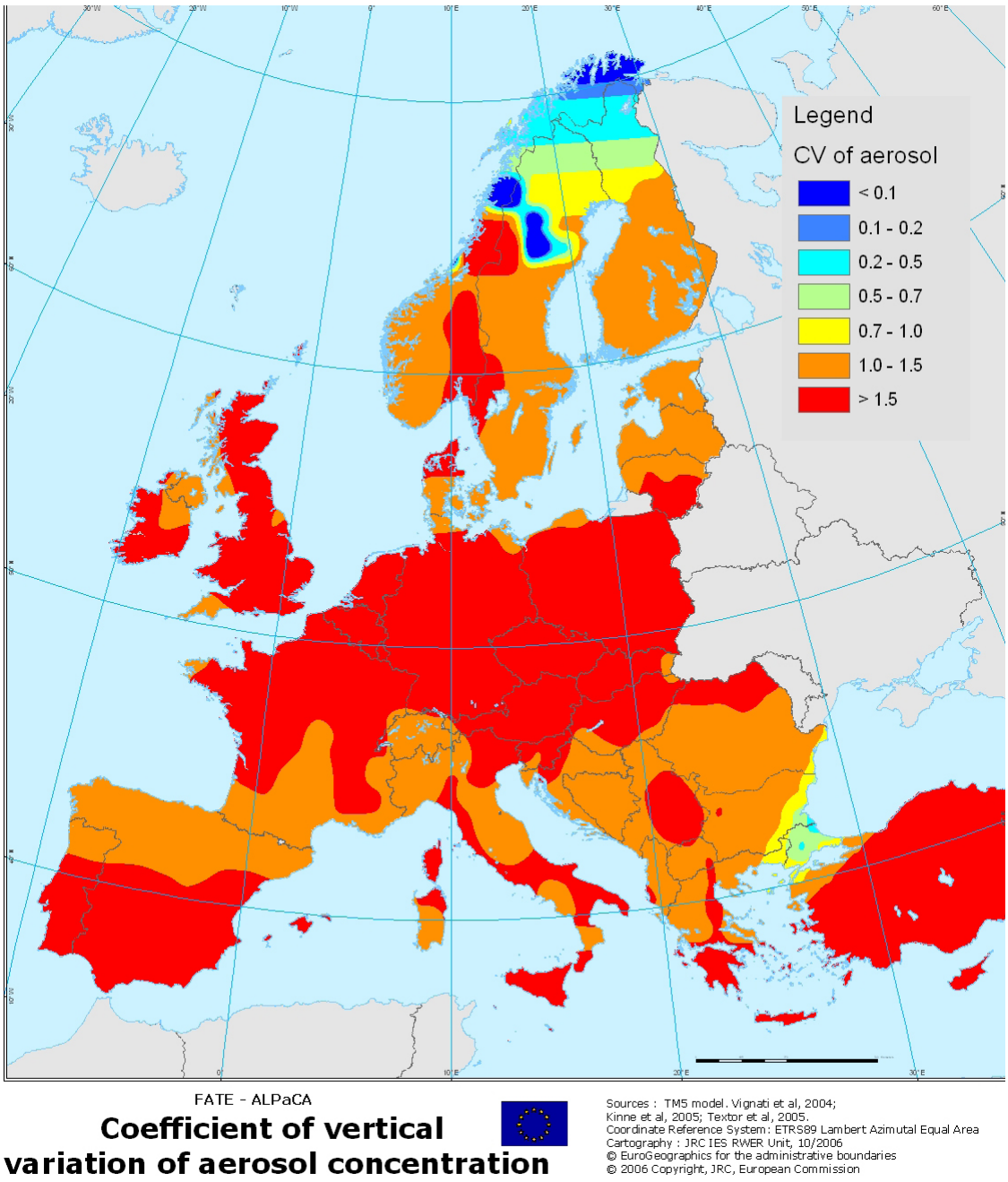

Map 8 – aerosol concentration coefficient of variation relative to the first 1000 m of height (TM5 model)

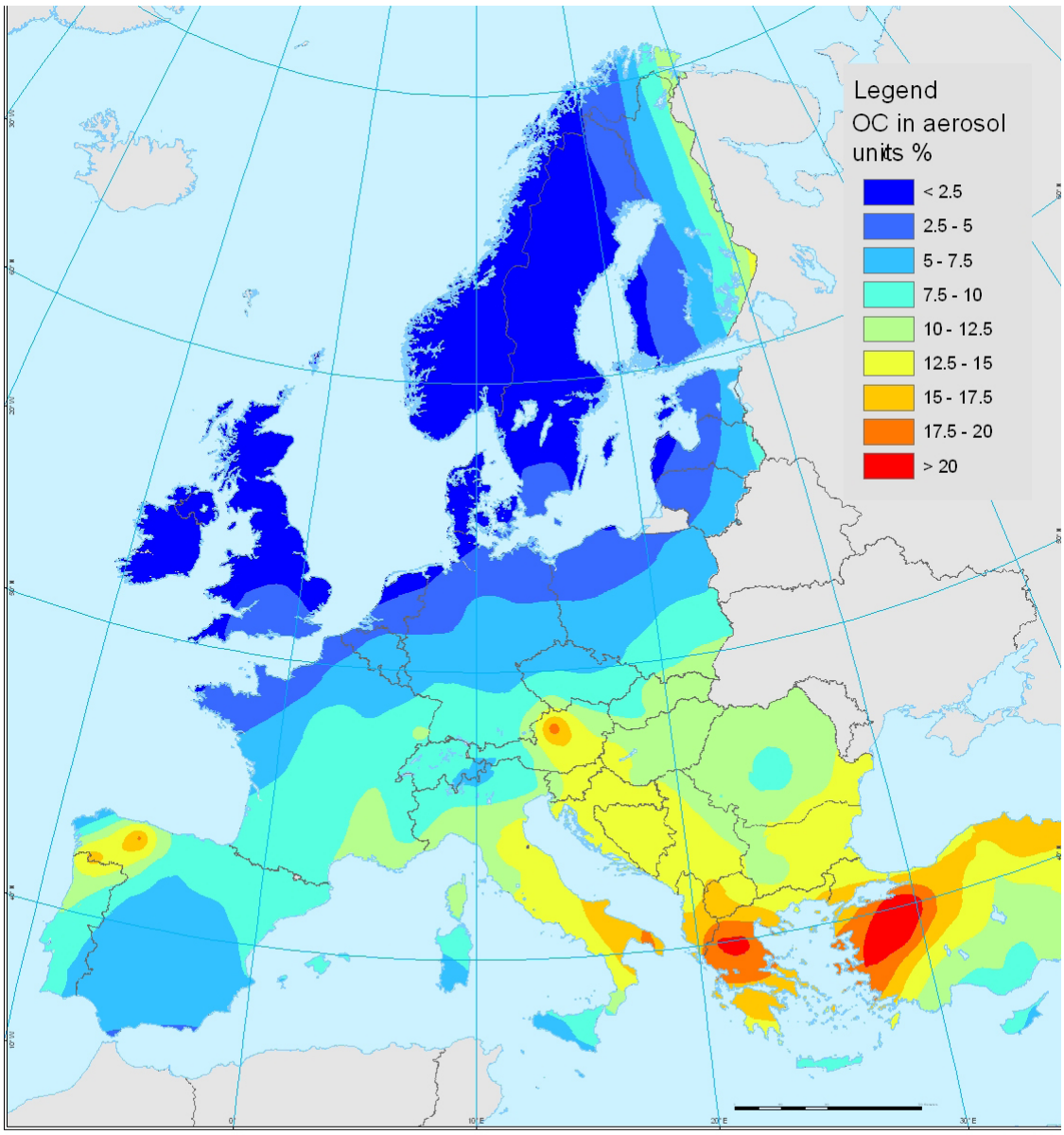

Map 9 - average OC relative to the first 1000 m of height (TM5 model)

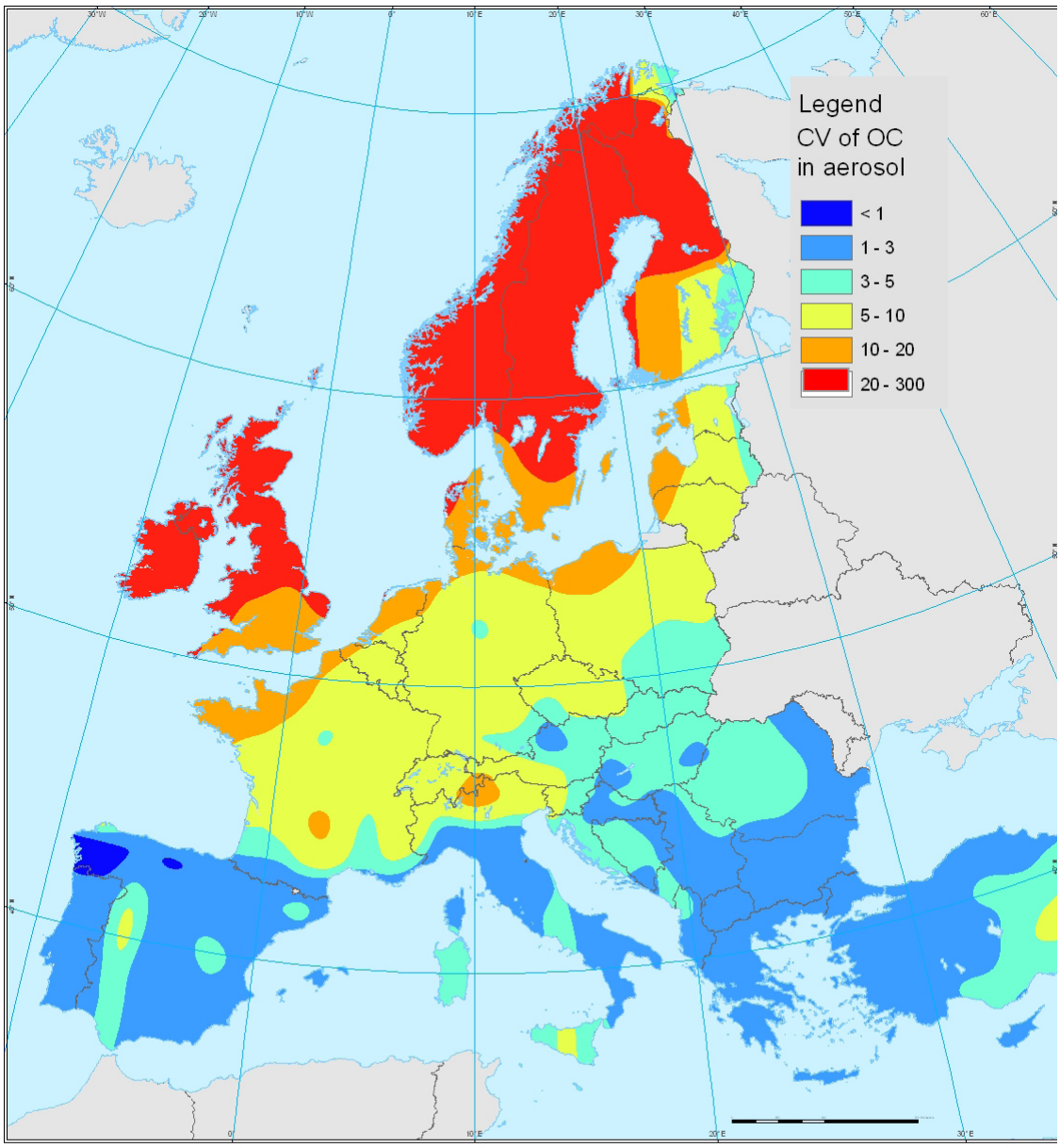

Map 10 – coefficient of variation of OC content relative to the first 1000 m of height (TM5 model)

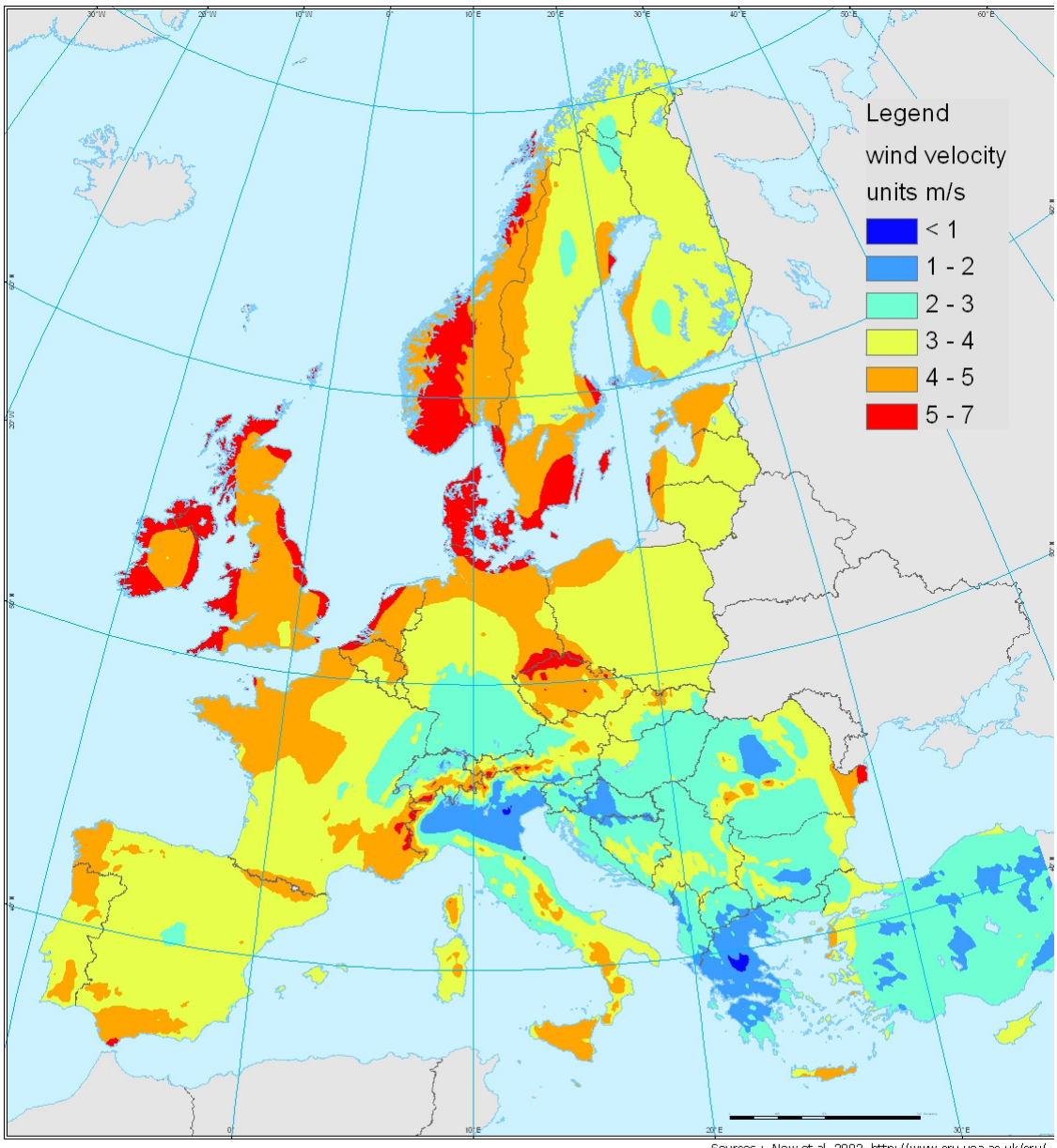

Map 11 - annual average wind speed at 10 m obtained from New et al, 2002 data

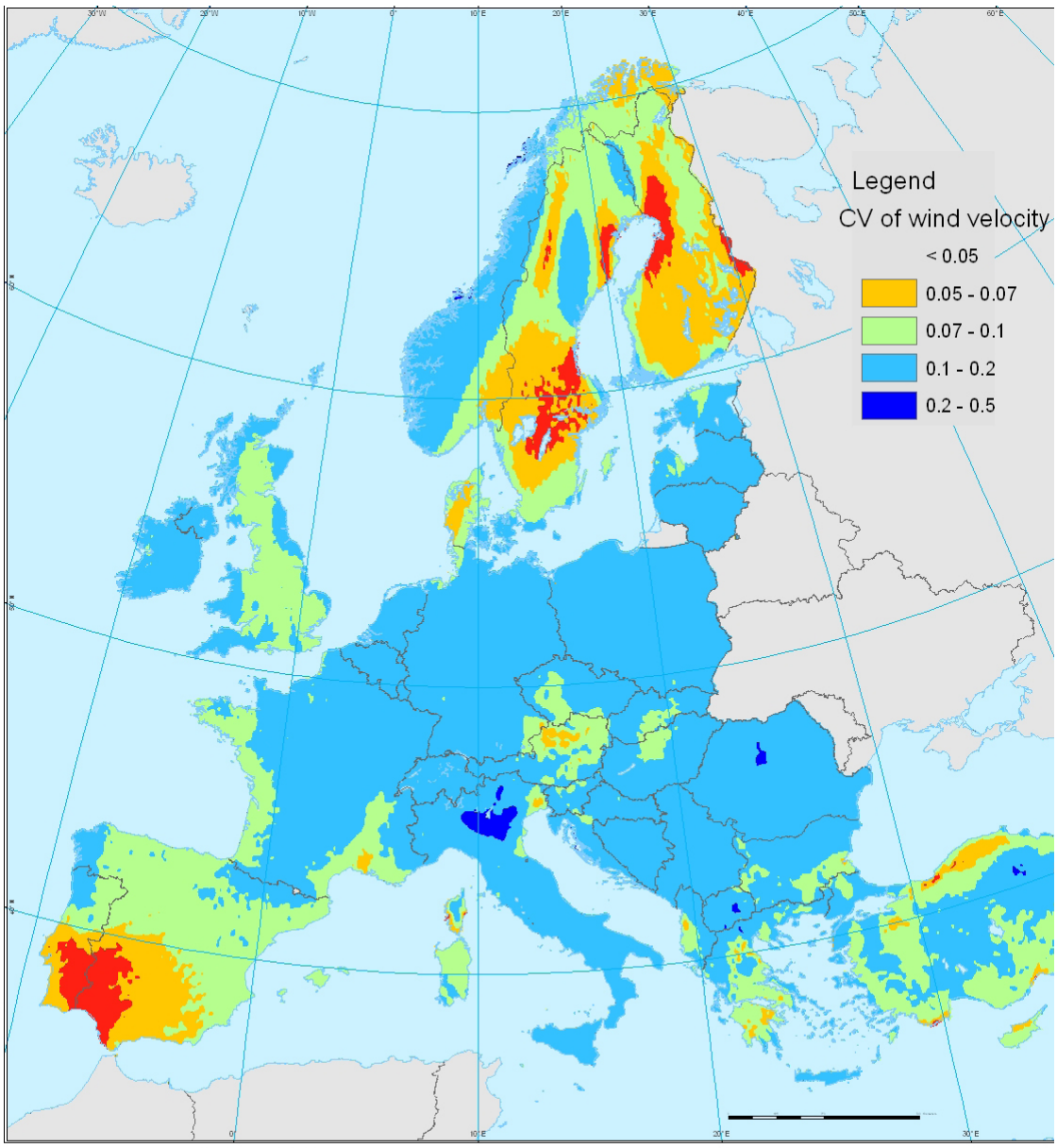

Map 12 - coefficient of variation of monthly values of wind speed at 10 m obtained from New et al, 2002 data

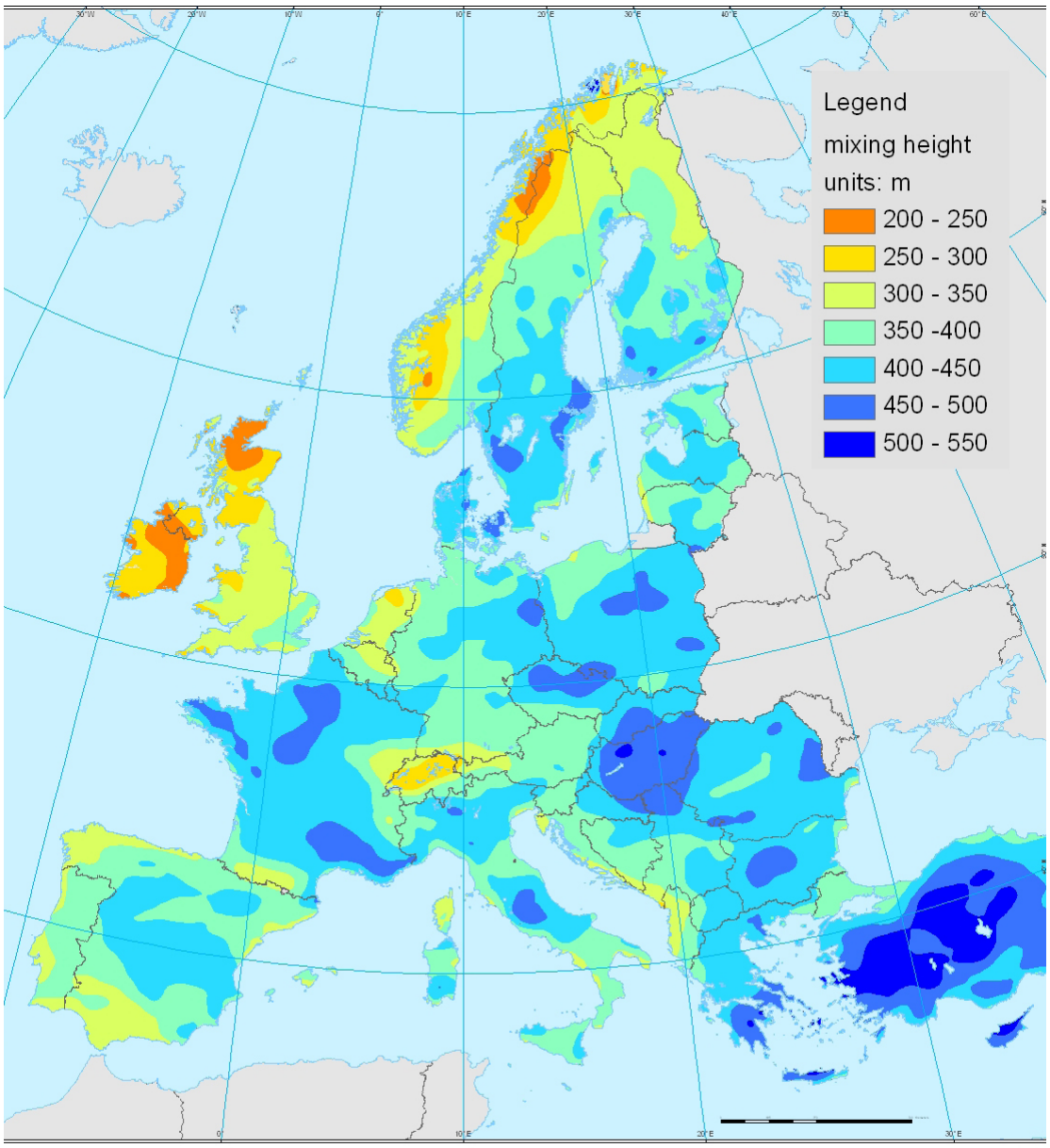

Map 13 – atmospheric mixing height from the ADEPT model

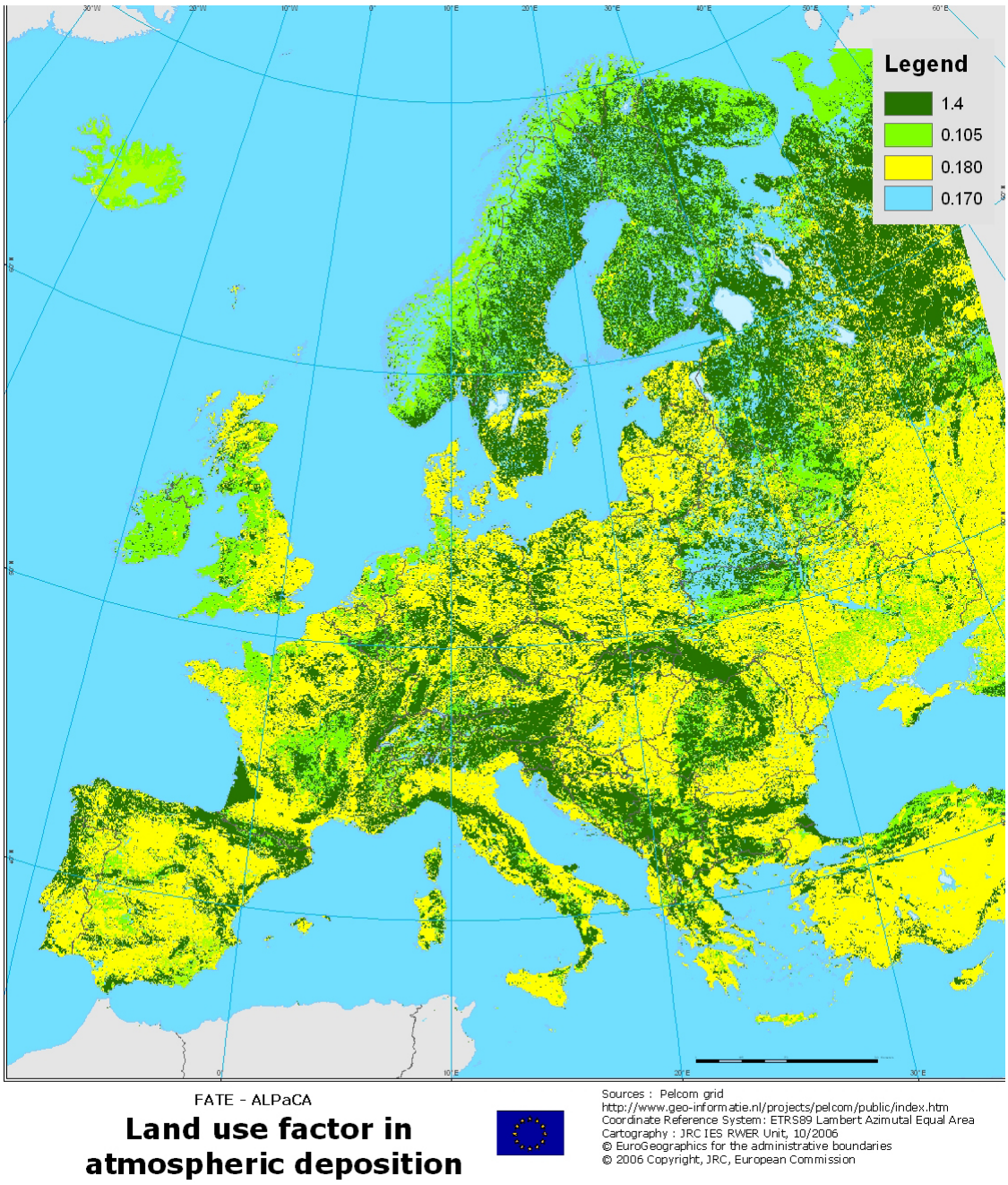

Map 14 - PELCOM map reclassified to account for relative deposition velocity depending on the surface roughness

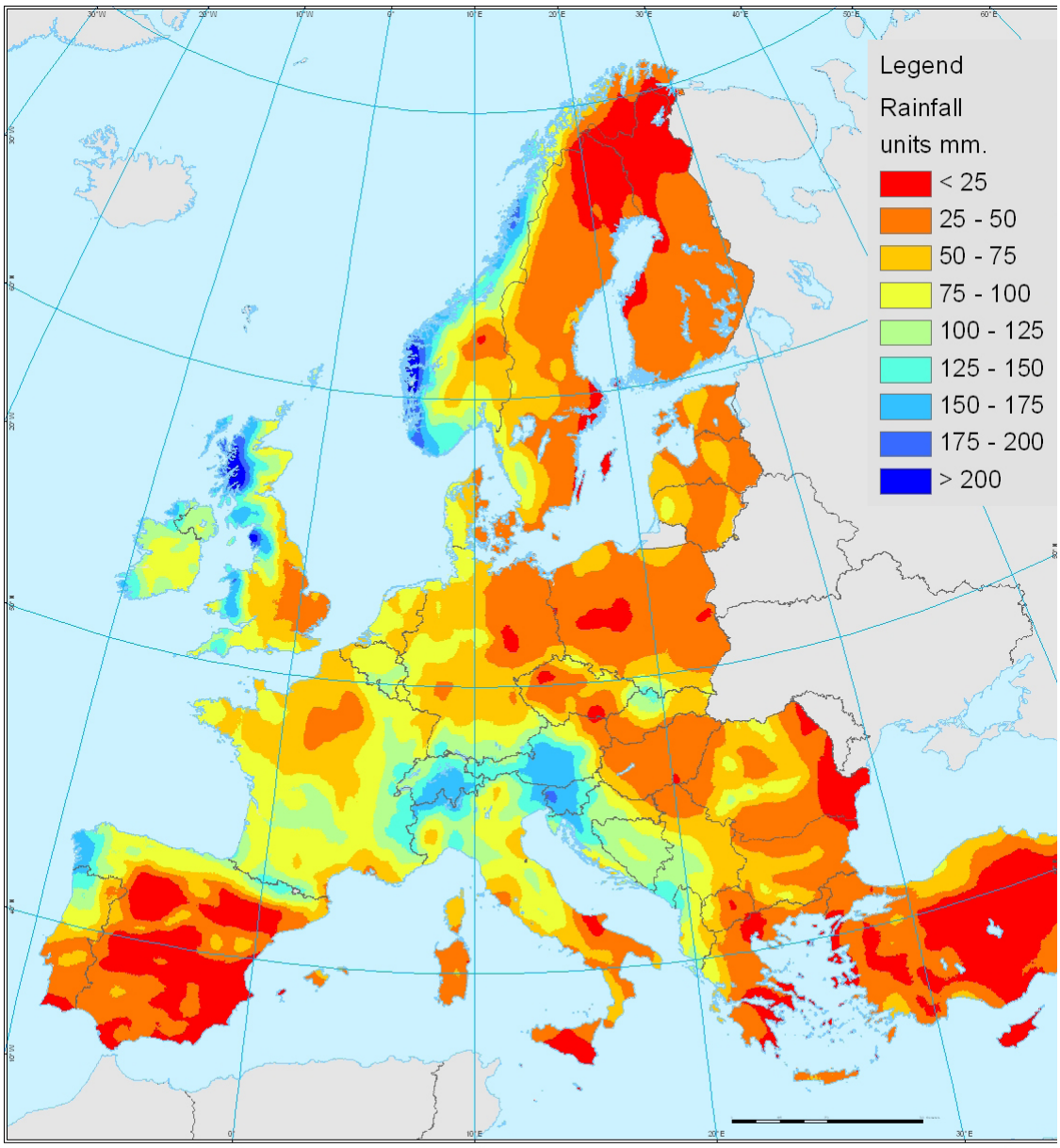

FATE - ALPaCA

Annual mean rainfall based on monthly values

Sources : New et al, 2002. http://www.cru.uea.ac.uk/cru/data
Coordinate Reference System: ETRS89 Lambert Azimutal Equal Area
Cartography : JRC IES RWER Unit, 10/2006
© EuroGeographics for the administrative boundaries

Map 15 –monthly average precipitation according to New et al., 2002

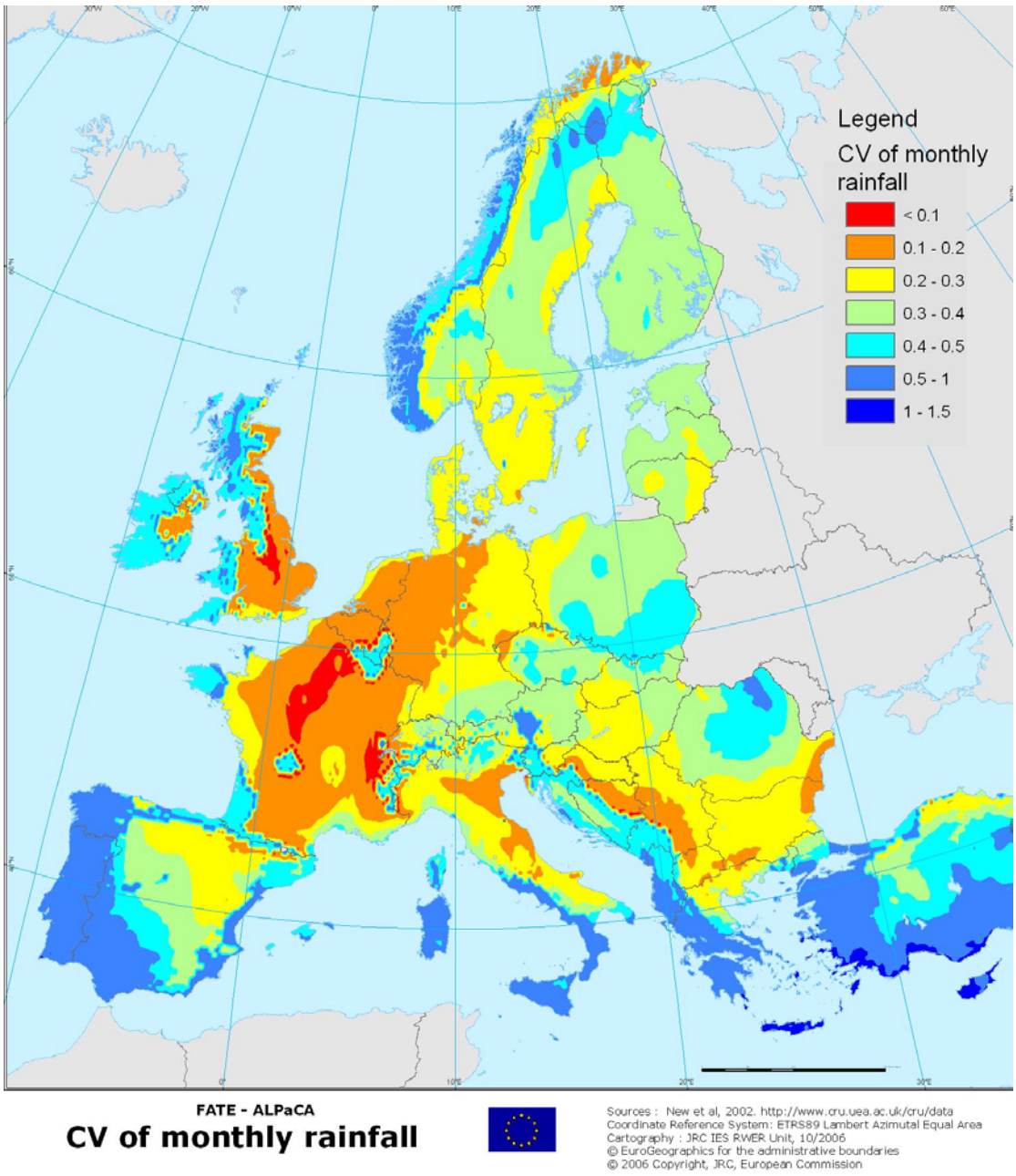

Map 16 – coefficient of variation of the monthly values of precipitation according to New et al., 2002

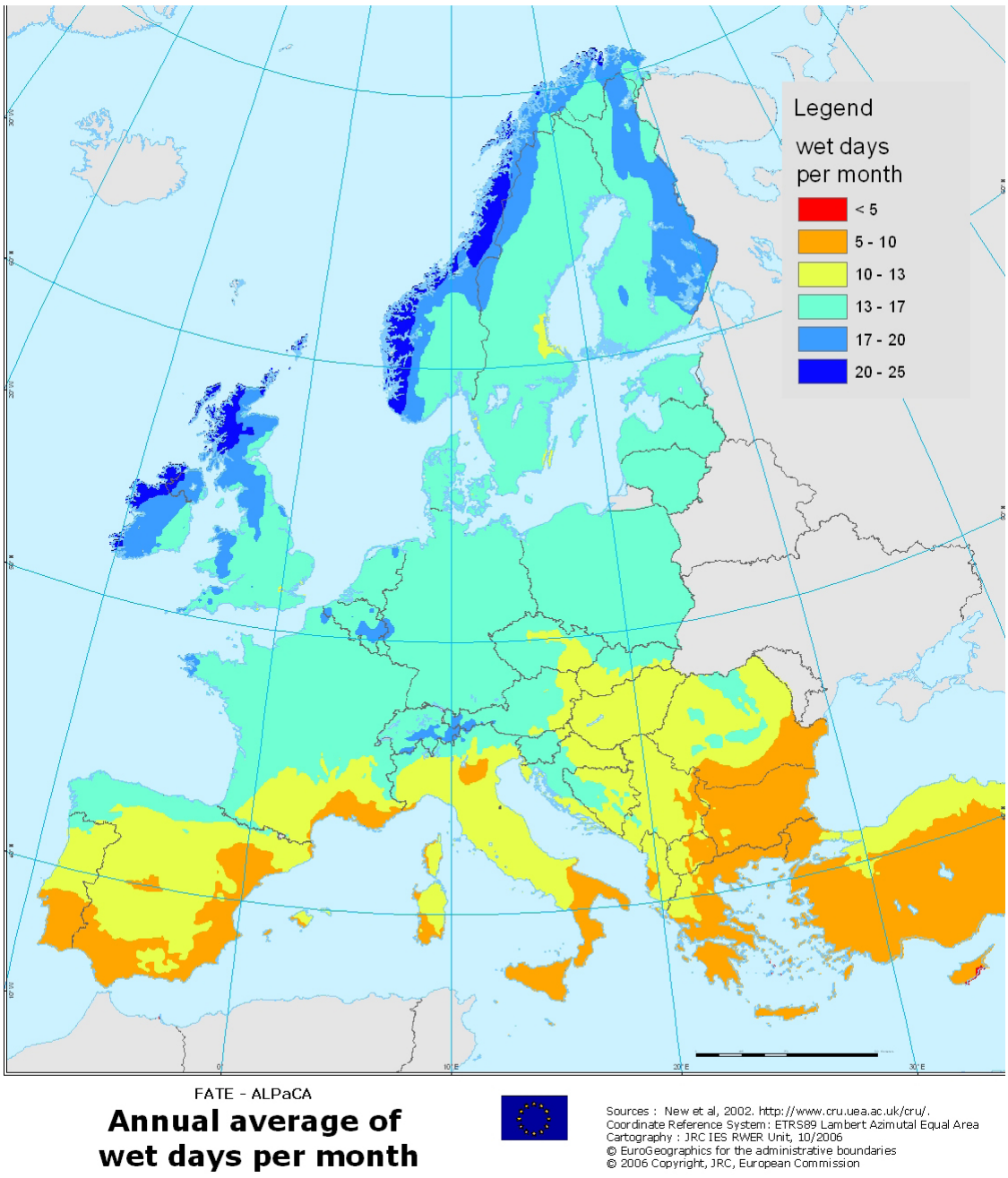

Map 17 - monthly average wet days according to New et al., 2002

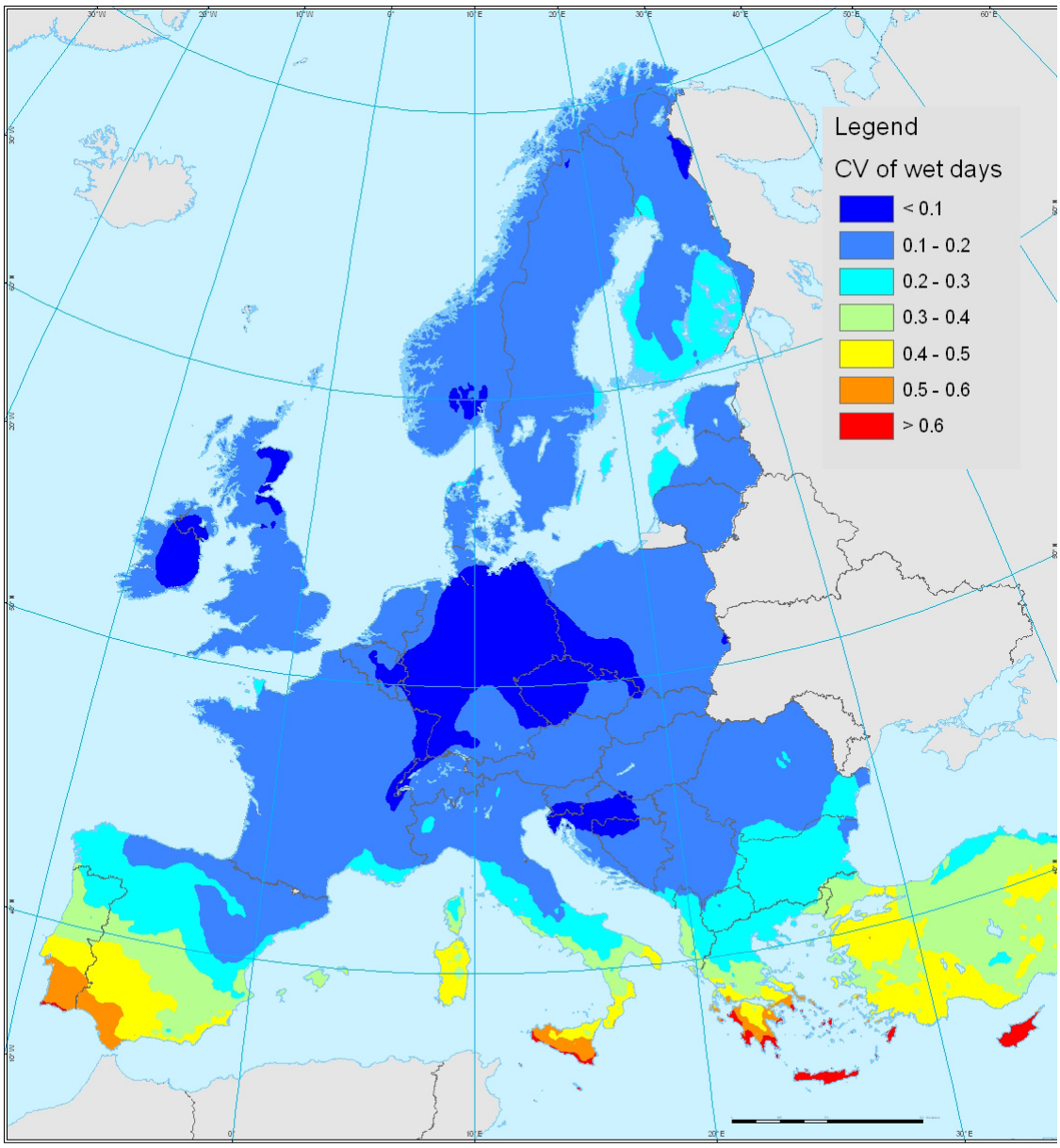

Map 18 - coefficient of variation of the monthly number of wet days according to New et al., 2002

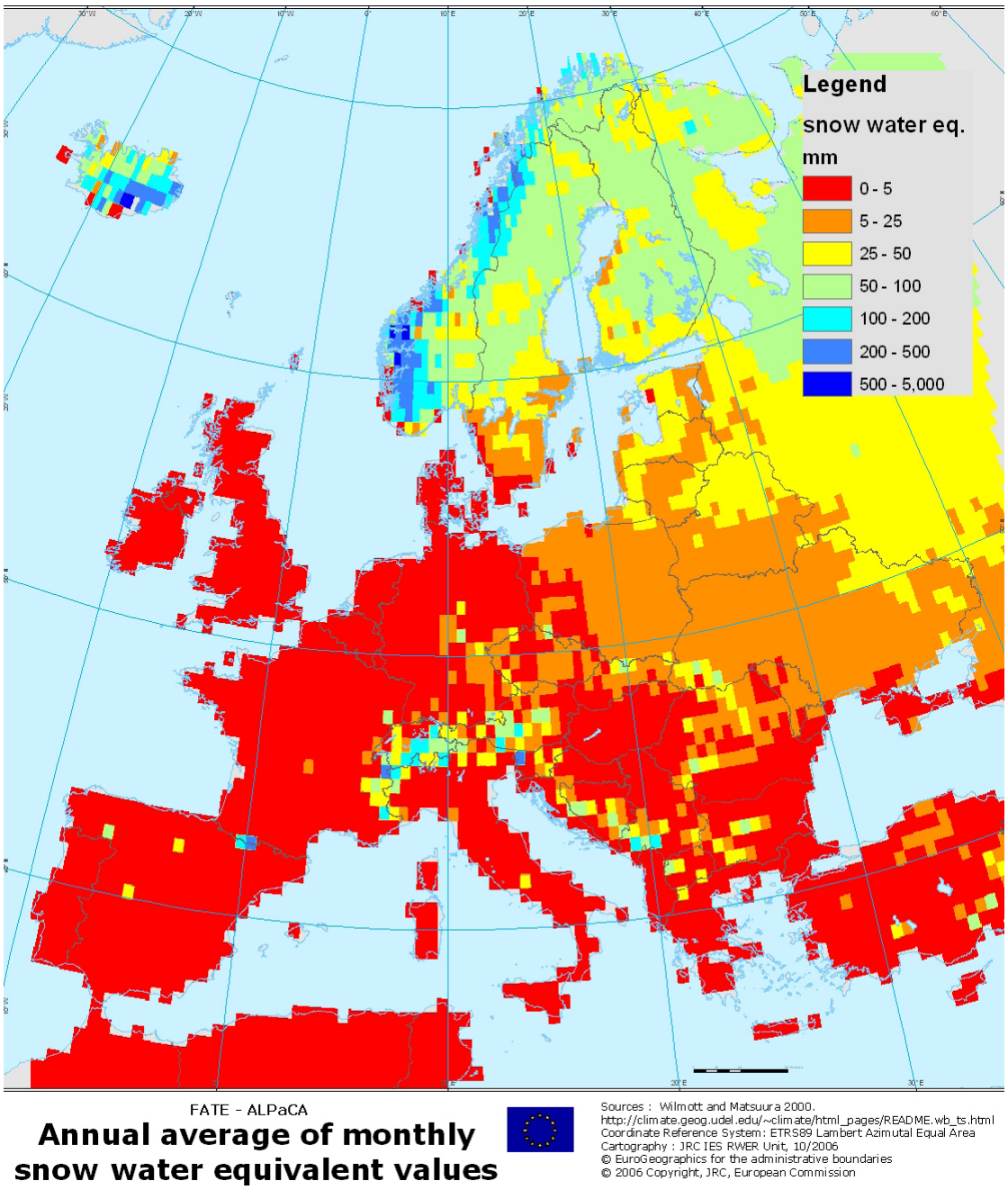

Map 19 – snowpack according to Wilmott et al., 1985.

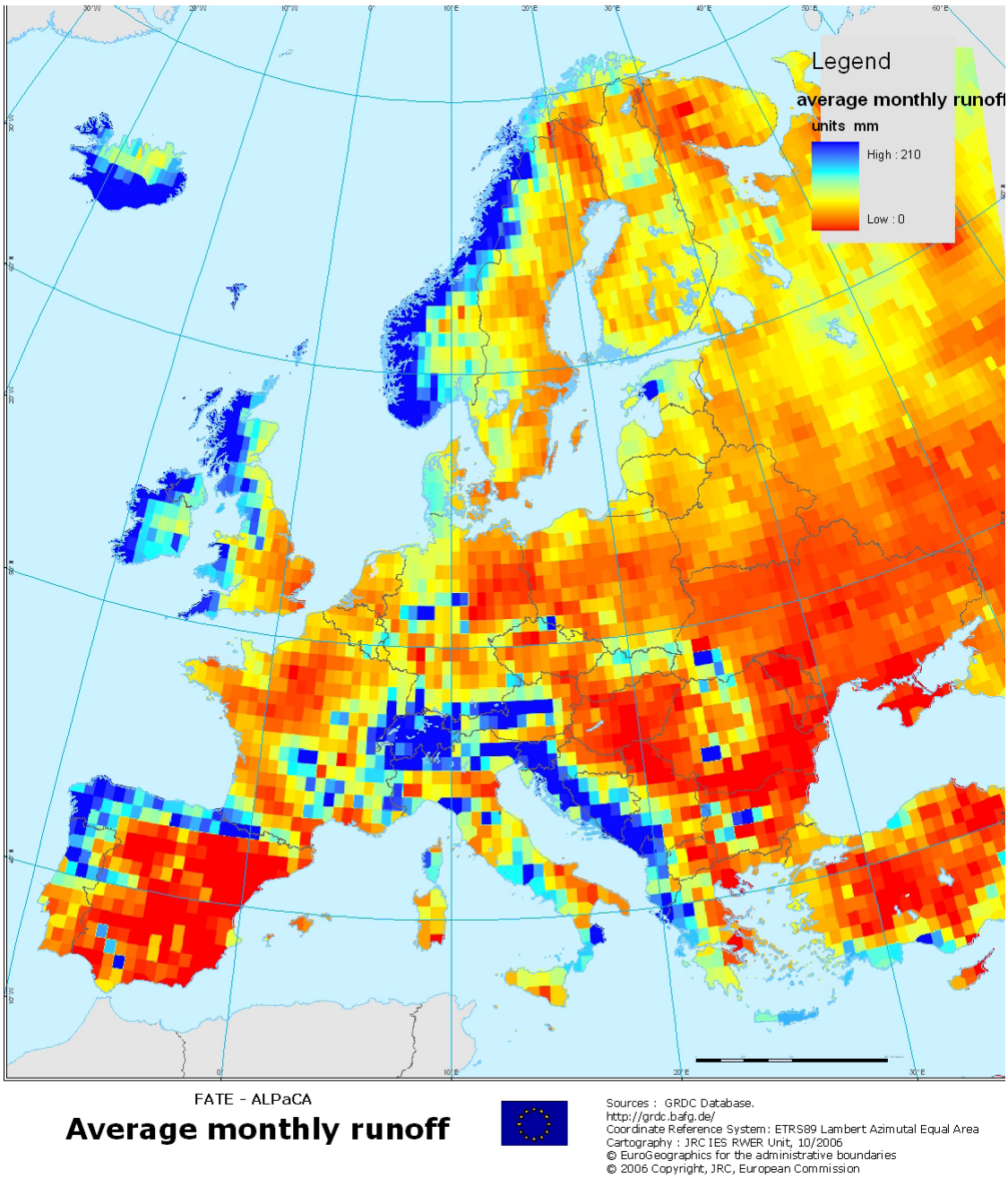

Map 20 –average monthly runoff (GRDC)

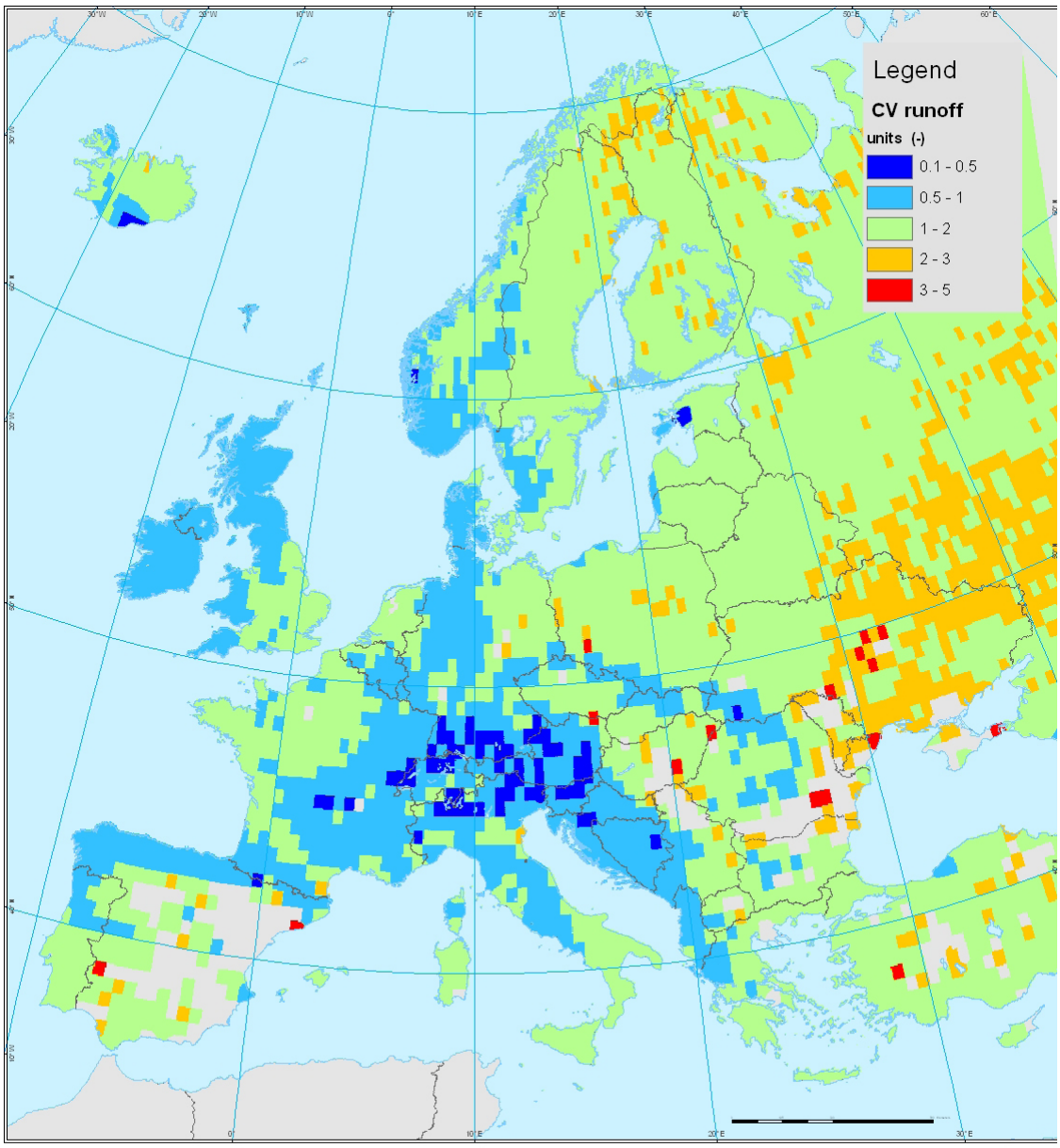

Map 21 – coefficient of variation of variation of the monthly values of runoff (GRDC)

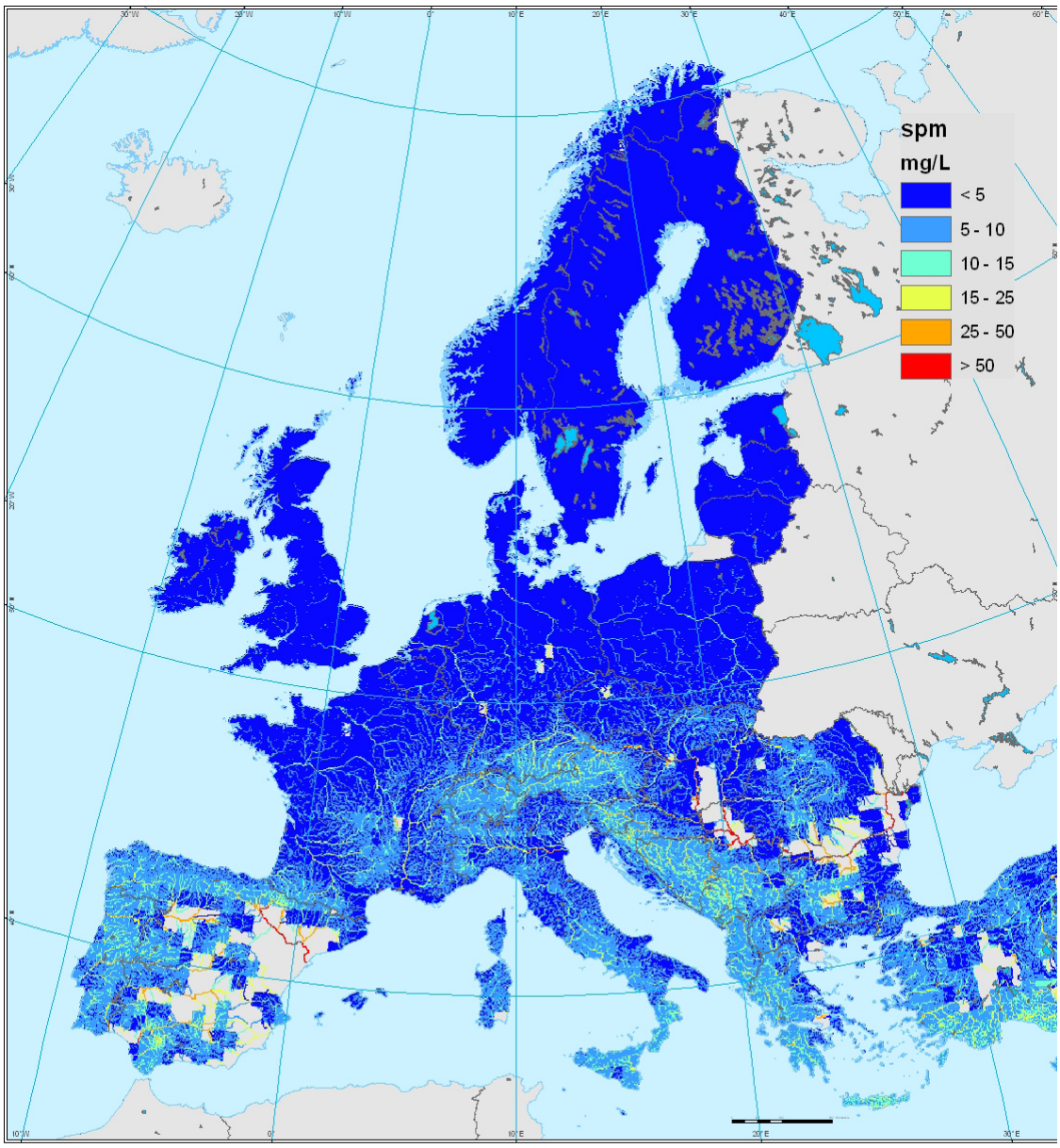

Map 22 – suspended sediment concentration according to Hakanson et al., 2005

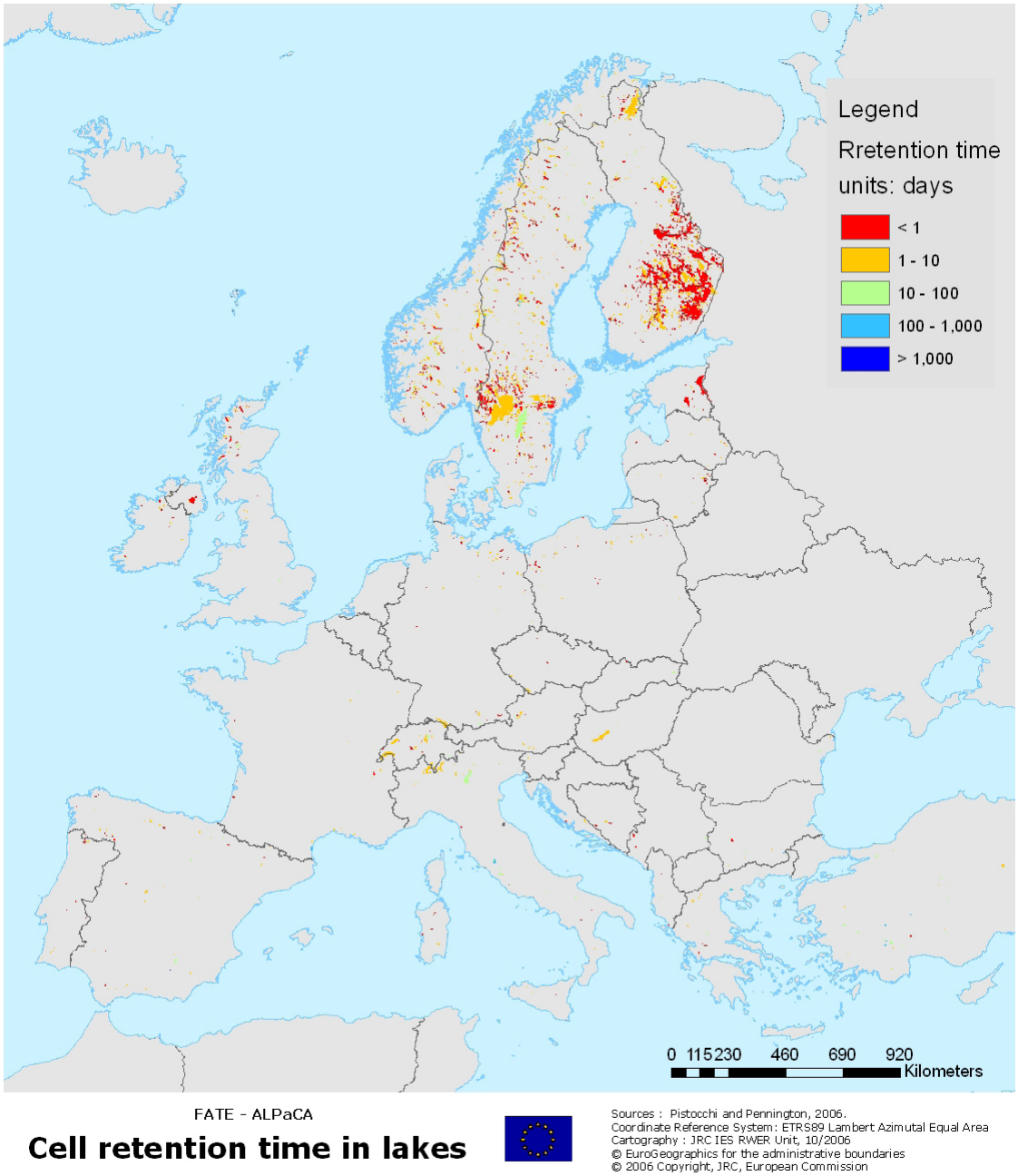

Map 23 – Cell retention time (1000 m. size cells) of European lakes.

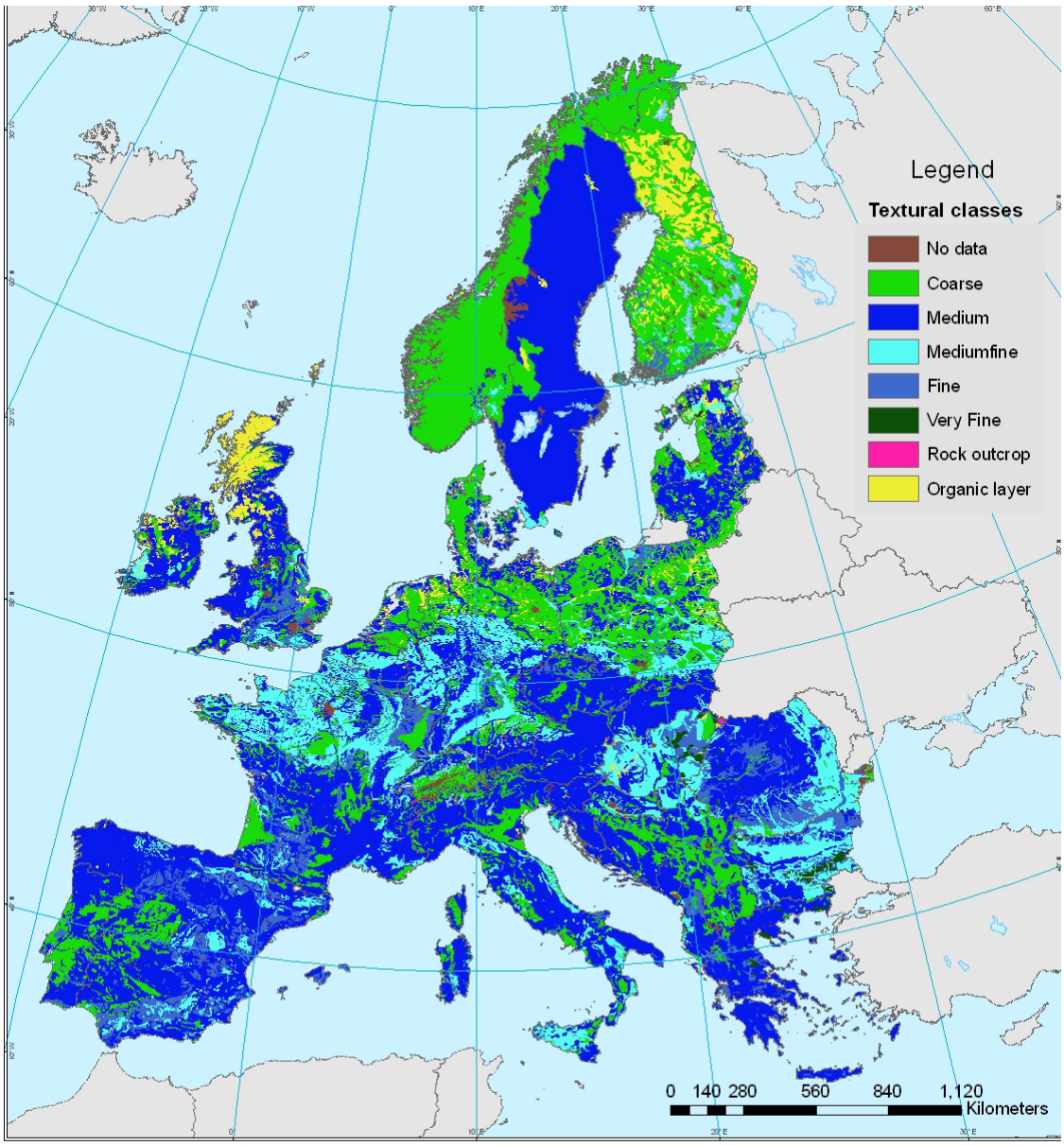

Map 24 – soil textural classes of Europe

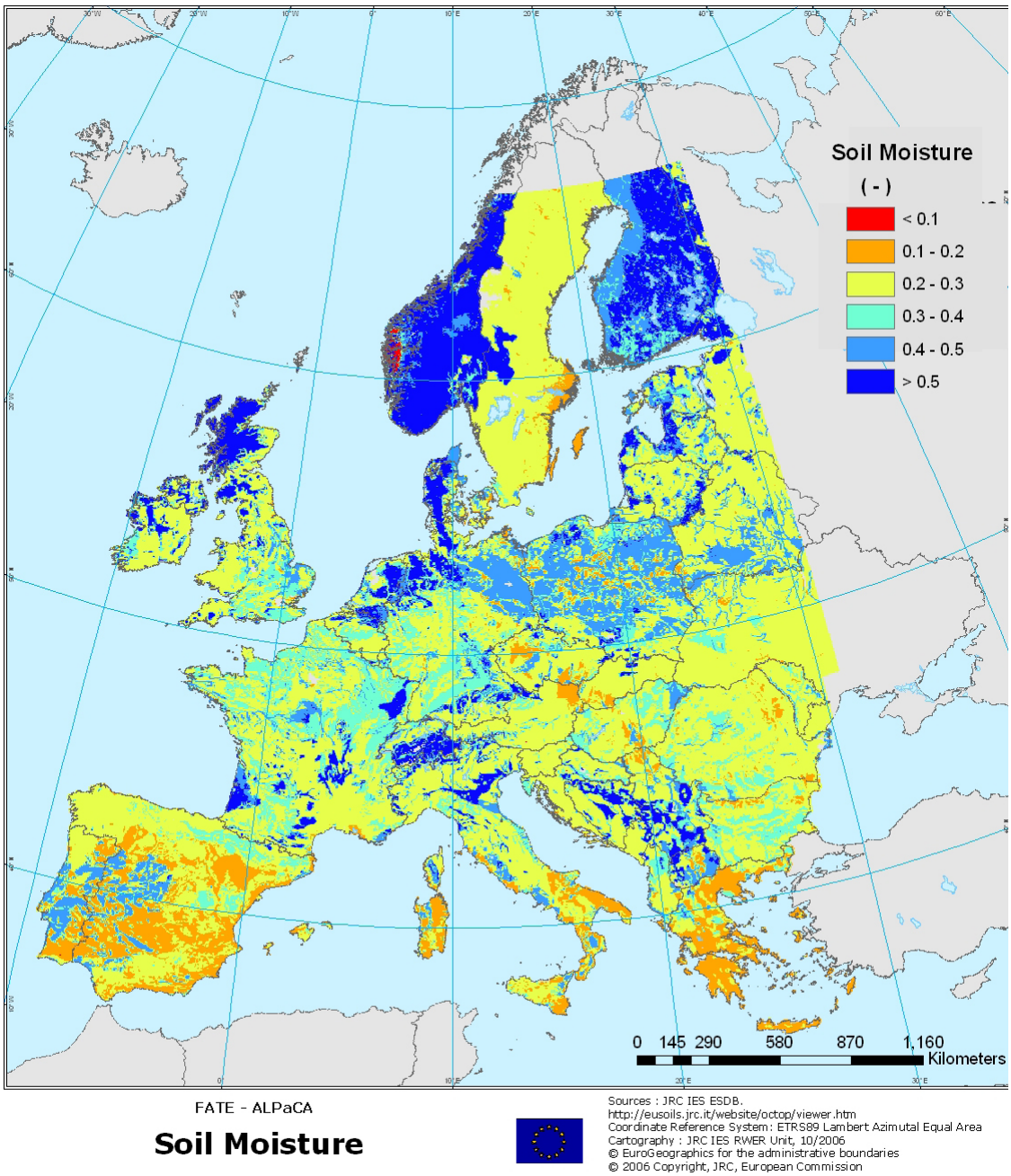

Map 25 – soil moisture computed as the average between field capacity and wilting point.

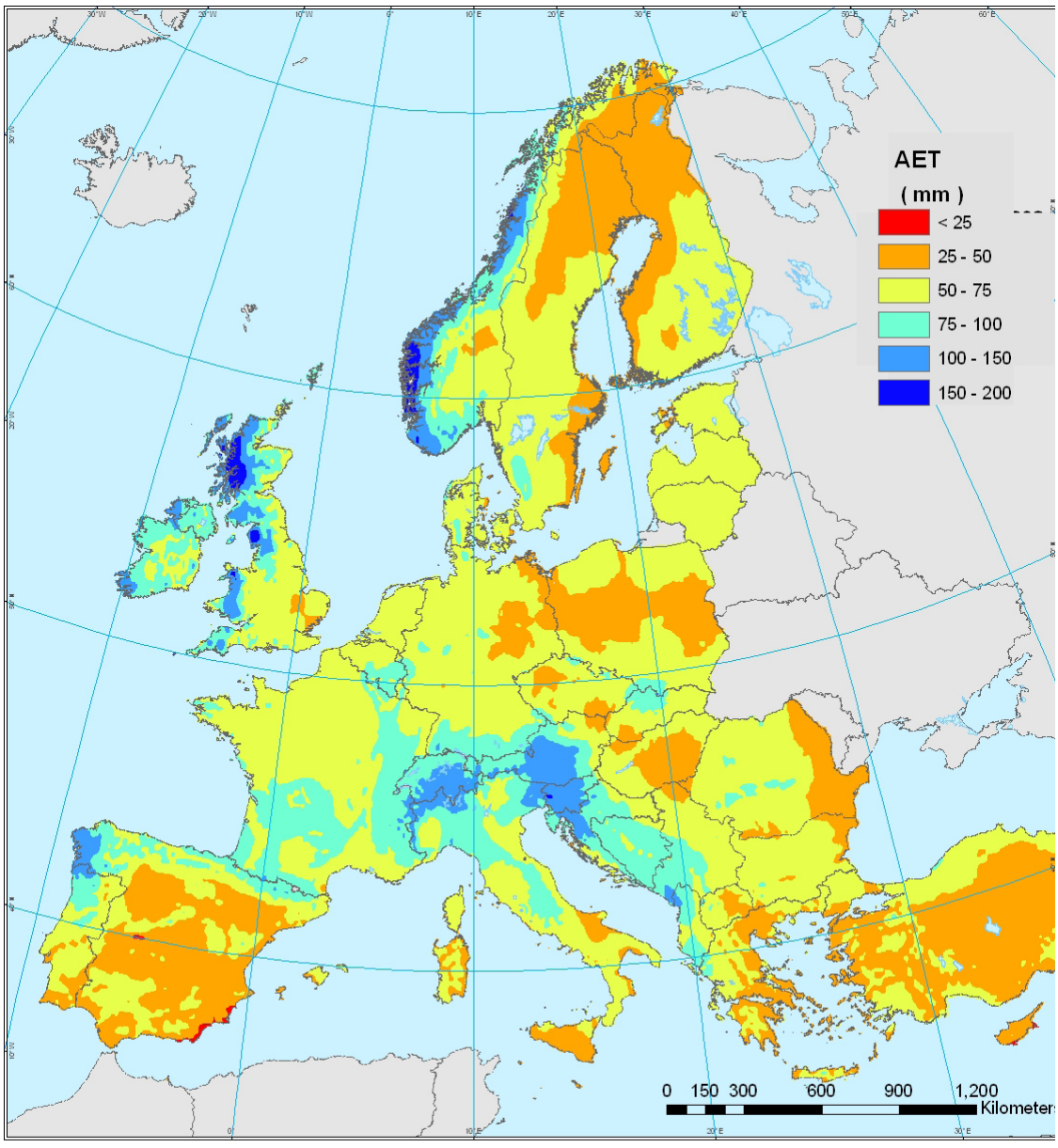

Map 26 – Annual Evapotranspiration according to Turc's formula

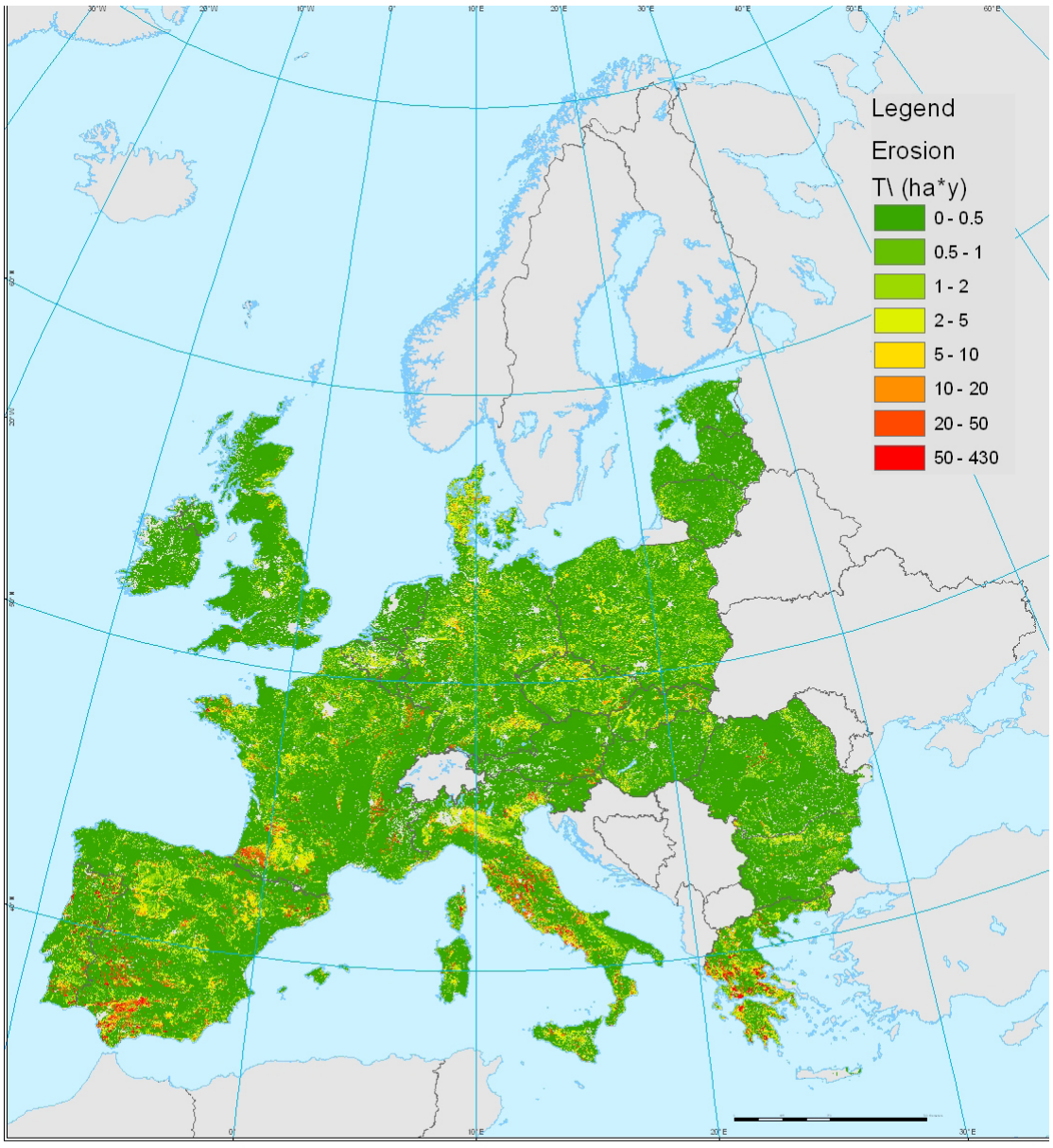

Map 27 – PESERA model results for soil erosion.

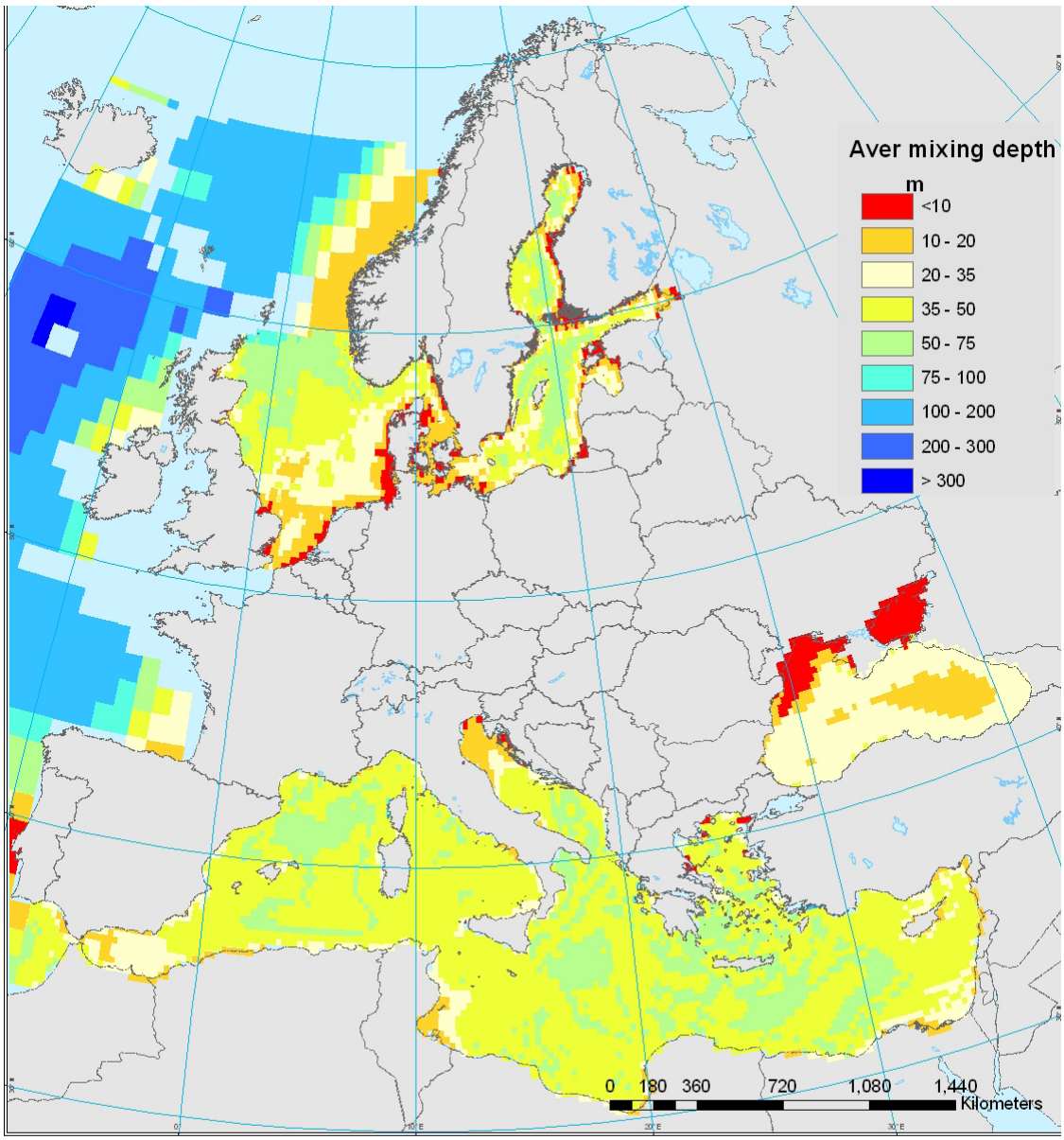

Map 28 -Seawater mixing depth (mean)

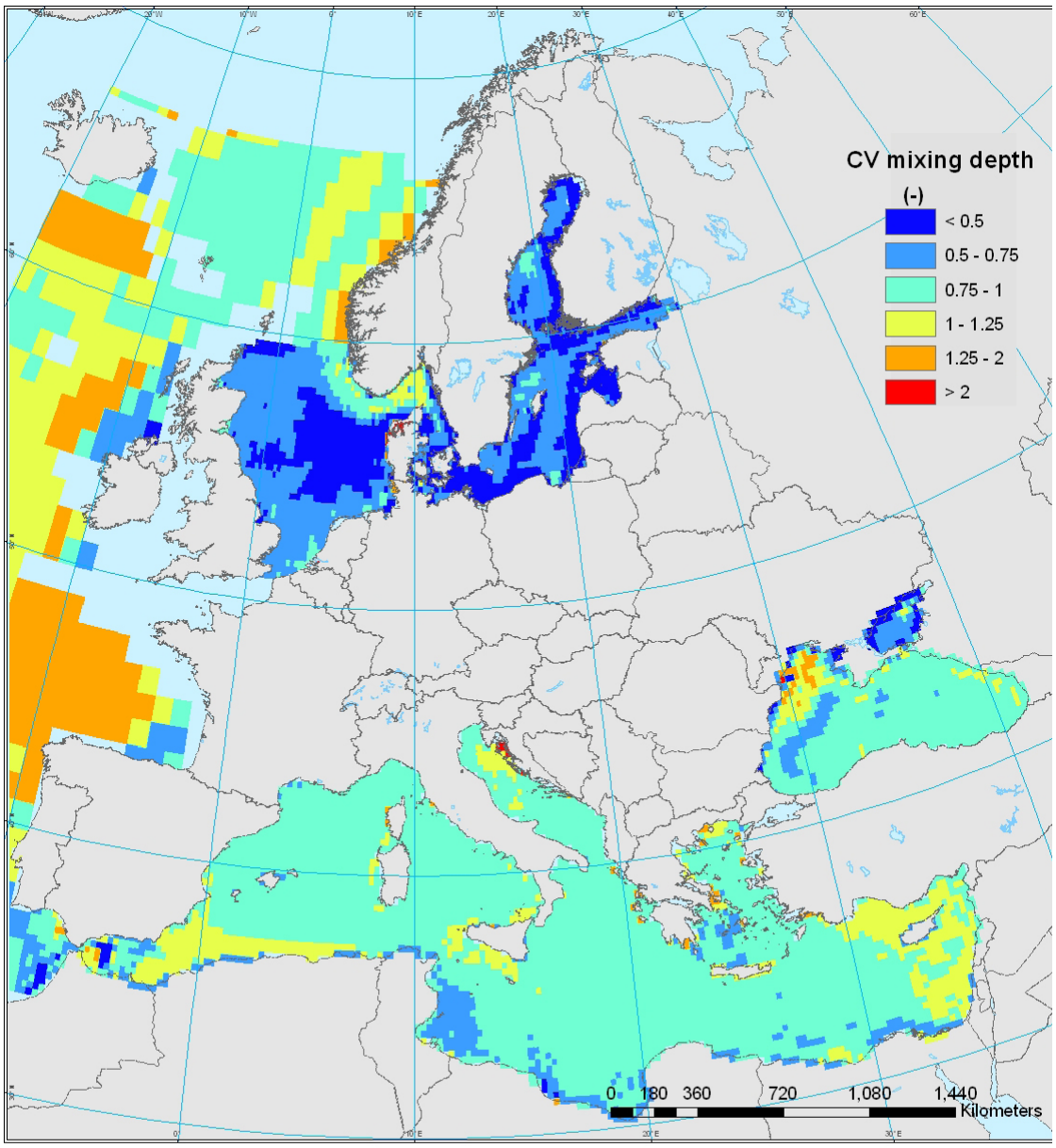

FATE - ALPaCA

Coefficient of variation of monthly values of Seawater Mixing Depth

Sources : Pistocchi et al, 2006. http://ensure.jrc.it
Coordinate Reference System: ETRS89 Lambert Azimutal Equal Area
Cartography : JRC IES RWER Unit, 10/2006
© EuroGeographics for the administrative boundaries
© 2006 Copyright, JRC, European Commission

Map 29 - Seawater mixing depth (coefficient of variation)

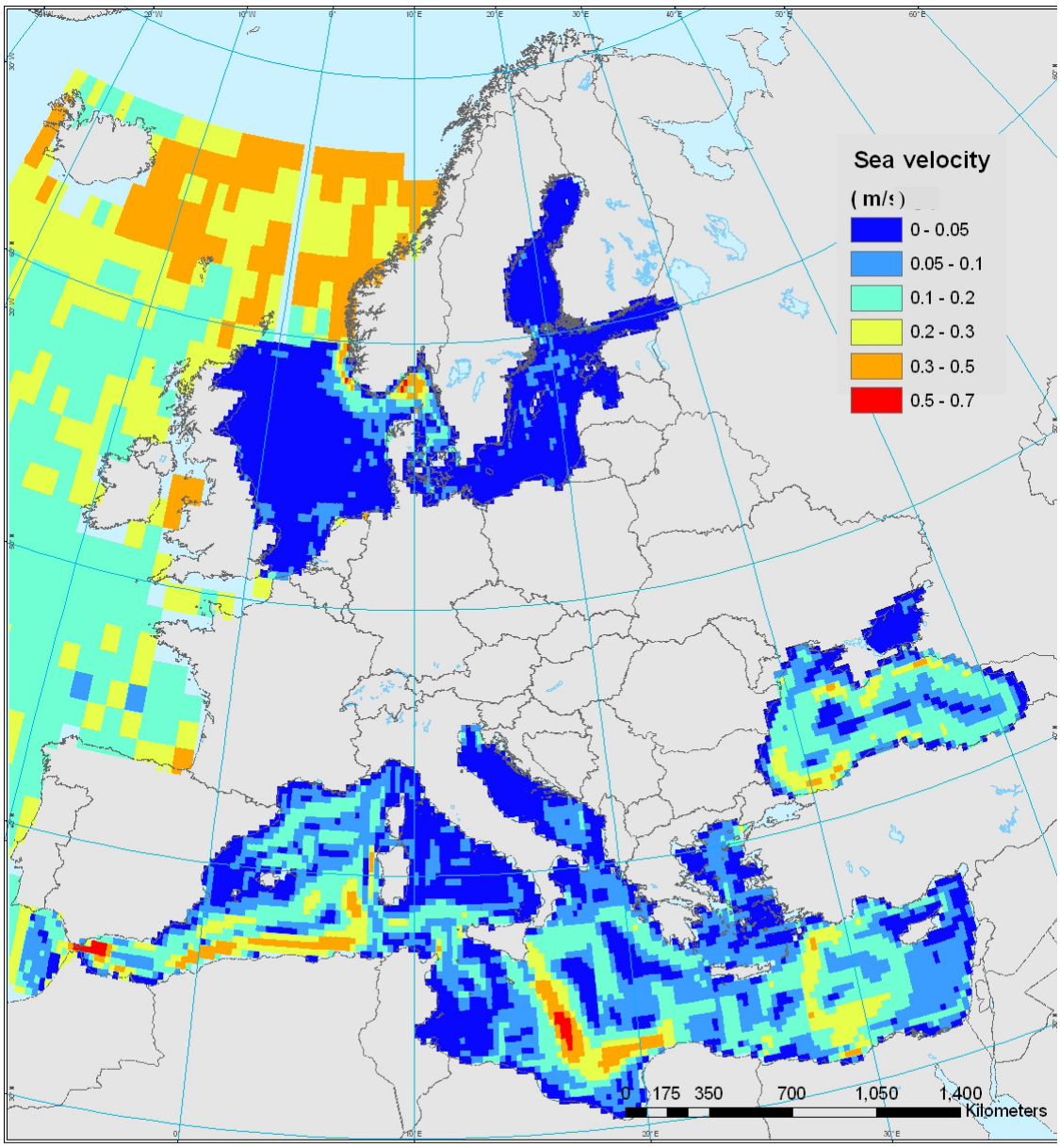

Map 30 - Seawater velocity (mean)

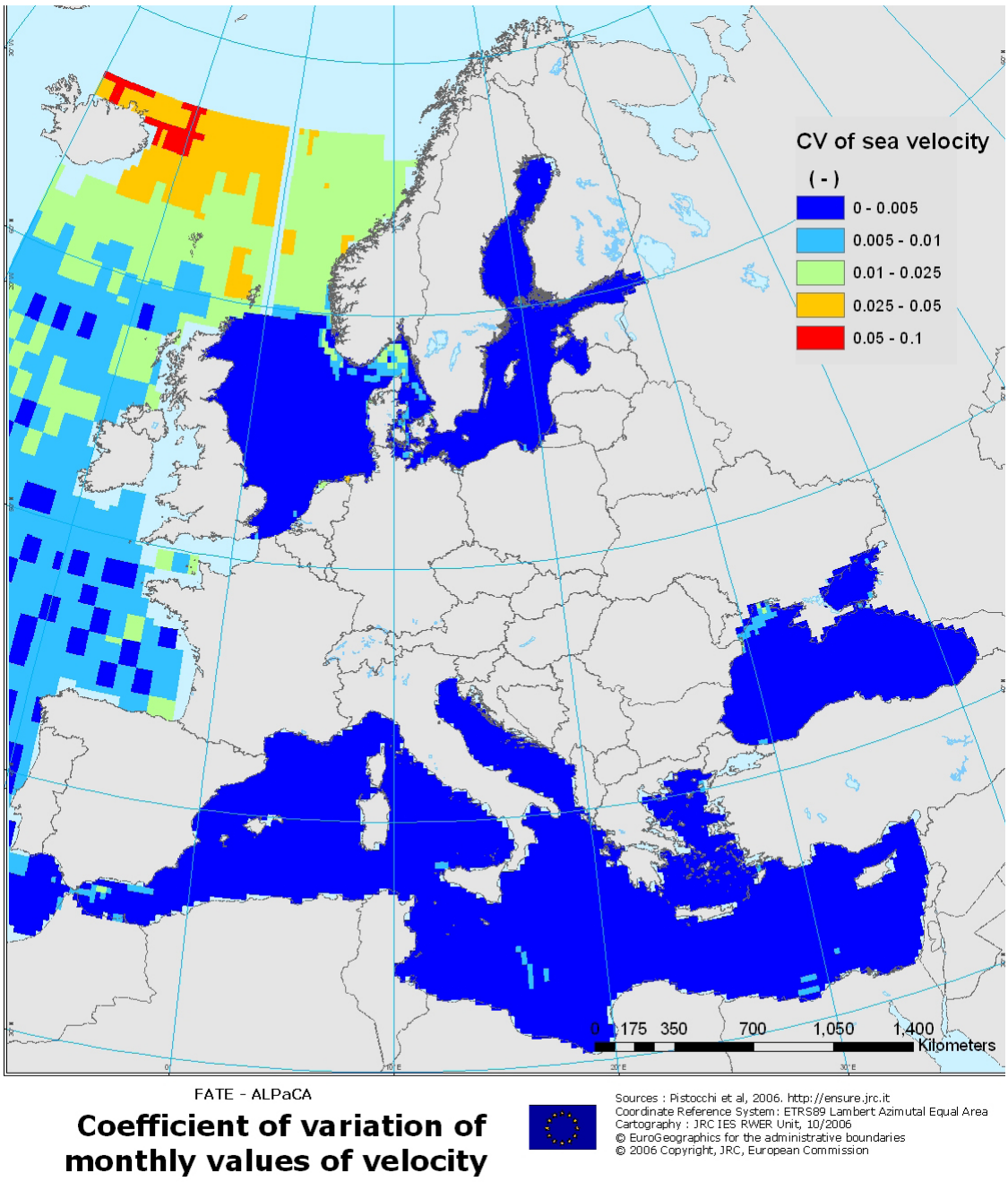

Map 31 - Seawater velocity(coefficient of variation)

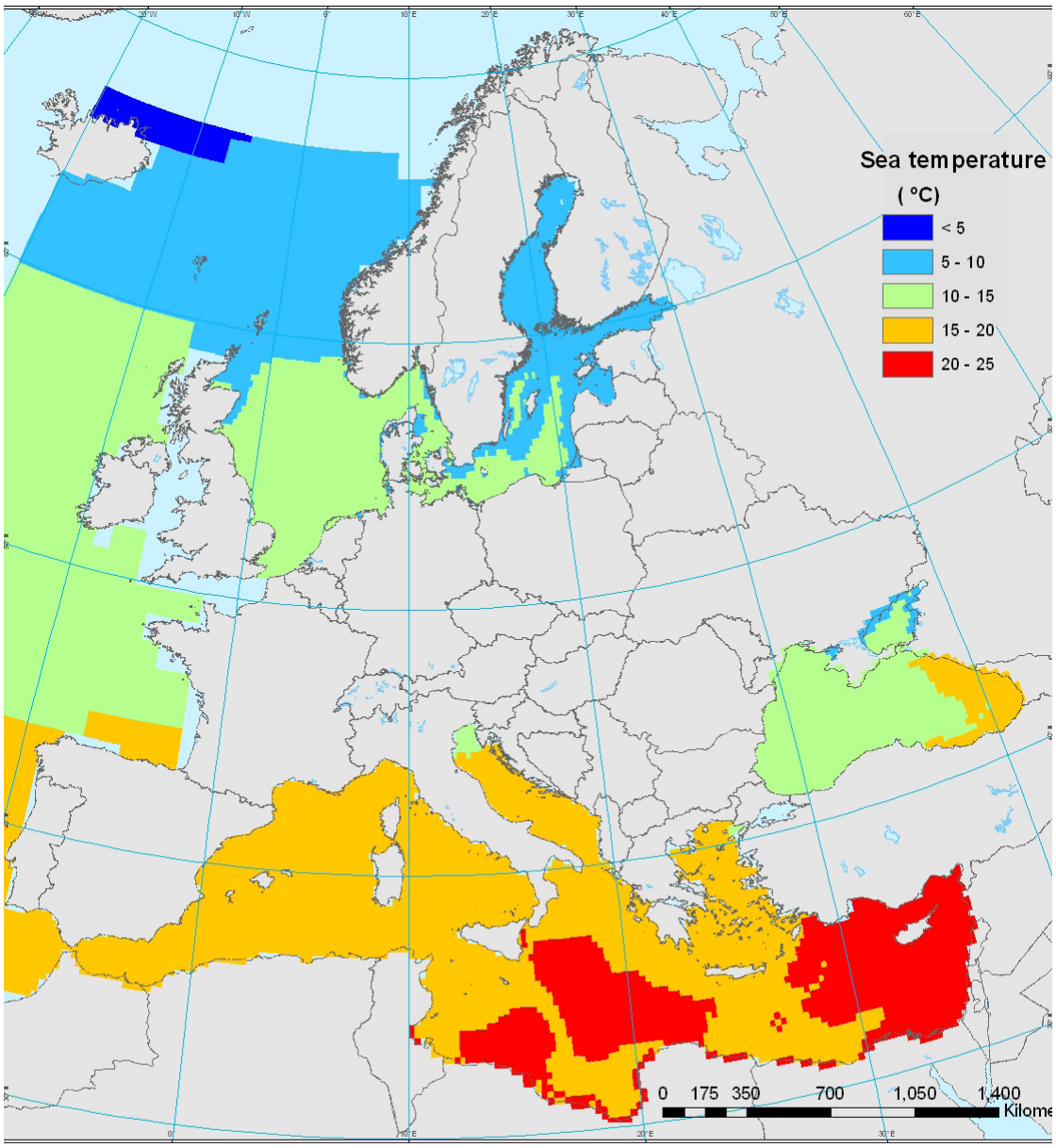

Map 32 - Seawater temperature(mean)

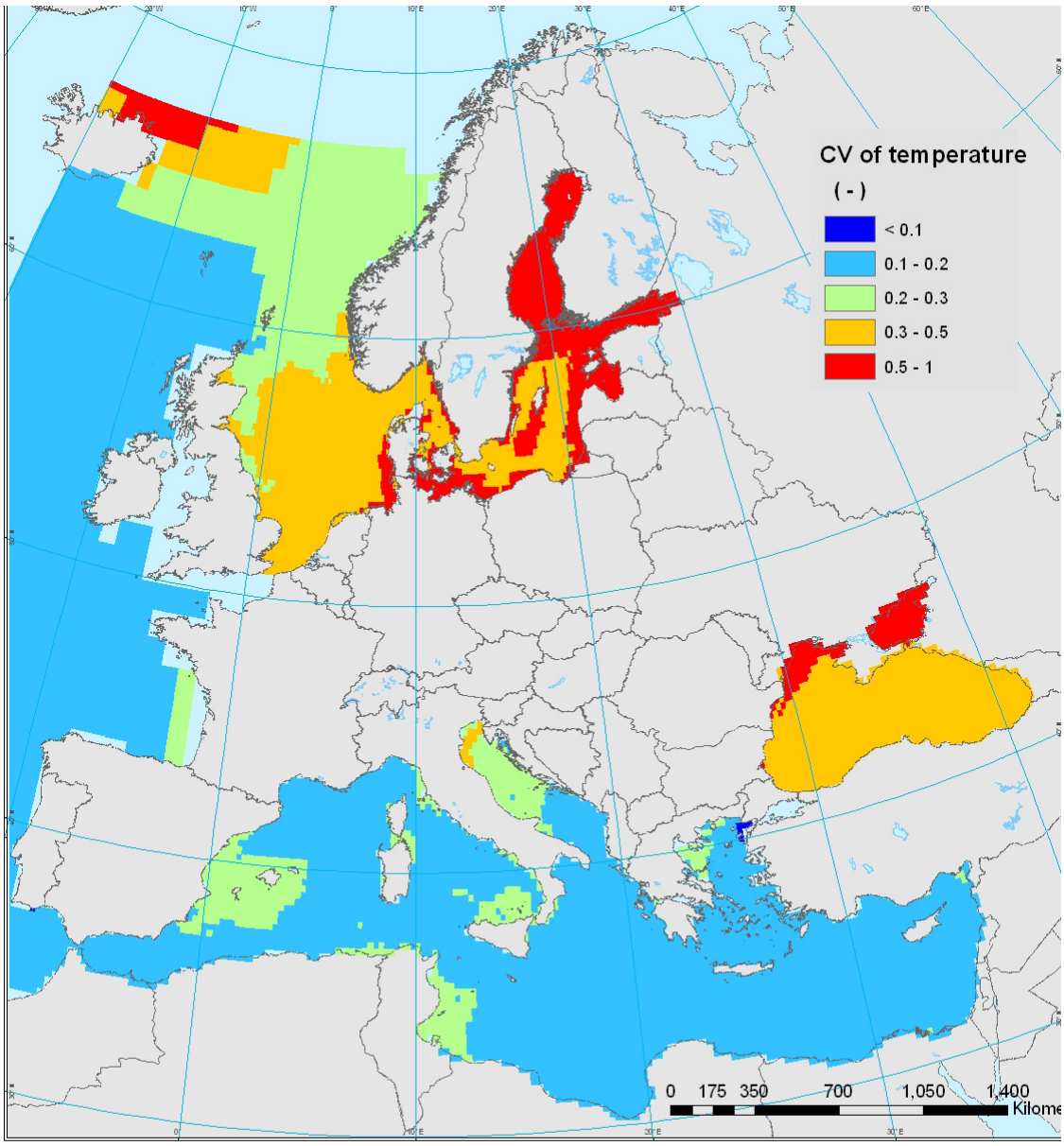

FATE - ALPaCA

Coefficient of monthly variation of sea temperature values

Sources : Pistocchi et al, 2006. http://ensure.jrc.it
Coordinate Reference System: ETRS89 Lambert Azimutal Equal Area
Cartography : JRC IES RWER Unit, 10/2006

Map 33 - Seawater temperature(coefficient of variation)

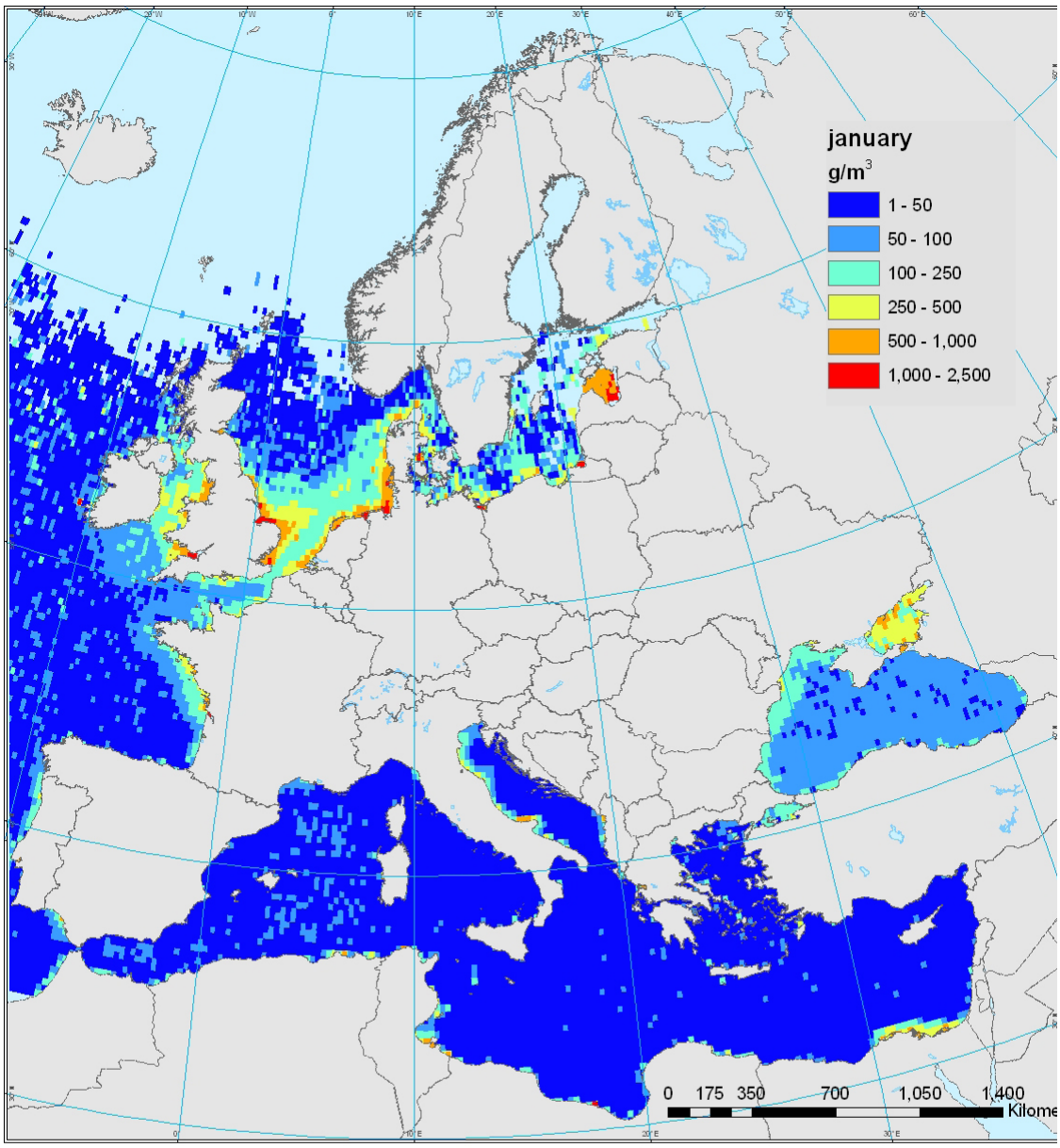

Map 34 - Seawater total suspended solids(january)

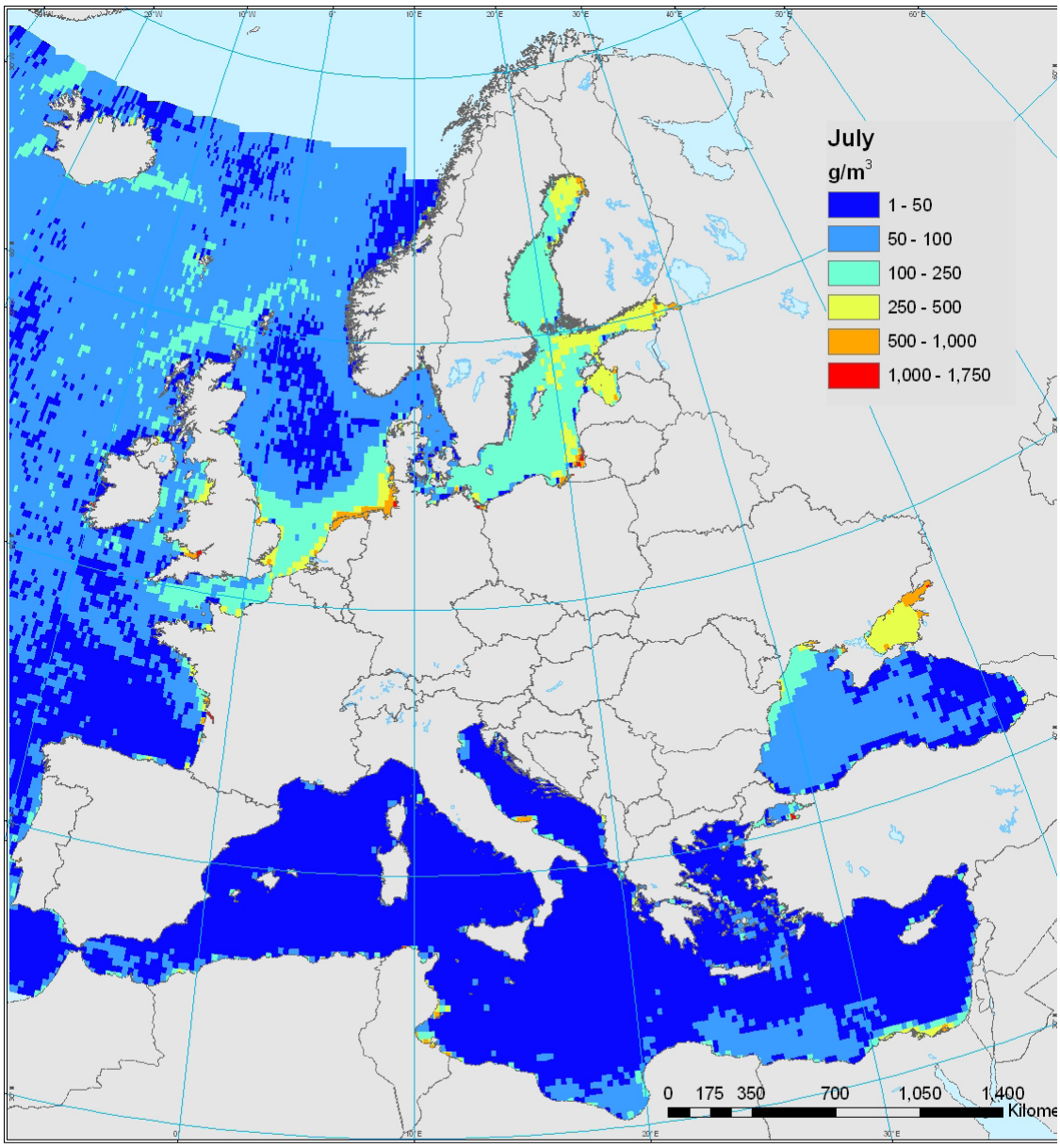

FATE - ALPaCA

Seawater total suspended solids values for July

Sources : Berthon et al., 2002
Coordinate Reference System : ETRS89 Lambert Azimutal Equal Area
Cartography : JRC IES RWER Unit, 10/2006

Map 35 - Seawater total suspended solids(july)

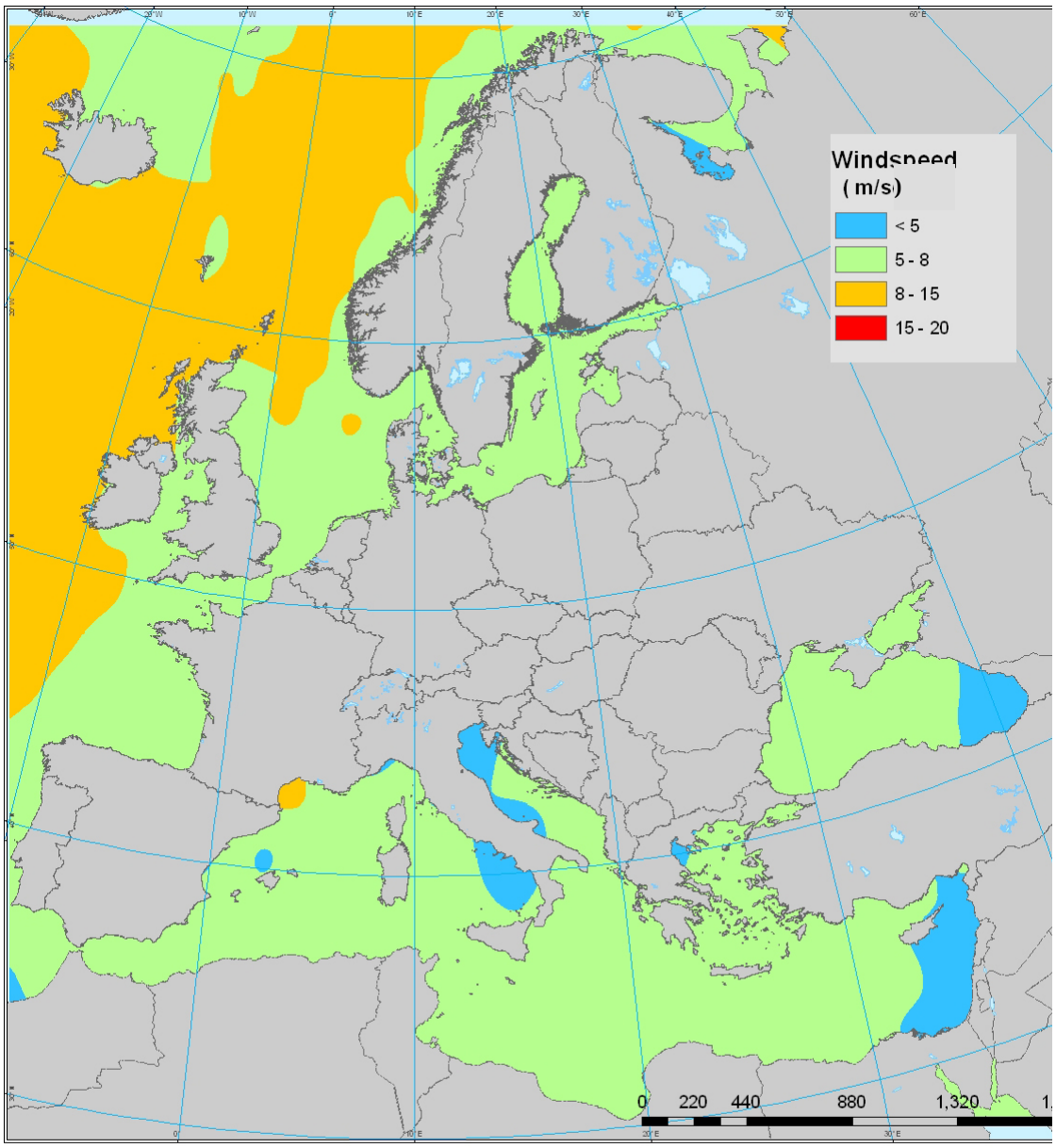

FATE - ALPaCA

Average of monthly values of wind speed on oceans

Sources : ICOADS
http://www.cdc.noaa.gov/cdc/data.coads.1deg.html
Coordinate Reference System: ETRS89 Lambert Azimutal Equal Area
Cartography : JRC IES RWER Unit, 10/2006

Map 36 - Wind speed on sea surfaces(mean)

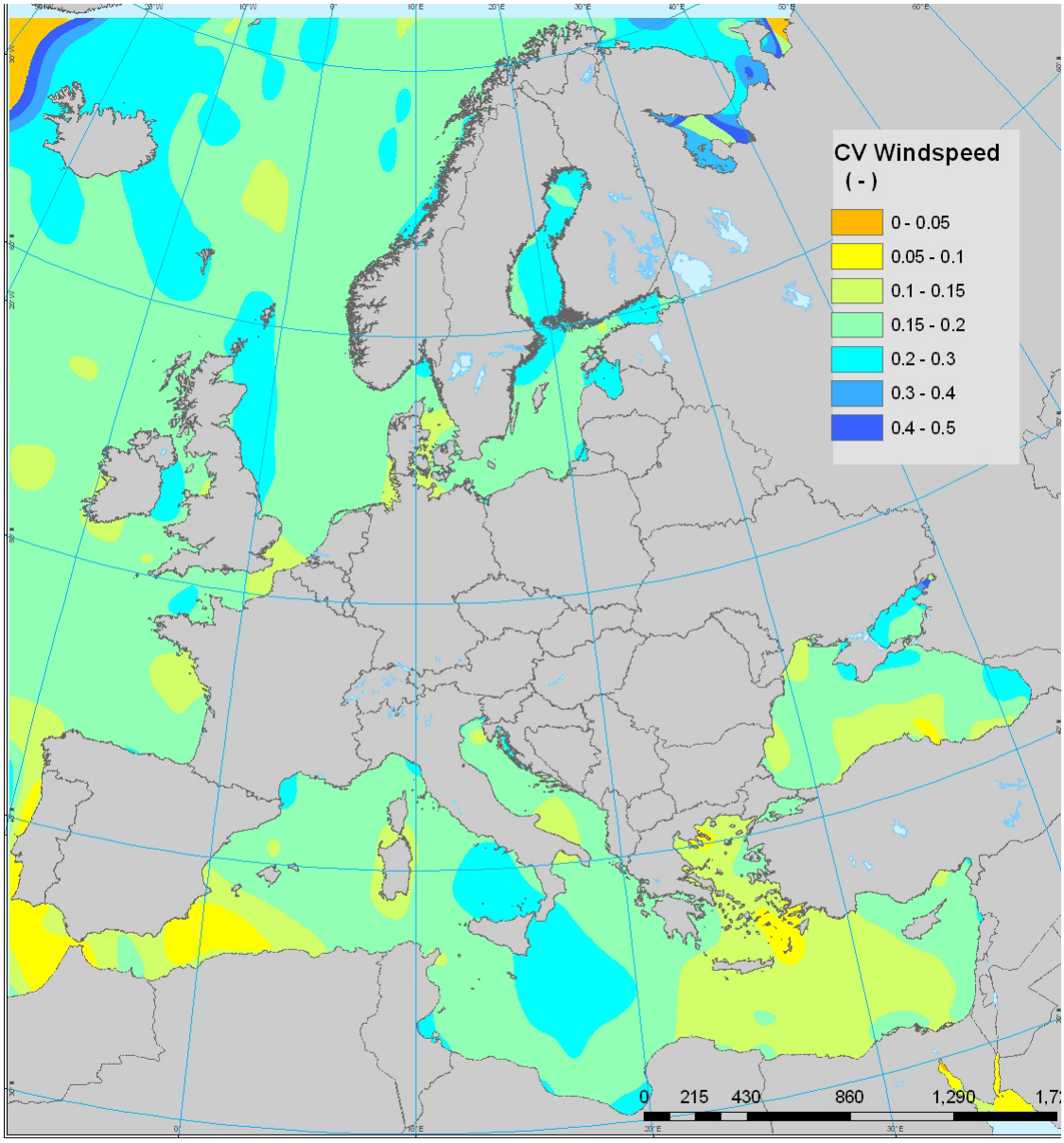

FATE - ALPaCA

Coefficient of monthly variation of Wind speed on oceans

Sources : ICOADS
http://www.cdc.noaa.gov/cdc/data.coads.1deg.html
Coordinate Reference System: ETRS89 Lambert Azimutal Equal Area
Cartography : JRC IES RWER Unit, 10/2006

Map 37 - Wind speed on sea surfaces (coefficient of variation)

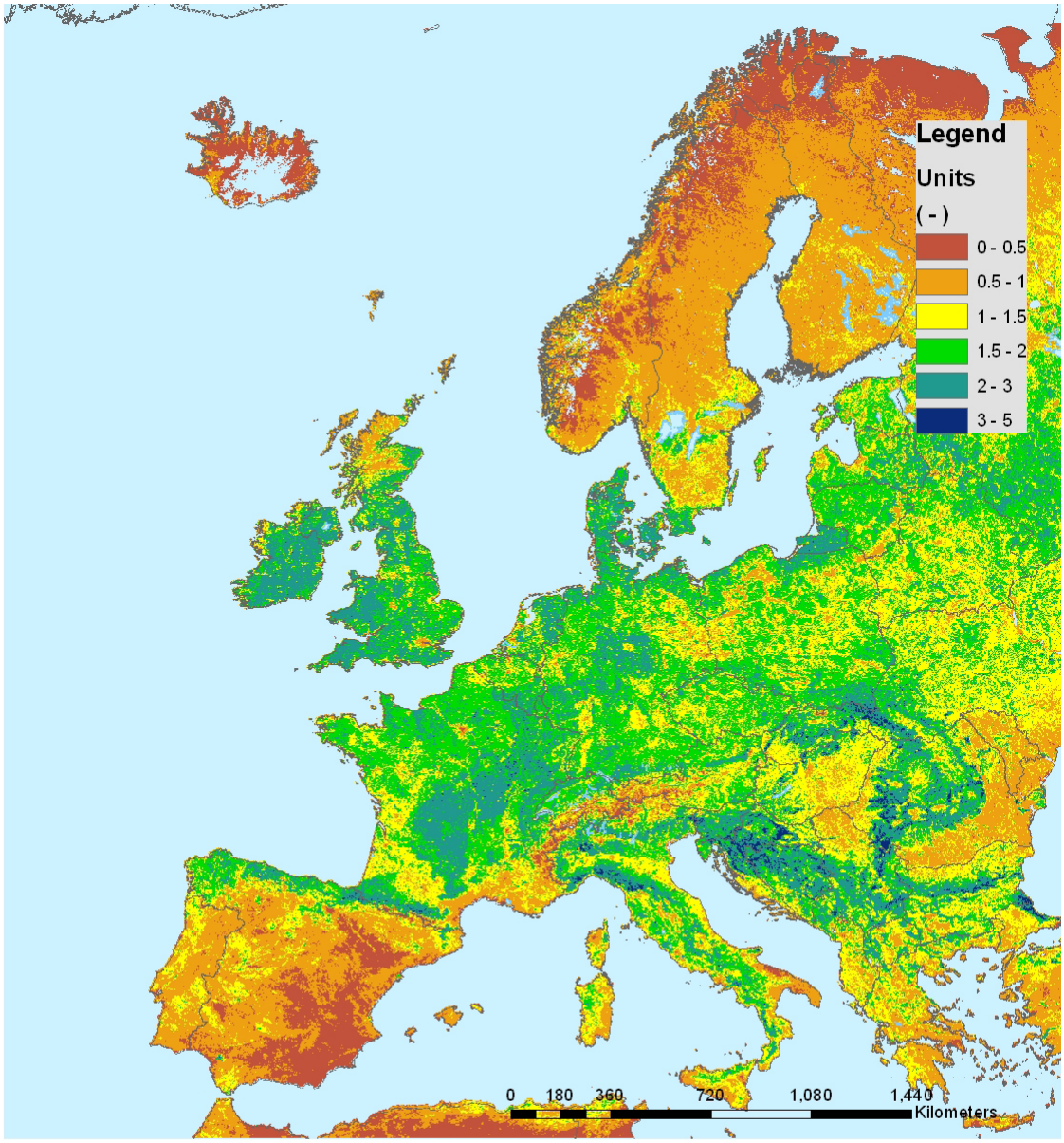

FATE - ALPaCA

Maximum LAI map of Europe

Sources : SeaWiFS FAPAR JRC product
(http://fapar.jrc.it/) as follows (Pinty et al., 2006)
Coordinate Reference System: ETRS89 Lambert Azimutal Equal Area
Cartography : JRC IES RWER Unit, 10/2006
© EuroGeographics for the administrative boundaries

Map 38 – Maximum values of LAI for Europe.

European Commission

EUR 22624 EN – DG Joint Research Centre, Institute for Environment and Sustainability (IES)
Title: Analysis of Landscape and Climate Parameters for Continental Scale Assessment of the Fate of Pollutants
Authors: Alberto Pistocchi, Pilar Vizcaino, David Pennington
Luxembourg: Office for Official Publications of the European Communities
2006 – 108 pp. – 21 x 29.7 cm
EUR - Scientific and Technical Research series; **ISSN 1018-5593**
ISBN 978-92-79-04809-8

Abstract

Landscape and climate variability is a key issue in multimedia environmental modeling. Predictions of chemicals fate and transport can be highly sensitive to some parameters, which in turn have high variability both across space and time. Hence it is important to characterize these parameters, in order to have appropriate information to supply to both spatially resolved and lumped models.

Evaluations using single default values for landscape parameters may be satisfactory when interested in small, homogeneous regions, while for continental or global scale predictions it would be more appropriate to refer to a whole range of the parameters, by performing e.g. calculations on a sufficiently representative set of unique combinations. In the present contribution, we illustrate a set of landscape and climate parameter maps of Europe, aimed at providing input to models of both distributed and lumped type. The parameters are provided in the form of maps, with a conventional spatial resolution of 1 km, and with a temporal resolution of one month whenever applicable. Actual spatial resolution may be well coarser than 1 km, depending on the data sources; however, as a number of parameters can be estimated at such resolution, it has been chosen to keep it as a reference. In future improvements of the data set, data at coarser resolution will be gradually replaced with finer ones if deemed necessary to improve model predictions.

The data set reflects average conditions in time. Although different data may often refer to different averaging periods, we don't have at present consistent estimates for all parameters throughout.

Inherent in the approach is also the impossibility to provide actual time series of the parameters. This may be limiting in many applications, but for the fate and transport of chemicals at continental or global scale overall knowledge of the emissions is still so weak that often referring to an average intra-annual variation of the landscape and climate parameters is fully satisfactory.

The parameters considered in this report reflect the input needs of most multimedia environmental models with three compartments, namely surface water, soil and air, together with atmospheric aerosol and suspended sediments in water. Also, Leaf Area Index (LAI) is included as a representative parameter for vegetation. The parameters are specifically designed to cope with the GIS-based modeling strategy proposed by Pistocchi, 2005, but similar to the input required by most multimedia models.

EUROPEAN COMMISSION
DIRECTORATE-GENERAL
Joint Research Centre

The mission of the JRC is to provide customer-driven scientific and technical support for the conception, development, implementation and monitoring of EU policies. As a service of the European Commission, the JRC functions as a reference centre of science and technology for the Union. Close to the policy-making process, it serves the common interest of the Member States, while being independent of special interests, whether private or national.

LB NA 22624 EN N

ISBN 978-92-79-04809-8